Status of Thesis

Title of thesis	Effect of Boost Pressure on Performance, Combustion and Exhaust Emissions in Direct Injection Compressed Natural Gas Engine

I GIRMA TADESSE

Hereby allow my thesis to be placed at the Information Resource Center (IRC) of Universiti Teknologi PETRONAS (UTP) with the following conditions:

1. The thesis becomes the property of UTP.
2. The IRC of UTP may make copies of the thesis for academic purposes only.
3. This thesis is classified as

	Confidential
X	Non-confidential

If this thesis is confidential, please state the reason:

_____

_____

____

The contents of the thesis will remain confidential for _____ years.

Remarks on disclosure:

_____

_____

____

Endorsed by

_____	_____
Signature of Author	Signature of Supervisor
Girma Tadesse Chala	
Universiti Teknologi PETRONAS	Name of Supervisor
Bandar Seri Iskandar, Tronoh, 31750	AP Dr A. Rashid A. Aziz
Perak, Malaysia	
Date: _____	Date: _____

UNIVERSITI TEKNOLOGI PETRONAS

Approval by Supervisor(s)

The undersigned certify that they have read, and recommend to The Postgraduate Studies Programme for acceptance, a thesis entitled "**Effect of Boost Pressure on Performance, Combustion and Exhaust Emissions in Direct Injection Compressed Natural Gas (CNG) Engine"** submitted by **Girma Tadesse** for the fulfillment of the requirements for the degree of Master of Science in Mechanical Engineering.

_____
Date

Signature : _____

Main Supervisor : AP Dr A. Rashid A.Aziz

Date : _____

Signature : _____

Co-Supervisor : Dr. Zainal Ambri

Date : _____

TITLE PAGE

UNIVERSITI TEKNOLOGI PETRONAS

Effect of Boost Pressure on Performance, Combustion and Exhaust Emissions in Direct Injection Compressed Natural Gas(CNG) Engine

By

Girma Tadesse

A THESIS

SUBMITTED TO THE POSTGRADUATE STUDIES PROGRAMME

AS A REQUIREMENT FOR THE

DEGREE OF MASTER OF SCIENCE IN MECHANICAL ENGINEERING

DEPARTMENT OF MECHANICAL ENGINEERING

BANDAR SERI ISKANDAR,

PERAK

SEPTEMBER, 2009

DECLARATION

I hereby declare that the thesis is based on my original work except for quotations and citations which have been duly acknowledged. I also declare that it has not been previously or concurrently submitted for any other degree at UTP or other institutions.

Signature: _____

Name : Girma Tadesse

Date : _____

ACKNOWLEDGEMENTS

My sincere appreciation and thanks goes to my supervisor Assoc. Prof. Dr. Abdul Rashid A. Aziz for all guidance, feedback, commitment and help in sharing valuable ideas for the successful completion of this work.

I would like to express my gratitude to all the members of Centre for Automotive Research for their efforts and encouragement throughout the course of this research. I would also like to thank staff of Postgraduate Office for their assistance and guidance.

My final gratitude goes to my fellow postgraduate students and all who co-operated in one or another way in giving suggestion for the success of this research.

ABSTRACT

There is an increasing interest in supercharging S.I. engines operating on natural gas mainly due to its superior knock resisting properties in comparison to traditional liquid fuels. With direct injection of gaseous fuel there is still some penalty in volumetric efficiency when injecting the fuel at early and partial direct injection. The present work reports the effect of low boost pressures on engine performance, combustion and exhaust emissions of CNG-DI engine. The experimental test was carried out in 4-stroke spark ignition CNG-DI engine with compression ratio of 14. The investigation was done at full load and homogenous piston for stoichiometric air-fuel ratio in order to assess the maximum output of the engine. The test includes variation of engine speed and boost pressure. Injection parameters are found to have significant influence on engine performance. Simulated port injection (Early injection) when inlet valves are still open (300° BTDC) and partial direct injection in which part of the injection occurs after the inlet valves are closed (180° BTDC) were varied at each operating speeds with variation of boost pressure from 2.5 to 10 kPa. Injection pressure was kept constant at 18 bars for all test points. Narrow angle injector (NAI) was used to get faster mixing rate at operating engine speeds of 2000 rpm to 5000 rpm. Ignition timing was set to get maximum brake toque (MBT). In order to examine effects of boost pressure experimental work was done for naturally aspirated engine and the results were compared to supercharging system.

For boost pressure above 7.5 kPa, it is observed that there is better performance at all operating engine speeds compared to naturally aspirated engine. With increasing supercharging pressure there is better heat release and mass fraction burned resulting in better combustion efficiency. In-cylinder pressure and temperature is high with increasing boost pressure giving high NOx emission. Supercharging system is found to reduce the penalty of volumetric efficiency at port and partial direct injections. With supercharging, partial direct injection gives better performance for speeds 2000 to 4000 rpm compared to early injection timings, whereas early injection timing gives better performance for engine speeds 4000 to 5000 rpm. At high engine speed, early injection timing gives enough time for mixture preparation with penalty for volumetric efficiency loss reduced by supercharging.

ABSTRAK

Kini terdapat minat yang mendalam dalam mengecas engine nyalaan bunga api yang beroperasi menggunakan gas asli terutama kepada ketahanan letupan yang tinggi dalam perbandingan kepada cecair bahan api. Dengan menggunakan suntikan terus gas asli, masih terdapat kerugian dalam kecekapan isipadu bila gas disuntik awal masa dan separuh masa. Kajian terkini melaporkan keputusan pada penambahan sedikit tekanan pada prestasi engin, pembakaran dan pencemaran dari ekzos oleh engin CNG-DI. Keputusan eksperimen dilakukan dalam 4 lejang dengan nyalaan bunga api engin CNG-DI dengan 14 nisbah mampatan. Penyelidikan dijalankan pada beban yang tinggi dan pencucuh dalam campuran sekata dalam nisbah udara dan gas untuk mendapatkan keputusan yang paling tinggi. Kajian ini meliputi pelbagai kelajuan engin dan penambahan tekanan. Parameter suntikan menunjukkan kesan yang ketara pada prestasi engin. Suntikan awal apabila injap dibuka (300^{o} BDTC) dan separuh suntikan terus dimana suntikan berlaku selepas injap ditutup (180^{o} BTDC) berbeza apabila ia beroperasi pada setiap kelajuan dan pelbagai tekanan udara dari 2.5 hingga 10 kPa. Tekanan suntikan ditetapkan pada 18 bar untuk semua titik ujian. Injektor sudut tirus digunakan untuk mendapatkan campuran yang cepat pada kelajuan 2000 ppm hingga 5000 ppm (ppm=pusingan per minit). Masa utnuk nyalaan bunga api ditetapkan bagi mendapatkan daya putaran brek yang tertinggi. Untuk menguji kesan penambah tekanan, kajian dijalankan pada engin tekanan biasa dan keputusan kajian dibandingkan dengan sistem peningkatan cas.

Untuk penambah tekanan melebihi 7.5 kPa, ia telah terbukti bahawa prestasi engine meningkat pada semua kelajuan engine dibandingkan dengan tanpa penambah tekanan cas. Dengan peningkatan cas pada enjin, terdapat pengeluaran haba yang lebih baik dan pembakaran pecahan jisim yang memberi hasil pembakaran yang lebih cekap. Tekanan dan suhu yang tinggi didalam silinder akibat peningkatan cas, menghasilkan penceramaran NOx yang tinggi. Sistem peningkatan cas didapati mengurangkan hasil kerugian oleh kecekapan isipadu di bukaan dan separuh masa suntikan. Dengan penambah cas, separuh suntikan terus memberi prestsi yang lebih baik untuk kelajuan 2000 ppm ke 4000 ppm berbanding suntikan di awal masa. Dimana sutikan awal dengan penambah tekanan akan memberi prestasi yang lebih

pada kelajuan 4000 ppm ke 5000 ppm berbanding dengan separa awal suntikan dimana ia mencukupi untuk persediaan campuran gas.

TABLE OF CONTENTS

LIST OF TABLES

LIST OF FIGURES

ABBREVIATIONS

ABDC	After Bottom Dead Center
AFR	Air Fuel Ratio
ATDC	After Top Dead Center
BMEP	Brake Mean Effective Pressure
BP	Boost Pressure
BSFC	Brake Specific Fuel Consumption
BTDC	Before Top Dead Center
CA	Crank Angle
CH_4	Methane
CNG	Compressed Natural Gas
CO	Carbon Monoxide
COV	Coefficient of Variation
CVCC	Compound Vortex Controlled Combustion
DI	Direct Injection
ECU	Engine Control Unit
EGR	Exhaust Gas Recirculation
ERI	Engine Remote Interface
FMEP	Friction Mean Effective Pressure
FTIR	Fourier Transform Infrared
HC	Hydrocarbon
IANGV	International Association for Natural Gas Vehicle
IC	Internal Combustion
IT	Injection Timing
IMEP	Indicated Mean Effective Pressure
IVC	Intake Valve Closed
LNG	Liquefied Natural Gas
LPG	Liquefied Petroleum Gas
MBT	Maximum Brake Torque
N/A	Naturally Aspirated
NAI	Narrow Angle Injector

N_2	Nitrogen
NO_X	Nitrogen Oxides
NO	Nitric Oxide
N_2O	Nitrous Oxide
NO_2	Nitrogen Dioxide
O_2	Oxygen
OBD	On Board Diagnosis
RCM	Rapid Compression Machine
RPM	Revolutions Per Minute
SI	Spark Ignition
TDC	Top Dead Center
UHC	Unburned Hydrocarbon
VRA	Vehicle Refueling Appliances
VVT	Variable Valve Timing
WAI	Wide Angle Injector
W/O	Without
WOT	Wide Open Throttle

CHAPTER 1

INTRODUCTION

1.1. Background

Nowadays, with the increasing demand of engine power output, fuel economy and severe emissions standard, supercharging technology has been widely used in truck and small industry engines [1, 2]. Supercharging will introduce air into an engine cylinder at a density greater than ambient. This allows a proportional increase in the fuel that can be burned and hence raises the potential power output.

The history of supercharging the internal combustion engine reaches back to Gottlieb Daimler and Rudolf Diesel themselves [3]. Supercharging the high-speed gasoline engine is as old as the engine itself. Gottlieb Daimler had supercharged his first engines, as his patent DRP 34926 obtained in 1885 as shown in Figure 1.1.

Supercharging found its first series application in aircraft engines, especially to increase high-altitude performance. In the years from 1920 to 1940, turbo compressors were continuously improved, in aerodynamics as well as in the circumferential speed of the impellers. From about 1920, automotive supercharged engines for racing, and also for the short-term power increase of sport and luxury vehicles, were equipped with mechanically powered and engageable displacement compressors. In most cases they were one or two-stage Roots blowers as shown in Figure1.2.

Exhaust gas turbocharged gasoline engines were first introduced into the U.S. market around 1960. For the supercharging of gasoline engines, the big break-through towards large-scale series production, with the exception of use in airplanes, only happened recently [3].

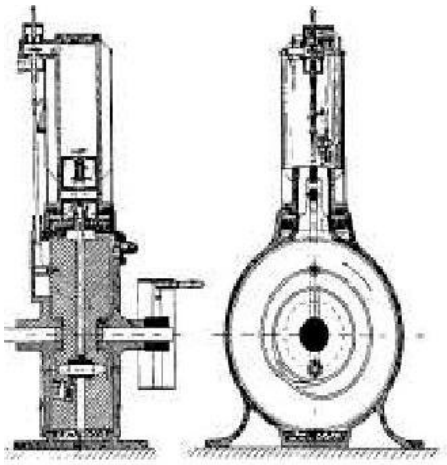

Figure 1-1

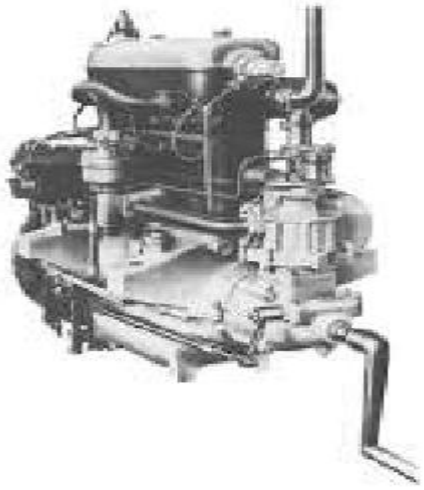

Figure 1-2

Figure 1-1 Patent drp 34926 from 1885 for the high-speed gasoline engine, by Gottlieb Daimler [3].

Figure 1-2 40/60 hp Passenger Car Compressor Engine with Roots Blower from 1921, by Daimler [3].

Rudolf Diesel also got involved with supercharging very early, as his patent DRP95680 demonstrates. With his layout, Diesel achieved a power increase of 30%. However, since he was primarily concerned about the efficiency of his engine and it dramatically deteriorated due to a totally incorrect size of the intake valve and the downstream plenum, he stopped these tests. This type of supercharging was, with correct dimensioning of the component, very successfully used 30 years later in marine diesel engine by Werkspoor [3].

The development of exhaust gas turbocharging is closely connected with the name and patents of the Swiss engineer Alfred Buechi [3]. As early as 1905, in patent DRP 204630, he described a turbocompound diesel engine although not meaningful in proposed form. But it took until 1925 for the first exhaust gas turbocharged diesel engines to be introduced into the market, in the form of engines for two passenger ships and one stationary diesel engine. In both cases, the exhaust gas turbochargers were still located beside the engine. All chargers were designed by Buechi.

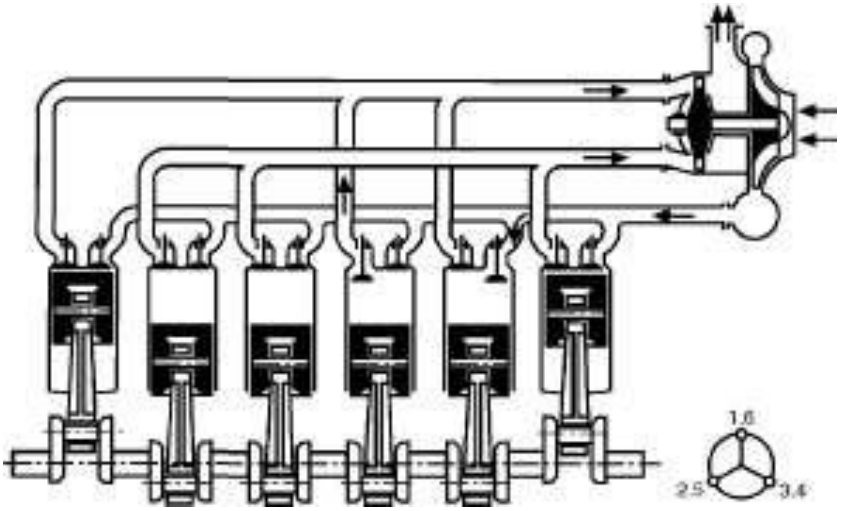

Figure 1-3 Buechi's Patent from 1925 for Pressure-Wave or Pulse Turbocharging via Flow Division [3].

The ever increasingly stringent emission requirements for internal combustion engines all around the world have presented serious challenges for researchers, designers, and manufacturers and operators to overcome. In order to solve the energy security and environmental problems, automotive industry has come out with systems that reduce fuel consumption and thus exhaust emissions. Technological developments such as direct injection (DI), variable valve timing (VVT), supercharging system, and exhaust gas recirculation (EGR) are proven to exhibit the ability to reduce fuel consumption and the emission levels to a low limit.

Attention has also been drawn to alternative fuels, including mainly common gaseous fuels such as liquefied petroleum gas (LPG), compressed natural gas (CNG) and H_2 [5]. Natural gas has emerged as the most promising energy source capable of matching both issues in the short and medium term. In fact natural gas combustion produces the fuels together with negligible amounts of suspended particles and photochemical smog promoters [1, 5]. Natural gas is the most widely used gaseous fuels considered a potential alternative to traditional liquid fuel mainly due to its relatively abundant resources and desirable combustion properties [4]. Because of its superior knock resisting ability, the interest to supercharge natural gas engines is increased nowadays. Over the past decades, air pollution has become increasingly a

serious concern worldwide mainly due to the ever increasing usage of vehicles, especially within urban areas. Correspondingly there is increasing interest to reduce the exhaust emissions of the regulated pollutants such as HC, CO and NO_X from internal combustion engines and for this a few possible approaches have been proposed, including application of low carbon fuels such as CH_4 [4,5].

However, the operation of vehicles on natural gas is not without disadvantages. The use of natural gas can lead to a significant reduction in maximum power production and torque at fully open throttle operation [1, 4 and 11]. This is due mainly to the displacement of some of the air by natural gas and loss of evaporation cooling associated with liquid fuels [4] that results in reduction of volumetric efficiency. In addition, natural gas has slower combustion in naturally aspirated engines which affects the performance of the engine [12]. Further, natural gas engine conversion from gasoline fueled engine requires some modifications, which includes valve trains, ignition system, storage and fuelling system [10,24].

Gaseous fuel like methane is clean-burning fuels, which in favorable conditions give a soot-free combustion and less harmful exhaust components than conventional liquid hydrocarbon fuels. However, to achieve low overall exhaust emissions, advanced engine technologies and control systems have to be applied. Thus, in addition to DI, the application of supercharging could recover the volumetric efficiency loss directly [13]. Internal combustion engine research is expected to focus on improving the fuel economy, reducing and finally eliminating exhaust emission while increasing the power density through either enhancing the design of the engine or boosting the intake mixture pressure through supercharging system [4, 13].

The power available from a given engine is limited by the amount of fuel that can be combusted efficiently within the cylinders. This fuel consumption rate in turn is limited by the amount of air which can be introduced into the cylinders during each engine cycle. Thus, the power available from a given engine can be increased by increasing the density of engine intake air prior to its introduction into the engine cylinders. One method of achieving this increased inlet air density is supercharging.

By mechanically increasing the volume of air that enters the engine, forced induction in effect increases atmospheric pressure giving the air more push as it enters the cylinder. The engine can breathe at a better volumetric efficiency compared to naturally aspirated engine depending on how much boost is built in to the system. As boost pressure is raised it is obvious that the maximum cylinder pressure achieved during combustion will also rise, generating high stress in many mechanical component so it is useful to obtain an idea of what level of boost pressure is involved [2].

1.2. Problem Statement

Natural gas has been largely unexploited in the transportation sector, mainly owing to the fuels gaseous state, which either significantly reduces engine power output or limits the vehicle operating range. This is due to the lower energy density of the stored fuel and the displacement of some of the air by natural gas which result in reduction of volumetric efficiency. The decrease in volumetric efficiency results in significant decrease in torque and power, when compared with the same engine using gasoline or diesel. It is found that natural gas vehicle gives 10% lower power output compared to equivalent gasoline-fuelled vehicles [8-11].

Because of slower combustion of natural gas [8, 20] in naturally aspirated CNG engines, there is a fall in brake power compared to those running with liquid fuels such as gasoline or diesel. The maximum efficiency of a spark-ignited gas engine is some 10-15% lowers compared to a good diesel engine [14]. A qualified estimate is that the energy consumption of a heavy-duty vehicle will, in most applications, increase 20-35% when switching from diesel to natural gas [14]. With direct injection of gaseous fuel there is a problem of reduction in volumetric efficiency when injecting the fuel at early and partial direct injection. This is because some of the air will be displaced by the gaseous fuel as the inlet valve is open during these injection timings. A supercharging system has been proposed to solve this problem.

Today, the primary goal to use supercharging for heavy-duty applications is still to raise the power to weight ratio, but it is more and more used as a help to optimize the engine to obtain lower emissions in order to manage future emission legislations while maintaining or even improving fuel efficiency [15,16].

1.3. Objective

The objective of this research is to assess the engine performance improvement attainable through supercharging and to define the best control strategies for this in terms of fuel consumption, exhaust emission, and optimal value of boost pressure. Furthermore, to study effect of supercharging on engine combustion parameters such as in-cylinder pressure, heat release, and mass fraction burned at different operating engine speeds. In addition, to determine experimentally the effect of supercharging on combustion process including the length of combustion duration and combustion stages. This research also studies the exhaust emission characteristics of a supercharged S.I.DI engine operated on compressed natural gas engine over a wide range of engine speeds and injection timings.

1.4. Scope of the Work

This research is basically focused on the effect of small boost pressure on CNG direct injection spark ignition engine. Supercharging pressure is optimized on injection parameters such as injection timing, injection pressure and injection spray angle on the range of operating engine speeds from 2000 to 5000 rpm. Previous researchs on injection parameters showed that injection timing has significant effect on engine performance. Thus, this thesis is focusing on optimizing of supercharging pressure at different injection timings while injection spray angle and injection pressure are kept constant. To assess the maximum performance of supercharging engine experiments were conducted at full load wide open throttle and stoichiometric air/fuel ratio conditions.

1.5. Thesis Organization

This thesis includes six chapters. Basically introduction, literature review, theoretical background, methodology, results and analysis, and conclusions and recommendations are included. Experimental work is done to meet the objective of the research.

Chapter 1 Describes the background of the research and the development of supercharging system to enhance the engine performance of spark ignition engine. Under chapter one the problem statement and the objective of the research is discussed. In addition the scope of the research is also explained under this chapter.

Chapter 2 Describes the literature survey to get more knowledge on what have been done before. Literature on fueling system technologies for spark ignition engine, development of natural gas as a fuel and supercharging the spark ignition engine are discussed in this section. In addition technology of injection system and emissions of CNG engine are stated in details.

Chapter 3 Here the theoretical background of an engine and its working cycles and theory on how to calculate the performance of an engine are discussed briefly. Combustion process characterization and models to calculate heat release and mass fraction burned are explained briefly.

Chapter 4 Methodology used to fulfill the objective of this research and parameters being researched are explained in detail. Discussion on equipment setup, its characteristics and measurement capabilities is given. Setup used for supercharging system is shown and discussion on how to conduct the experiment has been clarified in order to handle the problem of this research.

Chapter 5 This chapter comprises the experimental results and discussions. Engine performance parameters for supercharging system at partial and port injection timing are explained in detail. Indicated and brake torque and power are analyzed from the experiment. Other combustion parameters like brake mean effective pressure, brake specific fuel consumption and indicated mean effective pressure are analyzed from

experimental data. Combustion process is shown at partial and port injection timing for both supercharging and non supercharging system at operating engine speeds. Heat release and mass fraction burned are analyzed in detail for both boost and naturally aspirated engine at partial direct injection and port injection timing. Finally Emissions of CNG DI engine for both supercharging and non supercharging system at partial and port injection timings are analyzed based on experimental data's.

Chapter 6 Conclusion based on the result output are addressed with recommendation on the future proposed work for further study.

CHAPTER 2

LITERATURE SURVEY

2.1 Development of IC Engines Fuelled by Natural Gas

Currently because of the increasing number of automotive vehicles and high usage of liquid fuels, researchers are motivated to have alternative fuels that give the same performance as the traditional liquid fuels such as gasoline and diesel. Alternative fuels that are still being researched are natural gas, hydrogen, propane, and alcohol [5, 17].

Natural gas engine has been implemented as fuel vehicle since 1920s. Significant development of natural gas was seen during the oil shocks in 1974 and 1979. The performance of an engine running on natural gas depends on the sophistication of the engine, and whether the engine is dedicated for natural gas or not. Normally power loss of some 10% due to displacement of air can be expected when switching from gasoline to natural gas in light-duty vehicles [8-11]. In most cases there is power enough for satisfactory performance even when running on natural gas.

Natural gas has emerged as the most promising energy source capable of matching both issues in the short and medium term, thanks to its intrinsic environmental friendly features and to the favorable geopolitical distribution reservoirs. In fact, natural gas combustion produces the lowest green house gas emission among fossil fuels together with negligible amounts of suspended particles and photochemical smog promoters [15].

There are numerous benefits which originate from the simple chemical structure of methane, the main constituent of natural gas. The most important feature is that emissions from natural gas fuelled vehicles are less noxious than the exhaust emissions from gasoline and diesel vehicles. P.B.Sharma et.al [18] investigated experimentally the emissions and fuel consumption from CNG and Gasoline fueled SI engine powered vehicles. The results showed that exhaust emissions of CO and NO_X were significantly less with CNG as compared to gasoline. And because of higher

H/C ratio CNG combustion produces 25% less carbon dioxide than gasoline or, diesel considering the same engine efficiency [19].

Recently in automotive industry the application of compressed natural gas in spark ignition engines is more prevalent than before. Because of the higher octane number of the natural gas the compression ratio of S.I. engines can be increased, which increases the total combustion efficiency [4, 12]. Corresponding to the power result by natural gas as an output of the engine, natural gas has lower power output compared to gasoline [8-11]. Lower power output produced by natural gas is due to lower energy content of natural gas [9, 21, and 22], displacement of the air and longer combustion duration [23]. But natural gas has lower fuel consumption which considered as economic value of natural gas usage as fuel [18].

Most heavy-duty gas engines are diesel engines converted to spark-ignition Otto cycle engines. Low engine efficiency and low power output are a problem for natural gas engine. In normal service, natural gas engines can consume 25-35% more energy than their diesel counterparts [14]. In order to overcome the efficiency deficit, engine manufacturers are working towards lean-burn combustion, higher specific power output and some special supercharging and fuel injection systems [29, 33]. New engine technologies and electronics like variable valve timing, skip-fire etc. can help to enhance the performance of gas engines. Applying of two-stage turbocharging systems or mechanical chargers can fulfill the higher charging requirement [4, 30-32]. An increase in the S.I. engine compression ratio in comparison to the standard engines for naturally aspirated engine requires an increase in durability of all engine elements. Natural gas vehicle statistics is shown in Table 2-1 and Table 2-2 shows the principal effects of typical conversion from gasoline to compressed natural gas engine.

Table 2-1 Natural Gas Vehicle Statistics [7]

Position	Country	Number of Vehicles	Refueling Stations	Last Updated
1	Argentina	1,459,236	1,400	5-Dec-06
2	Brazil	1,357,239	1410	7-Mar-06
3	Pakistan	1,300,000	1230	7-Apr-06
4	Italy	410,000	558	6-Dec-06
5	India	334,658	321	Apr- 06
20	Malaysia	19,000	46	6-Dec-06
	TOTALS	6,080,582	10,068	

Table 2-2 Principal Effects of Typical Conversion from Gasoline to CNG [21]

CHANGES-CONVERSION FROM GASOLINE TO CNG	EFFCT	SCALE
Change in fuel	Loss of power	8%-15%
Lower energy of fuel	Loss of range	40% or more
Increase in fuel storage volume	Loss in available space	significant
Increase in storage weight	Loss of acceleration	noticeable
Improvement due to methane fueling	Improved emissions	significant
Fuel cost	Saving on fuel cost	30% or more
Saving on engine maintenance	Cleaner oil or longer life	noticeable

2.2 Development of Fuel Injection System

Fuel delivery system has been investigated over the years and developed to recent technology. The development of fuel delivery started from conventional carburetor system to a recent direct injection system. The pressure drop in a carburetor impairs the volumetric efficiency of an engine and reduces its power output [34]. The

problems of balancing multiple carburetors and obtaining even distribution in the inlet manifold can also be avoided with fuel injection. Engines using carburetors as fuel delivery system require modification for use of CNG. Studies showed power losses of about 13-30% for carbureted engines using CNG compared to gasoline [35].Early injection systems were mechanical and complex two dimensional cams have now been superseded by electronic systems. After carburetor the development of electronic fuel injection systems are as follows.

- Single point fuel injection(SPI)
- Multi point fuel injection(MPI)
- Direct injection

The single point fuel injection system is a cheaper alternative to multi-point fuel injection; it can lead to about a 10 percent lower power output than a multi-point injection system [34]. CNG engines with single point injection system would have 13.8% lower IMEP at rated speeds in comparison with the gasoline. CNG due to its gaseous state has very small effect on cooling the intake charge, therefore the inlet temperature is higher and thus reduced volumetric efficiency [36].

Multi-point injection has the potential for a higher power output, since the manifold can be designed for optimum air flow that includes some induction tuning features [37]. The fueling level is controlled by the fuel supply pressure, and the duration of the injection pulses. As with carburetors, the single-point injection system leads to fuel transport delays in the inlet manifold. In multi-point injection system the fuel flow rate through an injector is controlled by the differential pressure across the injector. In the case of a single-point injection system, the injector sprays fuel into a region at atmospheric pressure, so a constant gauge pressure is maintained by the fuel pressure regulator [34]. In contrast, the fuel injectors for a multi-point injection system inject into the reduced pressure of the inlet manifold. Thus, to make the fuel flow rate a function only of injection duration, the fuel pressure regulator senses the inlet manifold pressure, so as to maintain a constant differential pressure across the injector.

MPI systems use more sophisticated system compared to SPI system, since the ECU monitors and controls the injection parameters, such as injection timing, injection duration and the amount of fuel required by each cylinder [34, 38]. Engines employing MPI for CNG have a 3% to 5% better performance as compared to SPI-CNG systems, and have 10.4% lower IMEP values for rated speeds compared to MPI-gasoline [36]. Although fuel transport delays are reduced with multi-point injection systems they are not eliminated, and multi-point fuel injection systems can also be subject to other complications during load increase transient. Best mixture preparation and most uniform fuel distribution can be achieved with current sophisticated direct injection system. Here direct injection system is used and the development of this system will be discussed in detail in the following section.

2.2.1 Development of Direct Injection CNG Engine

Mixture of air and fuel is an important parameter to ensure good and stable combustion. So far fuel delivery system has been investigated over the past years from conventional carburetor system to a sophisticated direct-injection system. The fuel delivery systems include carburetor, single point injection (throttle body fuel injection), multi port injection (MPI) and the recent technology called direct injection (DI) system as mentioned in the above section. Here development of direct injection (DI) system will be discussed in detail.

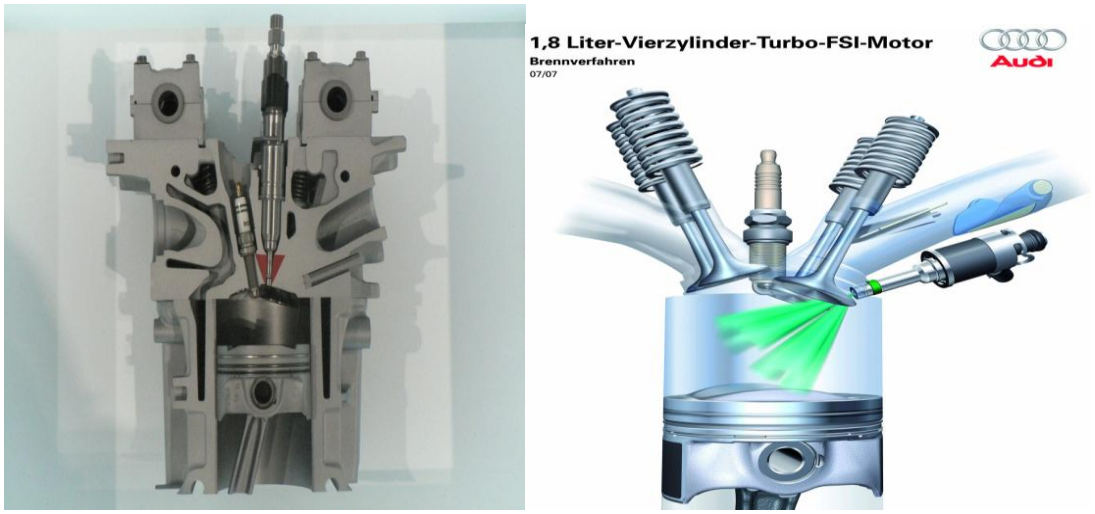

Figure 2-1 Direct Injection Systems [Source: www.bmw.com]

A typical spark ignition direct injection (SI-DI) engine consists of high pressure fuel pump, injector and ECU, where ECU function is to control the amount of fuel injected and injection parameters such as injection pressure and injection timing.

It is well known that the rate of combustion in SI engines is strongly influenced by turbulence and charge motion [39-42]. Because natural gas contains many hydrocarbons with varying concentration of the individual species the heat value of the fuel is not constant. It also influences the ignition process depending on lower ignition temperature of the fuel and energy induced by secondary circuit of the ignition coil. The future gas engines will be equipped with high pressure direct injection systems. Like the gasoline direct injected engine the gas engine operates mainly in two modes: a homogenous charge for full loads and a stratified charge for part loads. Injection of the gas fuel for full load takes place during the induction stroke after opening of inlet valves and this operation does not require so high injection pressure. For part load the fuel is injected during the compression stroke forming a bigger concentration of fuel near spark plug located in the central axis of the cylinder head. The timing of injection should correlate with the piston position BTDC and engine speed in order to enable the adequate stoichiometric mixture near the spark plug during the ignition. This mode requires higher injection pressure than in the first one [39].

The full load engine performance of DI-CNG, MPI-CNG and DI-Gasoline have been investigated. The engine torque of DI-CNG was higher than that of MPI-CNG because direct injection recovers the decrease of charging efficiency of MPI-CNG. It is considered that the larger fuel flow rate of DI-CNG injector and the improved combustion with suitable piston cavity shapes to improve mixture homogeneity and engine torque of DI-CNG at all engine speed [11, 39].

Jongwoo, K., et al [39] conducted some experiment on concept of direct-injection of CNG as a means for improving combustion, emissions and performance relative to manifold injection engines. Their result revealed that direct injection of CNG increases the volumetric efficiency of the engine and allows enhanced in-cylinder flow motion and charge stratification at the time of ignition, which results in faster

flame propagation and reduced cycle to cycle variations. They also concluded that increasing injection pressure leads to a slightly decrease in the jet cone angle and increase in the jet penetration. Furthermore, the experiment also revealed that direct injection of CNG offers advantages in terms of power output, extension of lean limit, and UHC emission levels. For example, they showed the IMEP for the late and early direct-injection strategies is higher by between 9% and 15% than that for manifold injection; this is mainly due to the increased volumetric efficiency achieved through direct injection of CNG into the cylinder [45, 46].

Direct gas injection leads to much better control of charge stratification while at the same time allowing homogeneous stoichiometric or lean mixtures to be formed by simply injecting the gas early during the induction stroke and by varying the fuel quantity to correspond to different air/fuel mixtures. This flexibility of electronically controlling the timing and quantity of gas injection offers the potential for reducing the exhaust emissions while maintaining high power output with much better fuel economy than conventional port-injected engines [44, 45]. However, CNG-DI engine tend to produce relatively higher levels of NO_x emission due to higher combustion temperature [43]. However, when considering the enormous interest in direct-injection engines and the possible advantages of direct gas injection, it is only a matter of time until advanced high pressure fuel injection systems become available that operate efficiently with short response times and with injection quantities appropriate for a wide range of engine sizes. Regulating injection parameters such as injection timing, injection pressure and spray angle of injector to control the mixture preparation is hoped to reduce emissions and it could increase the power output of the engine.

There are two types of mixture preparation method, homogenous charge and stratified charge [47-49].

2.2.1.1 Homogenous Charge Operation

Homogeneous charge can be achieved when fuel and oxidizer are well mixed before the start of combustion. By injecting fuel early in direct injection engine homogeneous charge is resulted. This is due to enough time available for the fuel and

the air to mix extensively and to be homogenous mixture. Different research has been done on effect of homogenous charge operation on direct injection engine. With direct injection homogenous systems it was shown that there is advantages in terms of emission and performance [50-53]. For instance, homogenous charge operations on gasoline are reported to produce lower emissions at stoichiometric conditions because of efficient three way catalysts operation at stoichiometric conditions. Homogenous charge operation on CNG are also reported and shown there is better emission and performance at stoichiometric conditions.

Zuohua Huang.et.al [49] investigated experimentally the effect of homogenous operation on CNG direct injection engine. They stated that combustion efficiency of homogenous mixture of CNG direct injection is higher than that of stratified at stoichiometric condition while lean operation has shown better combustion efficiency for stratified charge operation. Combustion efficiency for the homogenous mixture decreases greatly with leaner mixtures, which is probably due to the thicker quenching layer near the wall [52]. Homogenous charge operation of CNG direct injection has lower methane emissions and due to its higher combustion efficiency it resulted in higher NOx emission compared to stratified charge operation [52, 53]. With direct injection it has also been shown that fuel consumption has the possibility to reduce [50]. Injection parameters influence on the turbulence intensity is confirmed experimentally that the mixing process is mainly influenced by injection parameters at lower engine speeds [54]. Injection parameters such as injection timing [56-61], injection pressure [39, 43, 45, 47, and 62] and type of injectors [48, 62, and 63] have been proven to be important parameters that affect the combustion, emissions and performance of direct injection engines.

2.2.1.2 Stratified Charge Operation

Stratified charge is the mixture condition where a rich mixture is near the spark plug and lean in the rest of the cylinder before combustion takes place. This reduces fuel consumption significantly compared to homogenous charge operation. This condition is achieved by injecting the fuel relatively late and near the end of compression

stroke. The stratification of the charge depends on the location of the injector and the angles of injection nozzles. The primary use towards the development of stratified technology was fuel economy and engine emissions. Stratification is found to have better performance for lean mixture than stoichiometric. The operation range of lean-burn SI engines is limited by the level of cyclic variability in early development of the flame [64, 65]. Charge stratification in lean burn engines is an important parameter for combustion control [65]. With direct injection system controllable charge stratification can make the combustion better and thus injection parameters found to have a significant influence on charge stratification. Study showed that CNG-DI stratified combustion system has overall shorter combustion compared to homogenous system. This is due to the decrease in the time interval between injection timing and ignition timing. In addition, combustion efficiency can be maintained more than 0.92 in the range of equivalent ratio from 0.1 to 0.9 [49].

Stratified combustion strategy has been investigated using rapid compression machine with compression ratio of 10. Improved results for the emissions of CO and CO_2 are reported, while higher heat release rate and high peak pressure lead to high levels of NOx compared to homogenous charge operation [52]. Another study was done by Seunghwan, C., et.al [63] used a cylindrical constant volume combustion bomb to investigate the combustion characteristics and to analyze the simplified heat balance of stratified charge methane-air mixture by using 2-stage injection. The result showed that, the stratification is able to improve the combustion rates, such as maximum combustion pressure, the rate of heat release and the cumulative heat release, for the more lean condition than of near-stoichiometric conditions. Stratification for near-stoichiometric mixture does not have much advantage over lean mixtures.

2.3 Supercharging the Spark Ignition (S.I) Natural Gas Engine

The term supercharging refers to increasing the air (or mixture) density by increasing its pressure prior to entering the engine cylinder. Natural gas (NG) is the most widely used gaseous fuels and it is considered as a potential attractive to traditional liquid fuels. However, its direct application in conventional S.I. engine can lead to a significant reduction in brake power and torque at fully open throttle [66-70].

The superior properties of natural gas as a fuel have been highlighted in many papers over the years. Such fuel is widely used in S.I. engines and is considered a potential alternative to traditional liquid fuels. However, the use of natural gas in conventional S.I. engines can lead up to 11.3-22% reduction in maximum power production and torque at fully open throttle [4]. Over the years, the following factors have been demonstrated to cause power loss with gaseous fuels applications:

- The displacement of some of the air by natural gas. It occupies about 10% of the intake mixture for stoichiometric operation. This is much higher than the value of about 1.6% for gasoline operation.
- The loss in the volumetric efficiency due to the lack of the evaporation cooling normally associated with the application of liquid fuels. The intake mixture is cooled when the air mixes with liquid gasoline due to its evaporation. This would increase the volumetric efficiency by about 3%. For natural gas, such a cooling effect is absent.
- Slightly lowered heating value of the stoichiometric mixture of natural gas with air compared to that of gasoline.
- Slower flame propagation rates.

Over the years, a few approaches have been developed to recover the power loss associated with the application of natural gas. These included increasing the compression ratio, modifying combustion chamber shape to enhance the flame propagation, modifying the intake system such as varying timing and valve lift to increase volumetric efficiency, accurately mixing the fuel-air at the stoichiometric and optimizing the spark timing. However, the effects of these approaches on power production are generally quite limited. For example, for the conditions considered, the brake power increased only by about 2% when the compression ratio is increased from 10 to 13.6 [4].

Nowadays, supercharging technology has been widely used due to an increase demand of engine power output, fuel economy and severe emissions standards [71-75]. Recently, there is an increasing interest in supercharging S.I. engines operating

on natural gas mainly to its superior knock resisting properties in comparison to traditional liquid fuels. The usage of supercharging system in S.I. liquid fuels engines is restricted by the onset of knock [13]. The onset of knock also remains one of the main problems limiting the boost pressure ratio of supercharging S.I. natural gas engines. There are various approaches that have been developed and demonstrated over the past decades to effectively suppress the onset of knock. From those, suppressing the onset of knock through retarding the spark timing, decreasing the effective compression ratio, leaning the operating mixture or diluting the intake mixture through the application of cooled EGR are widely applied and recommended [51].

Moreover, application of after-cooler, which widely used in turbocharged SI engine, cools the compressed air before entry to the engine and reduces the tendency to knock when applied to supercharging S.I. engines [13]. When there is no after-cooler the performance gains from supercharging could be reduced by about 50 percent. Without after-cooler, the supercharger outlet temperature would be limited to about 80^{o}C (compared to 120^{o}c with inter-cooler), and after the inter-cooler the temperature might be about 50^{o}C [34]. The inter-cooler thus increases the output of the engine in two ways. Firstly, the higher pressure ratio and the cooler air temperature both increase the air density. Secondly, the lower temperature allows a higher boost pressure or compression ratio for knock-free operation with a given quality fuel. An inter-cooler system though offer option to boost engine performance while suppressing the onset of knock and tends to make supercharging spark ignition engine systems increasingly complex.

Traditionally, the supercharging S.I. engine is either operated under lean operation or on stoichiometric mixture combined with cooled EGR. Both approaches could operate S.I engine under optimized spark timing without involving the onset of knock. The former is highlighted by the high power production efficiency and its capability to meet the emissions requirements without adopting an after-treatment device. The latter acknowledged in achieving high brake power and best conversion efficiency of the three-way catalyst.

CHAPTER 3
THEORETICAL BACKGROUND

3. Thermodynamic Principles

3.1 Introduction

This chapter provides criteria by which to judge the performance of internal combustion engines. Most important are thermodynamic cycles based on ideal gases undergoing ideal processes. However, internal combustion engine follow a mechanical cycle, not a thermodynamic cycle. Air standard cycles have limitations as air and, in particular, air/fuel mixtures do not behave as ideal gases. Despite this, the simple air standard cycles are very useful, as they indicate trends. Most important is the trend that as compression ratio increases cycle efficiency should also increase. Working fluid does not go through a cycle in a thermodynamics sense but the mechanism does go through the system. During the operation, there is a continuous change in pressure and volume of the working fluid, there is an energy exchange between the system and surroundings, the processes are not ideal and the physical properties and composition of working fluids change.

Therefore, a quantitative analysis of the working cycle or the actual thermodynamic cycle using air and liquid or gaseous fuel is quite complicated and the best approach appears to be a series of approximations starting with air standard cycles and modifying them step by step for the various points of differences so that the analysis is complete. Air standard cycle will be corrected for characteristics of fuel-air mixtures and fuel-air cycle will be modified to account for losses in the cycle and finally Actual cycle will be achieved.

3.2 Ideal Air Standard Cycles

The following assumptions are made in the analysis of air standard cycles:

1. The working fluid is air, it behaves like an ideal gas, undergoes no chemical change during the cycle,
2. The compression and expansion processes are isentropic,
3. The combustion process is replaced by a heat transfer process, the addition

and rejection of heat energy takes place reversibly and can take place instantaneously,

4. Kinetic and potential energy of the working fluid is negligible and the operation of the engine is frictionless.
5. The cycle is a closed one.

Whether an internal combustion engine operates on a two-stroke or four-stroke cycle and whether it uses spark ignition or compression ignition, it follows a mechanical cycle not a thermodynamic cycle. However, the thermal efficiency of such an engine is assessed by comparison with the thermal efficiency of air standard cycle, because of the similarity between the engine indicator diagram and the state diagram of the corresponding hypothetical cycle. The engine indicator diagram is the record of pressure against cylinder volume, recorded from an actual engine. Pressure/volume diagrams are very useful, as the enclosed area equates to the work in the cycle.

3.2.1 The Ideal Air standard Otto Cycle (Constant Volume Cycle)

It is theoretical or ideal cycle for SI engines. It consists of four internally reversible processes: reversible adiabatic compression instantaneous heat addition at constant volume, isentropic expansion and instantaneous heat rejection at constant volume. The pressure-volume diagram of the cycle is shown in Figure 3-1. In air standard cycle analysis, it is assumed that the power required to push out the exhaust gases is equal to the power required to suck-in the charge and therefore, the net work done by the cycle is not affected by the suction and exhaust processes and the working fluid acts as a closed system.

The Otto cycle is usually used as a basis of comparison for spark ignition and high speed compression ignition engines. The cycle consists of four non-flow processes, as shown in Figure 3-1. The compression and expansion processes are assumed to be adiabatic (no heat transfer) and reversible, and thus isentropic. The processes are as follows:

1-2 isentropic compression of air through a volume ratio V1/V2, the compression

ratio r_v

2-3 addition of heat Q_{23} at constant volume

3-4 isentropic expansion of air to the original volume

4-1 rejection of heat Q_{41} at constant volume to complete the cycle.

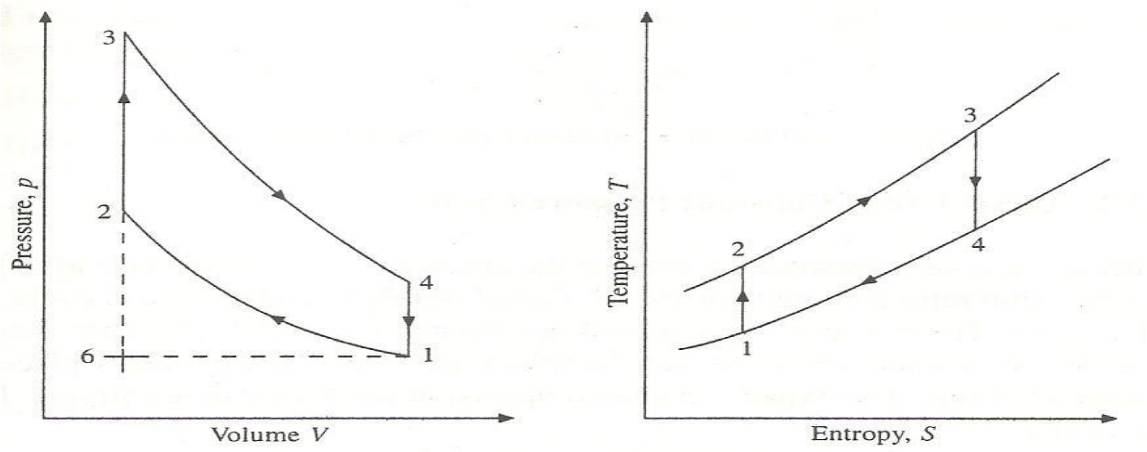

Figure 3-1 Air Standard Otto Cycle [94].

3.3 Fuel-Air Cycles

If we consider the physical properties of the actual working fluid before and after combustion, we can obtain a better analysis of the actual working cycles. A fuel-air cycle is defined in which:

1. The working fluid is a mixture of air and fuel or the products of combustion of fuel-air mixtures and it remains in chemical equilibrium before and after combustion.
2. The heat energy is generated within the system and is equal to the product of mass of fuel supplied and its lower heating value.
3. The specific heat c_p and c_v increase with temperature
4. The A/F ratio is varied during the operation of the engine and that will change the relative amounts of CO_2, CO and H_2O etc.
5. The working fluid undergoes idealized thermodynamics processes.
6. The combustion is complete and there is no heat interaction between the engine

cylinder and surroundings.

7. The intake and exhaust process are ideal, the velocities of the working fluid during the two processes are negligible.

Fuel-air cycles are usually assumed to begin at the start of compression process. The pressure and temperature at the start of compression process and the air-fuel ratio and the residual gas fraction are chosen to represent condition prevailing in a real cycle.

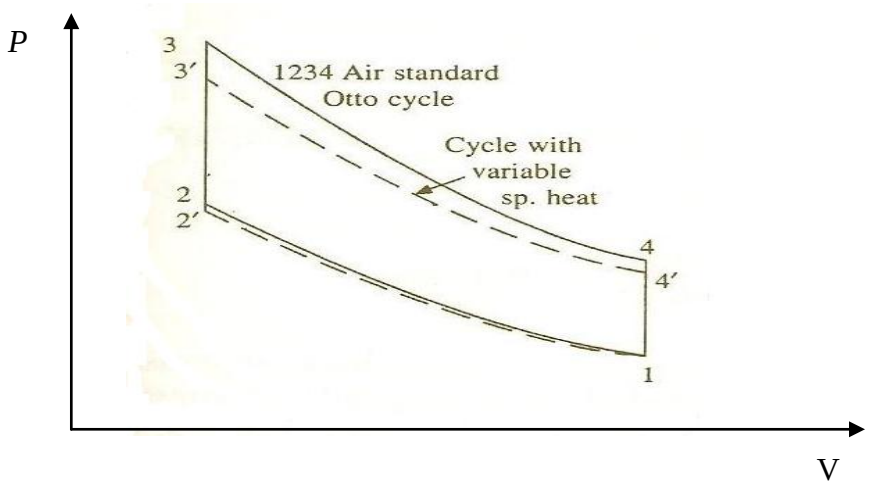

Figure 3-2 P-V Diagram for Constant Volume Fuel-Air Cycle [94].

3.4 Actual Cycles

The thermal efficiency and the power output of actual cycles is less than those calculated on the basis of fuel-air cycles. The differences are due to the following factors:

i. Variation of air-fuel ratio-the air fuel ratio varies from cycle to cycle and therefore the composition of the working fluid varies.
ii. Valve operation-valves do not open or close instantaneously.
iii. Finite combustion time-a finite time is required for the combustion of fuel inside the combustion chamber and the combustion is never complete, i.e. the exhaust gases always contain combustible elements.
iv. Dissociation-the available energy and the output decreases because the products of combustion dissociate into other compounds at very high

temperatures and this process is an endothermic one.

v. Heat transfer –there is always a heat transfer between the working fluid and the surroundings through cylinder walls because of high temperature inside the cylinder.

vi. Suction and exhaust processes-they are never ideal and there is a loss of work on the expansion stroke due to early opening of exhaust valve.

vii. Fluid friction-it is appreciable during suction and exhaust processes and also near the end of compression and during the first part of the expansion process.

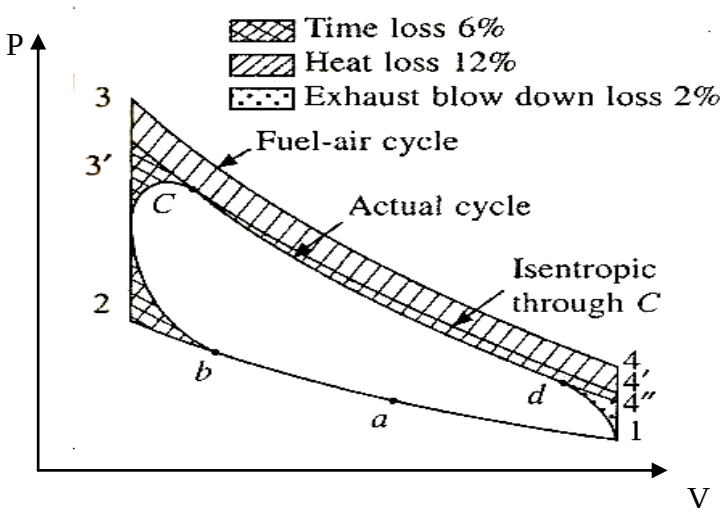

Figure 3-3 Constant Volume Real Cycle and its Equivalent Fuel-Air Cycle [94].

i. Time loss

Combustion does not occur instantly. The spark ignites the mixtures in the immediate vicinity of the spark plug, and a flame from proceeds spherically outward from here. It is necessary to start the combustion (ignition) considerably before TDC, and even so the combustion will go on substantially past TDC. The greatest efficiency usually is obtained when the point of ignition and the point at which combustion is complete are roughly symmetric with respect to TDC. The area to the left of ignition start and end of combustion shows time loss. It is a loss due to the finite time that the flame front takes to cross the combustion chamber. This unextracted work that accounts to 30% is due to time loss.

ii. Heat loss

As the intake charge is compressed on the compression stroke its temperature is raising, and it is consequently losing heat to the cylinder walls. This is not too serious, because its temperature and is not very high. After the combustion, however, its temperature is considerable, and as it expands on the power stroke, its temperature dropping, it is losing considerable heat to the walls of the cylinder and combustion chamber, resulting in a substantial reduction in its temperature and pressure at the end of the stroke. The difference of this and the ideal cycle represents work that cannot be extracted. The difference between the real and ideal cycle on the compression stroke is work that need not be done on the gas, but this is much smaller than the difference on the power stroke and is usually negligible. The area above 3-4 is heat loss. This resulted in around 60% of the total loss.

iii. Exhaust blow down loss

As the piston approaches BDC on the power stroke the exhaust valve is opened. Immediately the pressure begins to drop as the exhaust rushes out of the cylinder. This difference in pressure between the real and ideal cycle at this point in the cycle represents unavailable work, and is called exhaust blow down loss. This accounts 10% of the total loss.

There are other losses, usually quite negligible at full throttle but definitely not at partial throttle. In partial throttle during the intake stroke the pressure drops below atmospheric as the piston descends, drawing air into the cylinder, and it is above atmospheric on the exhaust stroke in order to expel the gases from the cylinder. This loop, consisting of exhaust and intake, represents work that must be done on the gases, and hence is lost energy. These losses are called pumping losses.

There are two other losses, both of which are small under normal circumstances; the first loss is because not all the fuel that is brought into the cylinder is burned, for several reasons. Finally we have leakage losses. The piston rings, and sometimes the valves, do not perfectly and consequently the cylinder pressures do not rise as high as they should, representing a small loss. For the engine in good condition this is

negligible, but for an old, worn engine, blow by, the loss past rings, results in a significant loss of power.

3.5 Basic Calculations of Performance Parameters for Internal Combustion Engines

This section will define engine performance parameters like torque, power, brake mean effective pressure and brake specific fuel consumption. The additional parameters relate to the work output per unit swept volume in terms of a mean effective pressure, and the effectiveness of the induction and exhaust strokes. There are two types of mean effective pressure, based on either the work done by the gas on the piston or the work available as output from the engine.

a) Indicated mean effective pressure (Imep)

The area enclosed on the p-v trace or indicator diagram from an engine is the indicated work (W_i) done by the gas on the piston. The imep is a measure of the indicated work output per unit swept volume, in a form independent of the size and number of cylinders in the engine and engine speed.

The imep is defined as:

$$\text{IMEP} = \frac{W_c}{V_d} \tag{3.1}$$

Where W_c = indicated work (Nm)

V_d = cylinder volume displacement (swept volume) (m^3)

In a four stroke cycle the negative work occurring during the induction and exhaust strokes is termed as pumping loss, and has to be subtracted from the positive indicated work of the other two strokes for aspirated engine. For supercharging system positive work occurring during the induction and exhaust so that it is going to be added to positive indicator work.

.

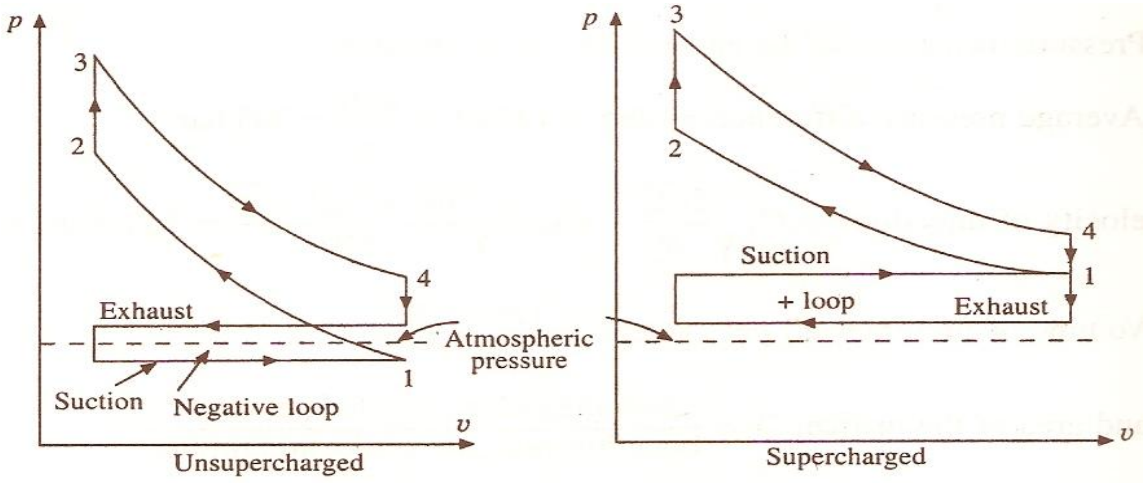

Figure 3-4 P-V diagrams for supercharged and unsupercharged SI Engine [94].

The pumping work can also be used to define a pumping mean effective pressure (pmep), Pp

$$Pp=\frac{W_p}{V_d} \tag{3.2}$$

Where W_p = pumping work (Nm)

V_d = swept volume (m^3)

Sometimes, the imep does not always incorporate the pumping work, and this leads to the use of the term gross imep and net imep:

Gross imep = net imep + pmep

Unfortunately, the imep does not always mean net imep, so it is necessary to check the context to ensure that it is not a gross imep. The imep bears no relation to the peak pressure in an engine, but is a characteristic of engine type. The imep in naturally aspirated four-stroke spark ignition engines will be smaller than the imep of a similar supercharging engine. This is mainly because the supercharging engine has greater air density at the start of compression, so more fuel can be burnt. The pumping work transfer will be to the cylinder gases if the pressure during the intake stroke is less

than the pressure during the exhaust stroke. This is the situation with naturally aspirated engines. The pumping work transfer will be from the cylinder gases to the piston if the exhaust stroke pressure is lower than the intake pressure, which in normally the case with highly loaded supercharging engines.

b) Brake mean effective pressure (Bmep)

The work output of an engine, as measured by a brake or dynamometer, is more important than the indicated work output. This leads to a definition of bmep.

$$Bmep = \frac{\text{brake work output (Nm) per cylinder per mechanical cycle}}{\text{swept volume per cylinder } (\text{m}^3)} \qquad (3.3a)$$

Or in terms of the engine brake power as:

$$bmep = \frac{Pn}{V_s N} \qquad (3.3b)$$

bmep can also be expressed in terms of engine torque:

$$bmep = \frac{2\pi.2T}{V_s} \qquad (3.3c)$$

Where: P = Power (kW)

T = engine torque (Nm)

V_s = cylinder Swept Volume (m^3)

n = number of crank revolutions for each power stroke

N = Revolutions per minute (RPM)

c) Frictional mean effective pressure, fmep

The difference between indicated work and brake work is accounted for by friction, and work done in driving essential items such as the lubricating oil pump. Frictional mean effective pressure, fmep, is the difference between the imep and the bmep:

$$\text{fmep} = \text{imep} - \text{bmep}$$

d) Brake torque

Engine torque is a measure of an engine's ability to do work. Engine torque represents control measuring parameter for any engine test. Engine torque is normally measured with a dynamometer. The bracing force acting via a lever arm is measured via strain gage load cells or via precision balances. Depending on the intended use and engine-power class of the supercharged engine to be tested various test benches may be utilized. The most common passive systems are eddy current brakes and hydraulic brakes. The engine is clamped on a test bed and the shaft is connected to the dynamometer rotor. Figure 3-5 illustrates the operating principle of a dynamometer. The rotor is coupled to a stator which is supported in low friction bearings. The stator is balanced with the rotor stationary.

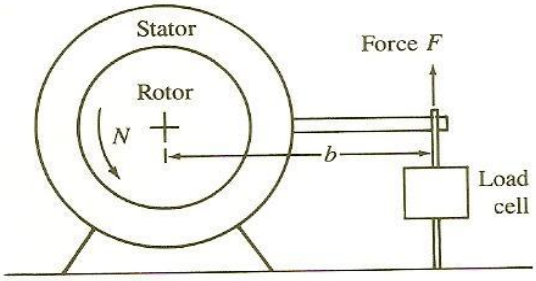

Figure 3-5 Schematic Principle of Operation of Dynamometer [51].

The torque exerted on the stator with the rotor turning is measured by balancing the stator with weights, springs, or pneumatic means.
The torque exerted by the engine is T:

$$T=F*b \tag{3.4}$$

e) Power (kW)

Power is defined as the rate at which work is done. The power P delivered by the engine and absorbed by the dynamometer is the product of torque and angular speed:

$$P = 2\pi NT \tag{3.5a}$$

Where N is the crankshaft speed. In SI units:

$$P(kW) = 2\pi N(rev/s)T(N.m)* 10^{-3} \tag{3.5b}$$

The value of engine power measured as described above is called brake power P_b. This power is the usable power delivered by the engine to the load.

f) Brake specific fuel consumption (bsfc)

Brake specific fuel consumption measures how efficiently an engine is using the fuel supplied to produce work. It is the ratio of fuel consumption to the power production and hence shows the fuel flow rate per unit power output. Thus low values of bsfc are desirable. The equation for specific fuel consumption is given as follows:

$$bsfc(g/kWh) = \frac{Fr(g/h)}{P(kW)} \tag{3.6}$$

Where: Fr =Fuel flow rate

P = brake power

g) Indicated work per cycle

Pressure data for the gas in the cylinder over the operating cycle of the engine can be used to calculate the work transfer from the gas to the piston. The indicated work per cycle, W_i, is obtained by integrating around P-V curve to obtain area enclosed on the diagram.

$$W_i = \text{imep} * V_S \tag{3.7}$$

Where: imep = indicate mean effective pressure

V_S = stroke volume

The power per cylinder, P_i is related to the indicated work per cycle by

$$P_i = \frac{W_i N}{n} \tag{3.8}$$

Where: n= number of crank revolutions for each power stroke

N= Revolutions per minute (RPM)

This power is the indicated power that is the rate of work transfer from the gas within the cylinder to the piston. It differs from the brake power by the power absorbed in overcoming engine friction, driving engine accessories, and (in case of gross indicated power) the pumping power. Indicated quantities are used primarily to identify the impact of the compression, combustion, and expansion processes on engine performance, etc. The gross indicated output is, therefore, the most appropriate definition. It represents the sum of the useful work available at the shaft and the work required to overcome all the engine losses. Brake and indicated are used to describe other parameters such as mean effective pressure, specific fuel, and specific emissions.

h) Air/Fuel Ratio

Engine operating conditions can be known after measuring air mass flow rate and fuel mass flow rate. Air/ Fuel ration thus defined as the ratio of air mass flow rate to fuel mass flow rate. Stoichiometric mixture defines when there is enough oxygen in the air to combine completely with the fuel in the combustion chamber and when the mixture is chemically balanced**.** When mixtures having AFR less than that of stoichiometric are called rich mixtures while mixture having excess air that is when the AFR greater than stoichiometric is called lean mixture. Each fuel has a specific air-fuel ratio for complete combustion. Stoichiometric, chemically balanced, AFR for natural gas can be calculated as follows:

When CH4 is burnt with air the reaction is

$$CH_4 + 2(O_2 + 3.76N_2) \Leftrightarrow CO_2 + 2H_2O + 2(3.76N_2) \tag{3.9}$$

Hence, AFR stoichiometric is:

$$AFR_{stoich} = {2*(1+3.76)*28.9}\Big/{(1*12)+(4*1)} = 17.19 \tag{3.10}$$

i) Volumetric efficiency

Volumetric is a measure of the effectiveness of the induction and exhaust process. The intake system comprises of air filters, intake runner, intake port and intake valves. The amount of air that enters the combustion chamber depends on the efficiency of the whole intake systems Volumetric efficiency can be defined as the ratio of mass of air inhaled per cylinder per cycle to mass of air to occupy swept volume per cylinder at ambient P and T. And it is shown as follows:

$$\eta_v = \frac{2\left(\dot{m}_a + \dot{m}_f\right)}{\rho_o V_d N} \tag{3.11}$$

Where: η_V = Volumetric Efficiency

$\dot{m}_a$ = Actual air mass that enters the combustion chamber (g)

$\dot{m}_f$ = Actual fuel mass (g)

V_d = Displacement volume (m^3)

ρ_o = Air intake density (kg/m^3)

In the equation, $\dot{m}_f$ is the mass of fuel inducted. For a direct injection system with injection after intake valve closed (IVC), $\dot{m}_f = 0$.

j) Indicated thermal efficiency

Indicated thermal efficiency is defined as the indicated power per cycle over the energy available from the fuel per cycle. It is given by the equation as follows:

$$\eta_{i\,ndicated} = \frac{P_i}{\dot{m}_f \cdot q_{HV}} \tag{3.12}$$

Where P_i is the indicated power

$\dot{m}_f$ is the fuel mass flow rate

q_{HV} is the lower heating value of the fuel.

3.6) Analysis of Combustion

Combustion is a chemical reaction in which certain elements of the fuel combine with oxygen liberating heat energy and causing an increase in temperature of the gases. The theory of combustion is a very complex subject and has been a topic of intensive research for many years. The fundamental difference between spark ignition (SI) and compression ignition (CI) engine lies in the type of combustion that occurs inside the cylinder. Here combustion process in the spark ignition engine will be studied. Combustion in spark ignition can occur either normally where with ignition from spark and the flame front propagating steadily throughout the mixture or it might be occur abnormally. Abnormal combustion can take several forms, principally pre-ignition and self ignition. Pre-ignition is when the fuel is ignited by a hot spot, such as the exhaust valve or incandescent carbon combustion deposits. Whereas self ignition is when the pressure and temperature of air/fuel mixture are such that the remaining unburnt gas ignites spontaneously. Normal and abnormal combustion will be discussed in the following section.

3.6.1 Normal Combustion

Normal combustion process in spark ignition engine is usually divided in to four distinct phases. These are: (1) spark ignition; (2) early flame development; (3) flame propagation; and (4) flame termination.

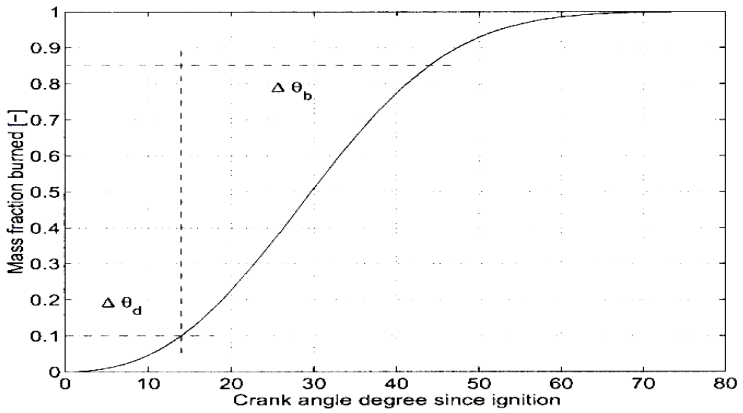

Figure 3-6 Combustion Stages in Spark Ignition Engine [51].

The first stage of combustion is the initiation of combustion by the spark ignition. When the piston approaches the end of the compression stroke, a spark is discharged between the sparking plug electrodes. The spark leaves a small nucleus of flame that propagates into the unburnt gas. Until the nucleus is of the same order of size as the turbulence scale, the flame propagation cannot be enhanced by the turbulence. This early burn period comprises the initial laminar combustion, and the transition to fully turbulent combustion, and the transition to fully turbulent combustion, and is sometimes referred to as the delay period. Ignition delay period, the time needed from the time of ignition to the start of combustion, can be determined by calculating mass fraction burned (mfb) from the pressure history, but there are uncertainties with this calculation.

The second phase of combustion is the early flame development or early burn period. The early flame development encompass the laminar burning phase and the transition to fully turbulent combustion. This period depends on the temperature, pressure and composition of the fuel/air mixture, in other words, when the laminar flame speed is highest. This stage also depends on the vicinity of the spark plug. Higher fuel availability around the spark can increase the combustion rate at this initial stage. The initial combustion duration is usually defined as the 0-10% mass fraction burn duration.

The third stage of combustion is rapid flame propagation or main combustion period. The main combustion period is dominated by turbulent combustion, and can be defined as the 10-90% mass fraction burn duration. This stage is affected in the same way as the early flame burn period, and also by the turbulence. The end of third stage of combustion occurs shortly after the peak pressure. In practice, the maximum cylinder pressure usually occurs 5-20° after top dead center [103]. Having better combustion rate at this stage would result in higher pressure and thus better combustion.

The final stage of combustion is flame termination where the flame front is contacting more of the combustion chamber, with a reduced flame front area in contact with the

unburned mixture, the remaining unburned mixture in the combustion chamber being burnt more slowly. The cylinder pressure should also be falling, so unburned mixture will be leaving crevices, and some of the fuel previously absorbed into the oil films on the cylinder wall will be desorbed. This final stage of combustion is very slow, and will not be complete by the time the exhaust valve opens. Even if there is some further oxidation in the exhaust port, combustion will still not be complete, as evidenced by the emissions of unburnt hydrocarbons. End of combustion occurs at the final 90-100 percent mass fraction burn duration.

Since combustion takes a finite time, the mixture is ignited before top dead center, at the end of the compression stroke. This means that there is a pressure rise associated with combustion before the end of the compression stroke, and an increase in the compression or negative work. Advancing the ignition timing causes both the pressure to rise before top dead center and also the compression work to increase. In addition the higher pressure at top dead center leads to higher pressures during the expansion stroke, and to an increase in the expansion or positive work. Obviously there is a trade-off between these two effects, and this leads to optimum ignition timing. Definition of each phase of combustion process can be analyzed using pressure reading from the engine data.

3.6.1.1 Analysis of Cylinder Pressure Data

Cylinder pressure is the main parameter that helps researchers to study the combustion process inside the cylinder. In cylinder pressure and temperature measurements are a common tool for analyzing combustion process in IC engines. Other observations such as flame propagation, flame visualization, in-cylinder flow behavior, and mixture distribution can also be used but needs complicated measurement systems and devices. It has been shown that cylinder volume change and combustion have the largest effect on the cylinder pressure changes with crank angle. This effect of volume change on the pressure can readily be accounted for and thus combustion rate information can be obtained from accurate pressure data provided models. Cylinder pressure is usually measured with piezoelectric pressure transducer. With this system cylinder pressure versus crank angle or volume can be

obtained that helps us to calculate heat release rate, mass fraction burned, indicate mean effective pressure and thus to study indicated performance parameters, burn rate and combustion efficiency using different combustion models. Pressure difference between the motoring cycle and the working cycle is called as the pressure build up due to combustion process. This pressure build up is used to calculate the heat release rate. The next section will show in detail how to determine the above combustion parameters.

3.6.1.2 Indicated Mean Effective Pressure (IMEP)

Indicated effective pressure is the basic parameter that helps to determine indicated engine performance parameters.

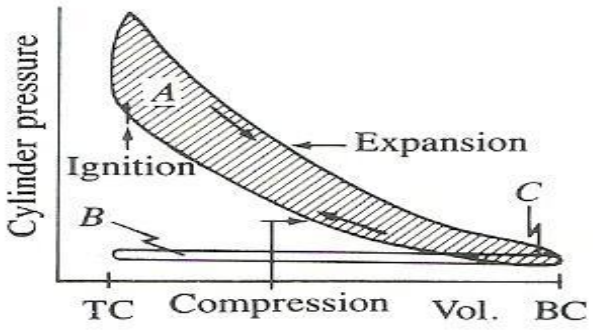

Figure 3-7 P-V Diagram for a Four-Stroke Cycle Engine [51].

Pressure analysis has been explained in the thermodynamics principal section. Pressure is built during compression stroke and will increase drastically as a result of combustion process inside the cylinder. It then starts to drop during expansion stroke and when exhaust valve open takes place. The area inside the cycle is considered as IMEP. This pressure helps us to determine the indicated work transfer from the gas to the piston. This is obtained by integrating around the curve to obtain the area enclosed on the diagram as shown in Figure 3-7:

$$W_c = \oint p dV \tag{3.13}$$

`

With the addition of inlet and exhaust strokes for the four-stroke cycle, some

ambiguity is introduced as two definitions of indicated output are in common use. These will be defined as:

I. Gross indicated work per cycle, W_c, work delivered to the piston by compression and expansion stroke

II. Net indicated work per cycle, $W_{c,n}$, is the work delivered to the piston over the entire four-stroke cycle.

3.6.1.3 Cyclic Variations in Combustion

Due to pressure developed in the cylinder is related to the combustion process, substantial variations in the combustion process on a cycle-by-cycle basis exist. Various measures of cycle-by-cycle combustion variability are used. It can be defined in terms of variations in the cylinder pressure between different cycles. Here we will define cycle-by-cycle variation of IMEP that helps us to define combustion variability. Coefficient of variation of indicated mean effective pressure has been the basic parameter to measure cyclic variability. It is defined as the standard deviation of IMEP divided by the mean IMEP, and is usually expressed in percent:

$$IMEP_{avg} = \frac{1}{n}\sum_{i}^{n} IMEP_i \tag{3.14}$$

Standard deviation of IMEP defined as:

$$\sigma_{IMEP} = \sqrt{\frac{\sum_{i=1}^{n}\left(IMEP_{avg} - IMEP_i\right)}{n-1}} \tag{3.15}$$

Thus coefficient of variation of IMEP is:

$$COV_{IMEP} = \frac{\sigma_{IMEP}}{IMEP_{avg}} * 100 \tag{3.16}$$

Where, n is the number of samples.

Coefficient of variation of IMEP defines cyclic variability in indicated work per cycle, and it has been found that vehicle driveability problems usually result when COV of IMEP exceeds 10% [51]. Three factors have been found to influence COV are:

a) The variation in gas motion in the cylinder during the combustion,
b) Cycle-by-cycle variation in the amounts of fuel, air, and residual gas to a given cylinder each cycle
c) Variations in mixture composition within the cylinder each cycle-especially near the spark plug-due to variations in mixing air, fuel, recycled exhaust gas, and residual gas.

3.6.1.4 Heat Release Analysis

In order to study the combustion process heat release analysis has been the basic parameter to be analyzed. Heat release analyses compute how much heat would have to be added to the cylinder contents, in order to produce the observed pressure variations. During analyzing heat release of an engine, the in-cylinder pressure has always been an important experimental diagnostic in automotive research due to its direct relation to the combustion and work producing processes [103]. Early models of the internal combustion engine were based on the air standard cycles. To improve the modeling effort, the fuel-air cycle and subsequently single zone models were introduced. In the single zone the usually assumption implies that the product and reactants are fully mixed. For instance, the early work of Rassweiler and Withrow [97] and Apparent model correlated the pressure rise due to combustion in the cylinder with the fraction of the mass burned and enabled it to be directly determined from the pressure-time diagram. This model uses the pressure-time history of the engine to analyze heat release that includes the effect of heat transfer, crevice flows, and spark ignition. Krieger and Borman [105] presented a diagnostic thermodynamic model for a spark ignition engine that helps to calculate heat release. In their model, the combustion chamber was divided into two zones: burned and unburned zones. Here in two-zone model the cylinder contents are divided into zones, considering the properties and composition of each zone. Two-zone methods are more accurate

compare to single-zone analysis. The disadvantages of two-zone model are the unburned and the burned zone heat-transfer areas must both now be estimated, and a model for the composition of the gas flowing into the crevice region must be developed. Due to this complexity crevice models are usually omitted. Single-zone method has been widely used in on-line processing to calculate heat release rate from pressure reading. This method needs less computational time compared to two-zone methods. In this research single zone model of Rasseweiler and Apparent method are used to calculate heat release from the fuel. The advantage of such an approach is that the pressure changes can be related directly to the amount of fuel chemical energy released by combustion, while retaining the simplicity of treating the combustion chamber contents as a single zone. This approach is based on the first law of thermodynamics. The first law of thermodynamics to calculate heat released by combustion is given by:

$$dQ_{ch} = dU + dW + \sum_i h_i dm_i + dQ_{ht} \tag{3.17}$$

Where:

dU is the internal energy changes of the charge in the system

dQ_{ch} is the chemical energy released by the combustion

$\sum_i h_i dm_i$ is the enthalpy flux across the system boundary

dW is work done by the systems

dQ_{ht} is heat transfer to the chamber walls

There are some assumptions that have been taken when using single-zone model [51]. These includes the in-cylinder contents are uniform throughout the chamber, heat release is assumed to be uniform in the chamber and the gas mixture is assumed ideal gas. The work done is the piston work and can be calculated using $dW = pdV$. Assuming the ideal gas law, the change in sensible energy U is given by $mu(T)$, where T is the mean charge temperature and m is the mass within the system boundary. And substituting $du(T) = c_v dT$. Where c_v is the value of specific heat at constant volume. Thus dU can be written as follows:

$$dU = mc_v(T)dT + u(T)dm \tag{3.18}$$

Crevice effects can usually be modeled adequately by flow into and out of a single volume at the cylinder pressure, with the gas in the crevice at a substantially lower temperature. The leakage to the crankcase can usually be neglected. Then substituting equation (3.18) into above equation (3.17) and assuming $dm_i = dm_{cr} = -dm$, the equation becomes:

$$dQ_{ch} = mc_v dT + (h' - u)dm_{cr} + pdV + dQ_{ht} \tag{3.19}$$

From the equation of state, $pV=mRT$, it can be written as follows:

$$mdT = \frac{1}{R}(pdV + Vdp) - Tdm \tag{3.20}$$

Substitution of equation (3.20) into equation (3.19) gives:

$$dQ_{ch} = \left(\frac{c_v}{R}\right)Vdp + \left(\frac{c_v}{R} + 1\right)pdV + (h' - u + c_v T)dm_{cr} + dQ_{ht} \tag{3.21}$$

When the heat or energy term, dQ_{ch}, is combined with the heat transfer and crevice terms, the combination is termed as net heat release. Net heat release can be calculated by subtracting the amount of heat transferred from the cylinder to the wall, dQ_{ht}, from the amount of heat released from chemical energy of the fuel, dQ_{ch}. From ideal gas, the specific gas constant R can be given as $R = c_p - c_v$ and the specific heat ratio is defined as $\gamma = \frac{c_p}{c_v}$, thus substitution gives:

Specific heat value at constant volume,

$$c_v = \frac{R}{\gamma - 1} \tag{3.22}$$

And $$\frac{c_v}{R} = \frac{1}{\gamma - 1} \tag{3.23}$$

Substituting this equation into the above equation,

$$dQ_{ch} = \left(\frac{1}{\gamma - 1}\right) V dp + \left(\frac{1}{\gamma - 1}\right) p dV + \left(h' - u + c_v T\right) dm_{cr} + dQ_{ht} \tag{3.24}$$

The convective heat transfer rate to the combustion chamber walls can be calculated from the relation

$$\frac{dQ_{ht}}{dt} = A h_c \left(T - T_w\right) \tag{3.25}$$

Where A is the chamber surface area, T is the mean gas temperature, T_w is the mean wall temperature, and h_c is the heat-transfer coefficient (averaged over the chamber surface area). For crevice effect a sufficient accurate model for overall effect is to consider a single aggregate crevice volume when the gas is at the same pressure as the combustion chamber, but at different temperature. And assuming the crevice gas is at the wall temperature due to these crevice regions are narrow and inserting this crevice model in to equation, with $\gamma(T) = a + bT$, gives the gross heat release rate:

$$\frac{dQ_{ch}}{d\theta} = \left(\frac{1}{\gamma - 1}\right) V \frac{dp}{d\theta} + \left(\frac{\gamma}{\gamma - 1}\right) p \frac{dV}{d\theta} + V_{cr} \left[\frac{T'}{T_w} + \frac{T'}{T_w(\gamma - 1)} + \frac{1}{bT_w} \ln\left(\frac{\gamma - 1}{\gamma' - 1}\right)\right] \frac{dp}{d\theta} + \frac{dQ_{ht}}{d\theta} \tag{3.26}$$

For more elaboration of the above equation, Figure 3-8 shows heat release versus crank angle. The lowest curve that is symbolized as Q_n shows net heat release from the system. On this net heat release addition of the heat transfer and crevice effect models gives chemical energy release during the combustion process. The curve at the top of the figures shows total input energy which can be calculate by multiplying the mass of the fuel within the combustion chamber and its lower heating value. The difference between the final value of Q_{ch} and total input energy ($m_f Q_{LHV}$) shows the

combustion inefficiency which is a few percent of $m_f Q_{LHV}$. Inaccuracies in the cylinder pressure data and the heat-release calculations will contribute to this difference.

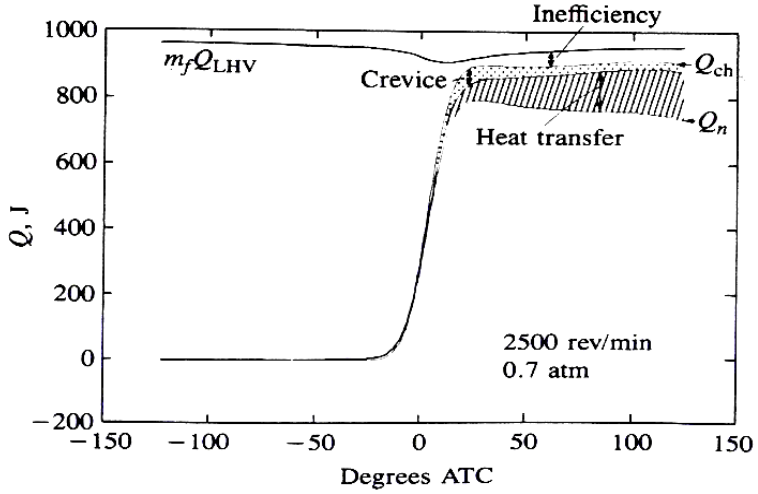

Figure 3-8 Heat Release Analysis Showing the Effects of Heat Transfer, Crevices, and Combustion Inefficiency [51].

From this basic equation of single-zone model there have been different models derived to calculate the amount of heat release from the combustion fuel. In this research Rassweiler-Withrow and Apparent models were used to calculate heat release and these will be explained in detail in the following section.

I. Rassweiler-Withrow Model

Rassweiler and Withrow [97] evaluated the polytropic index, k, to calculate mass fraction burned and heat release. Rassweiler-Withrow methods have high dependency on the accuracy of the polytropic index value. The polytropic index value for spark ignition engine is commonly in range of 1.25 to 1.35. So the determination of correct polytropic index value is very important before doing the cylinder pressure analysis. Polytropic index can be found using the cylinder pressure reading at the motoring cycle. The Rassweiler and Withrow method contains several assumptions. It is assumed that the referenced pressure rise due to combustion is proportional to the

mass fraction burned in each increment. There is no explicit allowance for heat transfer, dissociation, or change in composition of the gases; though to some extent an allowance is made, as the polytropic index is allowed to vary from the ratio of the gas specific heat capacities. Since the Rassweiler and Withrow method is simple to calculate, it is an appropriate and popular method when cycle-by-cycle variations in combustion are to be analyzed. This method assumes the pressure volume relation can be modeled as polytropic relation.

$$pV^n = \text{constant} \tag{3.27}$$

Where n is polytropic index and its value ranges from 1.25 to 1.35. These values give good fit to experimental data for both compression and expansion process. As mentioned Rassweiler-Withrow models have made some assumption on basic equation of (3.26). This includes no crevice effect taking into account and thus $\left(h'-u+c_vT\right)\frac{dm_{cr}}{d\theta}=0$. In addition heat transfer value is assumed zero, dQ_{ht}=0 and hence $dQ_{ch}=dQ$. Equation (3.26) will be written as follows:

$$dQ=\frac{1}{\gamma-1}Vdp+\frac{\gamma}{\gamma-1}pdV \tag{3.28}$$

Assuming there is no release of chemical energy during the compression phase prior to the combustion or during the expansion phase after the combustion, therefore $dQ=0$. The specific heat value can be assumed as constant value and represented as polytropic index, $\gamma=n$. This assumption gives to:

$$dp=\frac{\gamma p}{V}dV \tag{3.29}$$

When considering combustion, equation (3.27) can be rewritten as

$$dp=\frac{n-1}{V}dQ-\frac{np}{V}dV=dp_c+dp_v \tag{3.30}$$

Where dp_c is the pressure change due to combustion and dp_v is the pressure change due to volume changes. In Rassweiler-Withrow models, the actual pressure change $\Delta p=p_{j+1}-p_j$ during the interval $\Delta\theta=\theta_{j+1}-\theta_j$, is assumed to be made up of a pressure due to combustion Δp_c, and pressure rise due to volume change Δp_V.

$$\Delta p = \Delta p_c + \Delta p_v \tag{3.31}$$

Pressure changes due to volume of cylinder change during interval $\Delta\theta$ is given by polytropic relation, and can be written as follows:

$$\Delta p_v(j) = p_{j+1,v} - p_j = p_j\left(\left(\frac{V_j}{V_{j+1}}\right)^n - 1\right) \tag{3.32}$$

Applying $\Delta\theta = \theta_{j+1} - \theta_j$, using equations (3.31) and (3.32) yields to the pressure change due to combustion as:

$$\Delta p_c(j) = p_{j+1} - p_j\left(\frac{V_j}{V_{j+1}}\right)^n \tag{3.33}$$

The total heat released by the combustion can be approximated by

$$\frac{dQ}{d\theta} = \frac{V_{j+1/2}}{n-1}\Delta p_c(j) \tag{3.34}$$

Where the volume during the interval j is approximated with $V_{j+1/2}$ (the volume at the middle of the intervals).

II. Apparent Heat Release Models

Heat release model that is derived from the first law of thermodynamics was also proposed by Krieger and Borman [95]. It computes the net heat release in the cylinder. Like Rassweiler, Apparent heat release model also assumes there is no heat transfer and crevice effect. Hence this model, the apparent heat release dQ, can be shown as follows:

$$dQ = \frac{1}{\gamma - 1}Vdp + \frac{\gamma}{\gamma - 1}pdV \tag{3.35}$$

Compared to Rassweiler and Withrow method this method shows slightly shorter combustion duration. Both method calculates heat release with a small different in values. Both methods are preferable for combustion analysis because of the least computational time, and less parameter required to analyze the combustion in the engine [105].

3.6.1.5 Burn Rate Analysis

a) Rassweiler and Withrow Method

A burn rate analysis is usually applied to the combustion data from spark ignition engines to calculate the mass fraction burned (mfb). A widely used technique is the approach proposed by Rassweiler and Withrow. That states the pressure rise Δp after the start of combustion during a crank angle interval $\Delta\theta$ is assumed to be made of two parts: a pressure rise due to combustion (Δp_c) and a pressure change due to the volume change (Δp_V):

$$\Delta p = \Delta p_c + \Delta p_v \tag{3.36}$$

As the crank angle θ_j increments to its next value θ_{j+1} the volume changes from V_j to V_{J+1}, and the pressure changes from p_j to p_{j+1}. As mentioned before it is assumed that the pressure change due to the change in volume can be modeled by a polytropic process with an exponent n and thus pressure rise due to the combustion is given by:

$$\Delta p_c(j) = p_{j+1} - p_j\left(\frac{V_j}{V_{j+1}}\right)^n \tag{3.37}$$

The end of combustion occurs after N increments, and it is defined by the pressure rise due to combustion becomes zero. By assuming the pressure rise due to the combustion is proportional to the mass fraction burned then it can be written as:

$$x_b(j) = \frac{m_b(j)}{m_b(total)} = \frac{\sum_{i=0}^{j} \Delta p_c(i)}{\sum_{i=0}^{N} \Delta p_c(i)} \tag{3.38}$$

Where Δp_c is given in equation (3.37) and N is the total number of crank angle intervals. The summation of the pressure rise due to combustion, the denominator of the above equation, contains information about the completeness of combustion. By looking at the distribution of the pressure rise due to combustion, it is possible to set an upper bound for its value, and then to calculate a completeness of combustion. This generates S-curve as the graph of mass fraction burned. From this mass fraction burned, we can also determine combustion process like start of combustion, combustion duration, end of combustion and ignition delay.

b) Wiebe Function

The prevailing combustion model is the vibe function, which is often called Wiebe function. Wiebe function represents typical heat release and burn fraction curve for spark ignition engine. Heywood et.al [51] developed a cycle simulation model of the S.I. engine and used a Wiebe-type mathematical function to represent the fuel burning rate. Hong [1990] also used a Wiebe-type function to represent the fuel burning rate and examined single zone model. The ignition and combustion duration were determined through curve fitting. He claimed that the effects of choosing different combustion models, single-zone or two-zone models, on the development of the pressure-time diagram were small. Wiebe function often used to represent the mass fraction burned versus crank angle curve:

$$x_b = 1 - exp\left[a\left(\frac{\theta - \theta_0}{\Delta\theta}\right)^{m+1}\right] \tag{3.39}$$

Where:

θ is the crank angle, θ_0 is the start of combustion, $\Delta\theta$ is the total combustion duration ($x_b = 0$ to $x_b = 1$), and a and m are adjustable parameters. Varying a and m changes the shape of the curve significantly. Actually mass fraction burned curves have been fitted with $a = 5$ and $m = 2$. Further, the burn rate can be written in its differential form as:

$$\frac{dx_b(\theta)}{d\theta} = \frac{a(m+1)}{\Delta\theta}\left(\frac{\theta-\theta_0}{\Delta\theta}\right)^m exp\left[a\left(\frac{\theta-\theta_0}{\Delta\theta}\right)^{m+1}\right] \quad (3.40)$$

3.7 Combustion Efficiency

Combustion efficiency is the difference between available energy (fuel) and the final value of heat released by combustion. It is defined as

$$\eta_c = \frac{Q_{out}}{Q_{in}} = \frac{Q_{ch}}{m_f q_{HV}} \quad (3.41)$$

Where, Q_{ch} is the total heat released by combustion process, m_f is fuel mass, and q_{HV} is the specific heating value of fuel.

Finally, density of air coming into the engine can be calculated by using ideal gas law as follows:

$$\rho = \frac{p}{RT} \quad (3.42)$$

Where p is the absolute pressure; R is the gas constant; and T is the absolute temperature of the gas.

CHAPTER 4

METHODOLOGY

4.1 Experimental Engine and Techniques

In this section the experimental equipment setup with its components is shown and discussed briefly. Supercharging system is displayed together with the engine. Data taking of basic parameters of engine performance and combustion is illustrated. In addition, equipment for measuring engine output emissions is demonstrated. Further, this section shows engine set-up for naturally aspirated engine and test conditions are discussed here.

4.1.1 Engine Setup for Naturally Aspirated System

Here schematic diagram of engine set-up with supercharging system is shown in Figure 4-1.

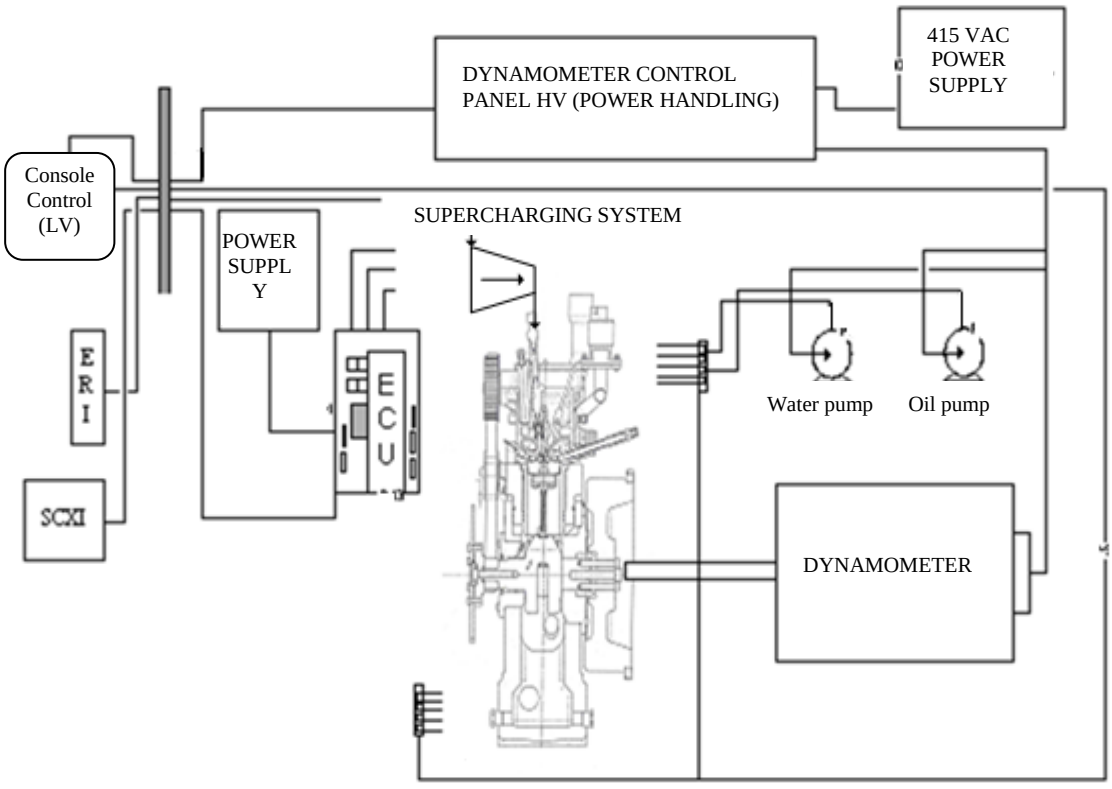

Figure 4-1 Schematic of test Set-up with Supercharging System

This engine is a four stroke single cylinder direct injection compressed natural gas spark ignition research engine with compression ratio of 14. Figure 4-2 shows photographic view of naturally aspirated engine. Experimental data's were also taken with naturally aspirated engine in order to compare with supercharging results.

Engine control parameters such as injection timing, ignition timing and air-fuel ratio are controlled by engine control unit (ECU) that is connected to ECU Remote Interface (ERI) installed in a personal computer. In addition, ignition timing is adjusted to achieve the maximum (MBT). The main specifications of the engine are given in Table 4-1.

Table 4-1 Engine Main Specifications

Engine Properties	
Displacement volume	399.25 cm^3
Cylinder Bore	76 mm
Cylinder Stroke	88 mm
Compression Ratio	14
Exhaust Valve Closed	ATDC 10°
Exhaust Valve Open	BBDC 45°
Inlet Valve Open	BTDC 12°
Inlet Valve Closed	ABDC 48°
Dynamometer	Direct Current with maximum reading of 50Nm
ECU	Orbital Inc

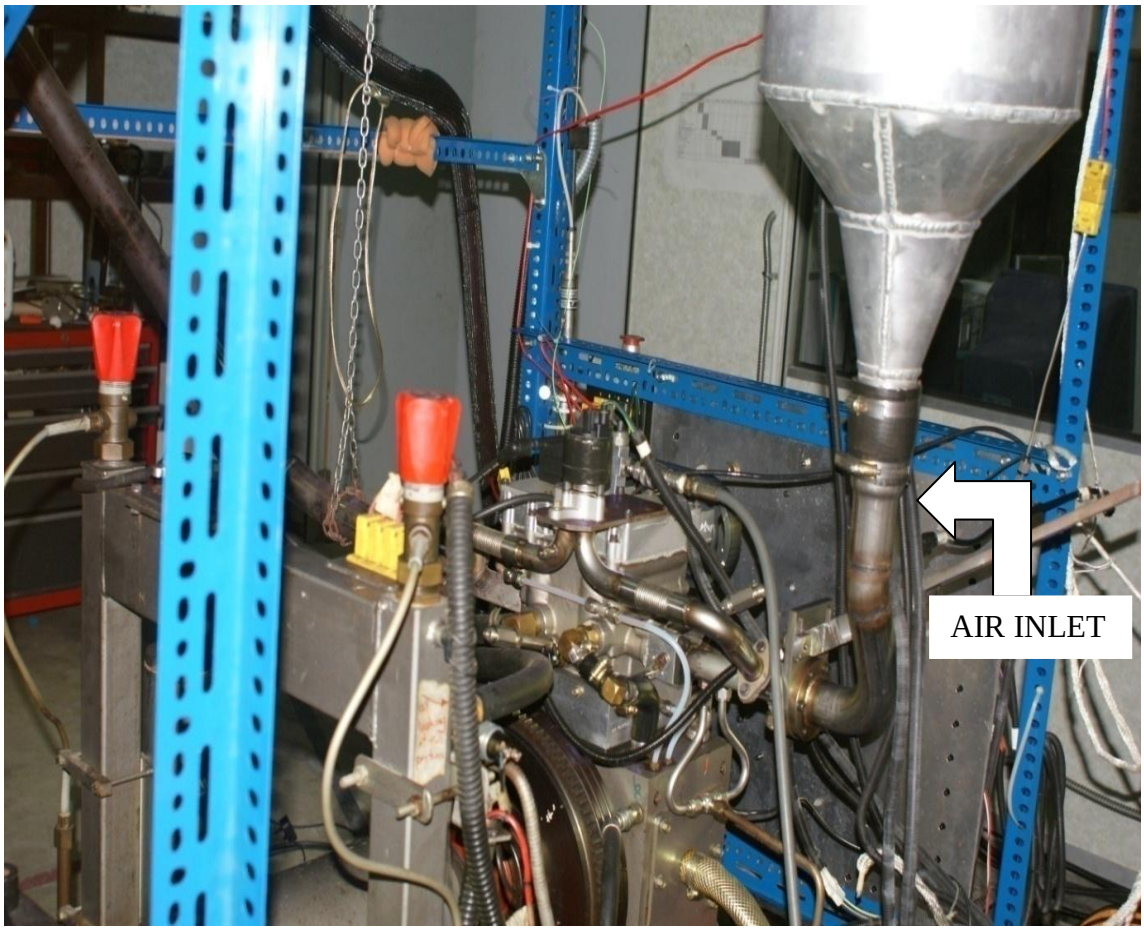

Figure 4-2 Photographic View of Naturally Aspirated Engine

4.1.2 Boost Pressure System

Detailed layout of Boost pressure system is shown in Figure 4-3. Boost pressure system is used to create boost pressure and this research investigates the effect of this boost pressure on engine performance, combustion and exhaust emissions of CNG-DI engine. For supercharging system centrifugal compressor has been set close to the engine. In order to get adjustable boost pressure, the compressor is controlled by DC motor by varying the motor speed using controller. The benefit of this arrangement is that we can vary boost pressure by varying motor speed for engine operating speeds ranging from 2000 rpm to 5000 rpm. Specification for compressor-motor assembly is shown in Table 4-2.

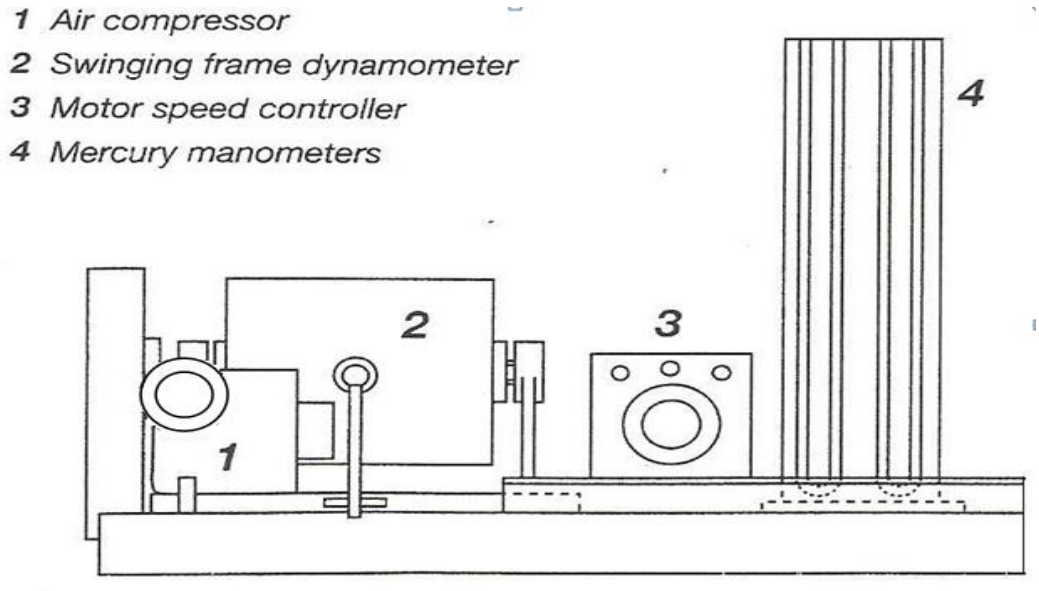

Figure 4-3 Detailed Layout of Boost Pressure System

Table 4-2 Specification for Compressor-Motor assembly

Type	four-stage centrifugal
Motor shaft speed	Variable from 0 to 2800 rpm (max)
Pulley ratio	4:1
Corresponding Blower speed	11200 rpm (max)
Output	0.3 kg/s and Pressure ration of 1.15 at 17,000 rpm
Impeller belt driven by a three phase 415 V/50HZ motor	Controlled by DC inverter
Inlet port bore	51mm

The distance between motor shaft center line and weight hanger (i.e. torque arm) is 0.342m. The input power (P_I) is given by $P_I=\omega T_r$. The power input to the compressor will be slightly less than the motor power owing to the mechanical losses in the belt drive. Power absorbed by the air can be assumed by $P_I= \dot{m}_a C_{Pair} \Delta T$.

Where C_{Pair} is the specific heat of air at constant pressure in kJ/kgk and is evaluated at the temperature of across the compressor from the following relation [106].

$$C_{Pair} = \frac{8.314}{28.97}(3.653 - 1.337 * 10^{-3}T + 3.294 * 10^{-6}T^2 - 1.913 * 10^{-9}T^3 + 2.763 * 10^{-13}T^4) \quad (4\text{-}1)$$

Thus power absorbed by the air can be calculated as follows:

$$P_I = (\dot{m}_a C_{Pair} T)_{outlet} - (\dot{m}_a C_{Pair} T)_{inlet}. \quad (4\text{-}2)$$

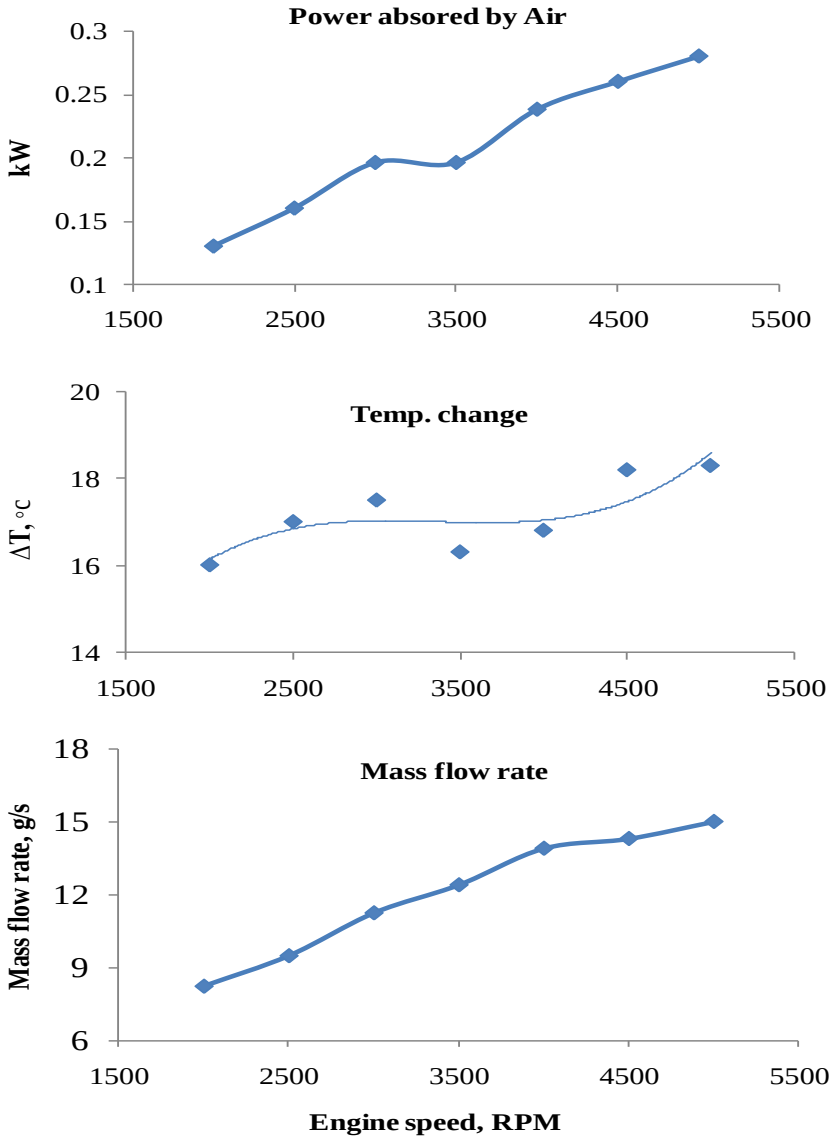

Figure 4-4 Characteristics of Compressor at 10 kPa Boost Pressure

Figure 4-4 above shows power absorbed by air, mass flow rate through compressor and temperature change between inlet and outlet of the compressor at operating engine speeds of 2000 to 5000 rpm for 10 kPa boost pressure. Engine set-up with supercharging system is shown in Figure 4-5 below.

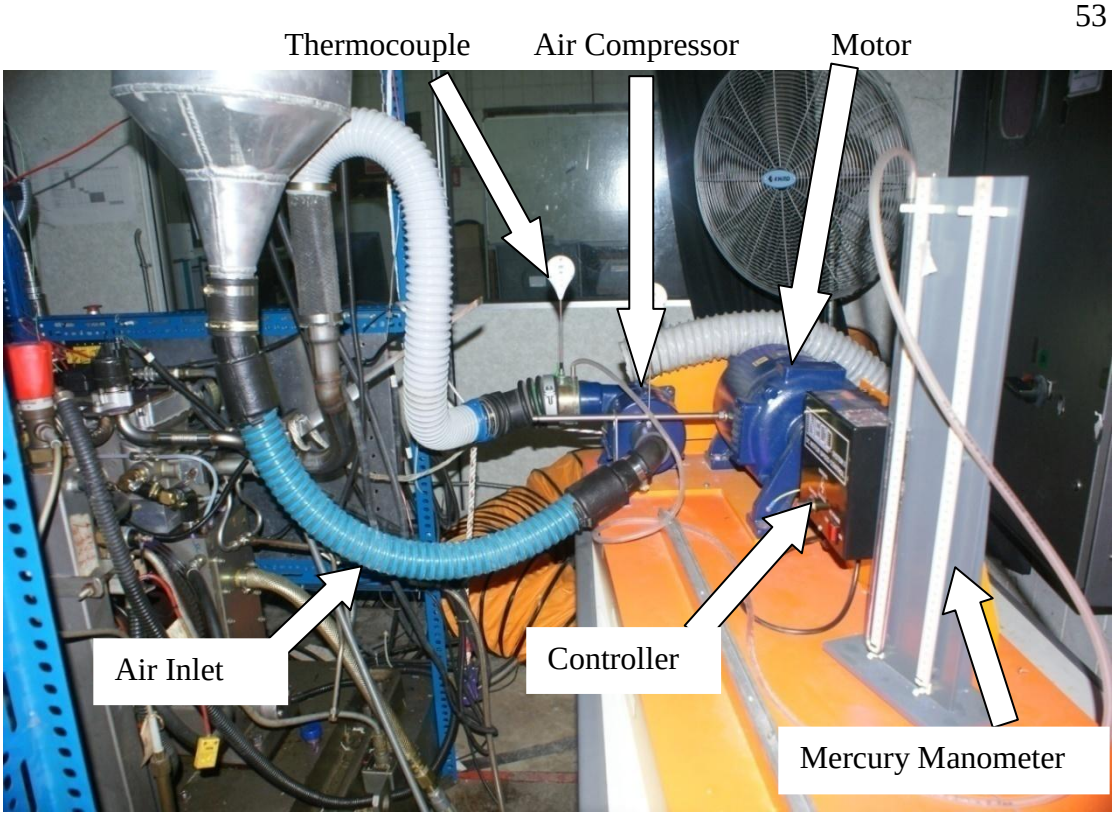

Figure 4-5 Photographic View of Engine with Supercharging System

4.1.3 Injector and Spark Plug Position

Figure 4-6 shows the geometry of the combustion chamber with injector and spark plug location. The injector is placed at the centre of the combustion chamber with the spark plug next to it with an offset of 6mm. Spark plug with a longer tip is used compared to the standard one to improve the combustion of CNG.

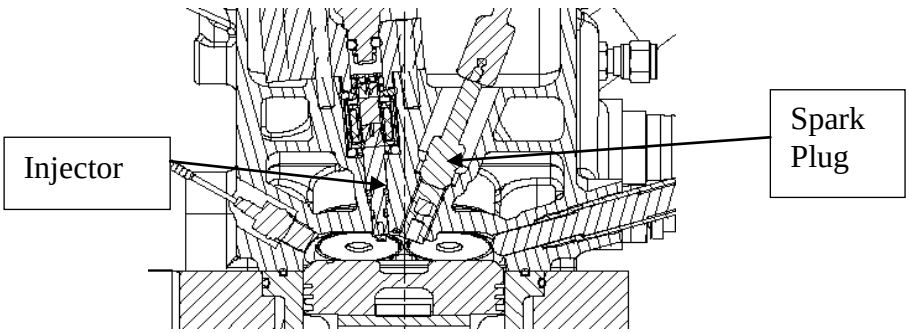

Figure 4-6 Injector and Spark Plug Position

Figure 4-7 illustrates the sectional view of the relative position of injector and the spark plug.

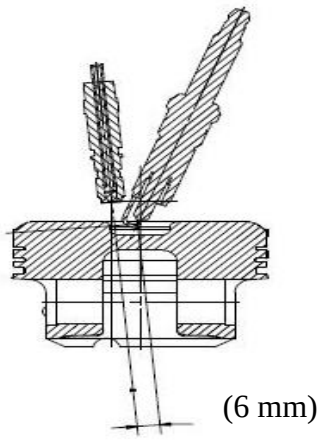

Figure 4-7 Relative Position of Injector and Spark Plug

4.1.4 Injectors

Quick and complete combustion is ensured by a well designed fuel injector. By atomizing the fuel into very fine droplets, it increases the surface area of the fuel droplets resulting in better mixing and subsequently combustion. Atomization is done by forcing the fuel through a small orifice under high pressure. Injector is the most influential component in direct-injection systems. Injector properties have a great influence on the mixing, charge stratification and combustion stability of the engine. Spray angle, penetration length, fuel delivery rate are known to be the critical characteristics of an injector.

Figure 4-8 shows the injector spray image at atmospheric condition for injector, WAI and NAI. Narrow angle injector (NAI) has a spray angle of 30 degree while wide angle injector (WAI) has 70 degree spray angle. The image is taken at 18 bars injection pressure at atmospheric conditions.

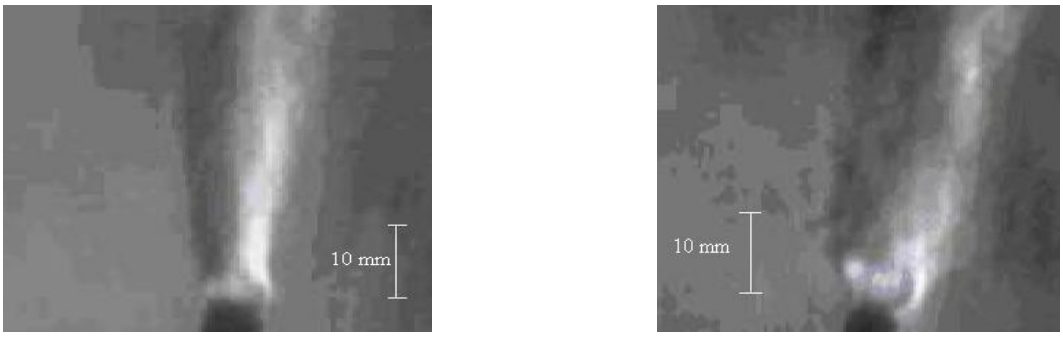

NAI WAI

Figure 4-8 Injector Spray Cone Angle

4.1.5 Pistons

Homogeneous and Stratified pistons are used to carry out homogeneous and stratified conditions respectively. In Figure 4-9 a homogeneous piston is shown. The sectional view is also given for the detailed illustration. This piston has a small cup placed in the centre of the crown.

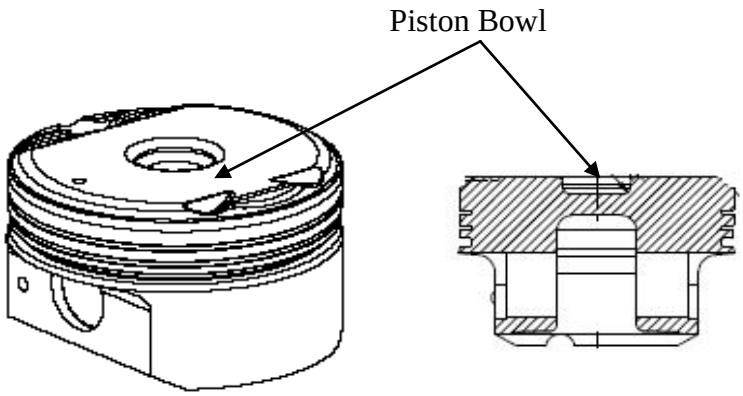

Figure 4-9 Homogeneous Piston

Stratified piston has a bigger cup compared to that of homogeneous piston and is position away from the centre. This design helps to achieve stratified conditions, in which fuel is deflected back from the piston head to the spark plug, so that a rich mixture is near the spark plug.

4.1.6 Dynamometer

Measurement of brake power is one of the most important measurements in the test schedule of an engine. It involves the determination of the torque and the speed of the engine output shaft. Dynamometer is a machine that used to measure torque and rotational speed of the engine and thus brake power can be calculated. There are different types of dynamometers such as:

- Prony Brake
- Rope Brake
- Hydraulic Dynamometer
- Eddy Current Dynamometer
- Swinging Field DC Dynamometer
- Fan Dynamometer
- Transition Dynamometer
- Chassis Dynamometer

Eddy current dynamometer is used in the experimental work to get the power ratings of the engine. The dynamometer is coupled with the engine to measure the brake torque as the engine output.

4.1.7 Fuelling System

Fuelling system is shown in Figure 4-10. Pressure of the compressed natural gas in the tank is 200 bars. This pressure is reduced to 20 bars using pressure regulated that is placed in between of the engine and the tank. Micro-motion mass flow meter is used to measure the flow rate to the engine and it has a sensitivity of 0.0001 g/s. The specifications of micro-motion mass flow meter are given in Table 4-3. After fuel flow meter, there is inlet fuel pressure control system. This system is coupled with a compressor to maintain the pressure along the fuel trail to injector.

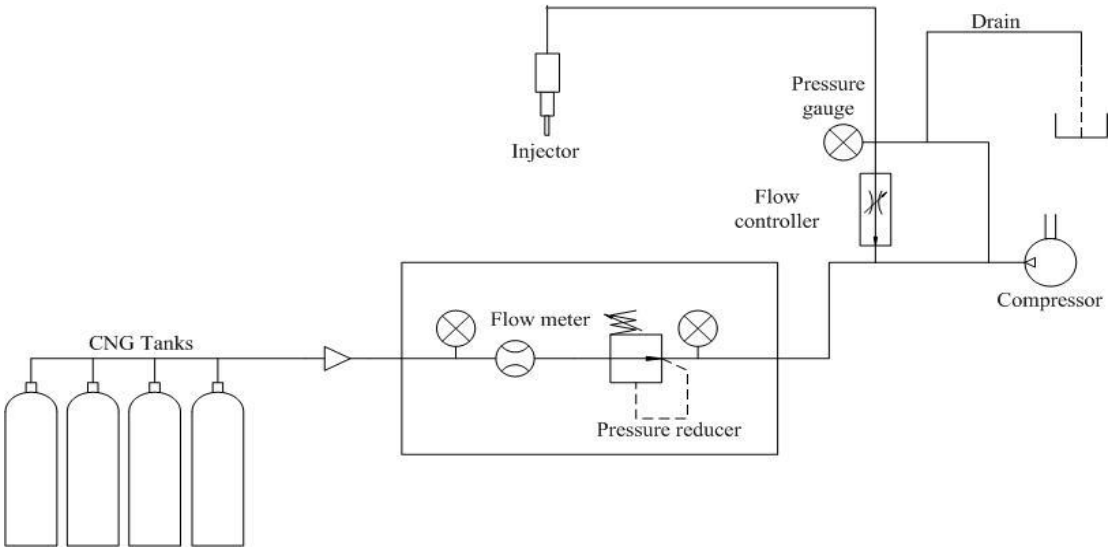

Figure 4-10 Compressed Natural Gas Fuelling System

Table 4-3 Micro-motion Fuel Flow Meter Specifications

Flow accuracy:	+/-0.05% of flow rate
Gas accuracy:	+/-0.35% of flow rate
Density accuracy:	+/-0.0002 g/cc
Wetted materials:	304L, 316L Stainless Steel or Nickel Alloy
Temperature rating:	-400 to 800°F (-240 to 427°C)
Pressure rating:	1450 - 6000** psi (100 to 413** bar)

4.1.8 Pressure Sensors

In order to investigate the individual cycles and combustion characteristics pressure transducer has been developed to measure in-cylinder pressure. The transducer is usually fitted in the cylinder head just like a spark plug without projecting into the combustion space. Of all the pressure transducers currently available the piezoelectric transducer are most satisfactory for all normal uses in internal combustion engine measurements as far as the sensitivity is concerned. Piezoelectric transducer is shown in Figure 4-11.

Piezoelectric transducer generates an electric signal in proportion to the pressure to which it is subjected. There are two primary piezoelectric effects: (1) the transversal effect in which charges on the x-planes of the crystal result from the forces acting upon the y-plane, and (2) the longitudinal effect in which charges on the x-planes of the crystal result from forces acting upon the x-plane. Piezoelectric transducer can be obtained with internal cooling passage and with a temperature compensator. Increasing temperature will make the casing expand and uncompressed crystals from load. Cooling is important operational procedures to get correct pressure reading. A crank angle encoder is used to establish the top dead centre position and the phasing of cylinder pressure to crank angle. Specification of pressure transducer is provided in Table 4-4.

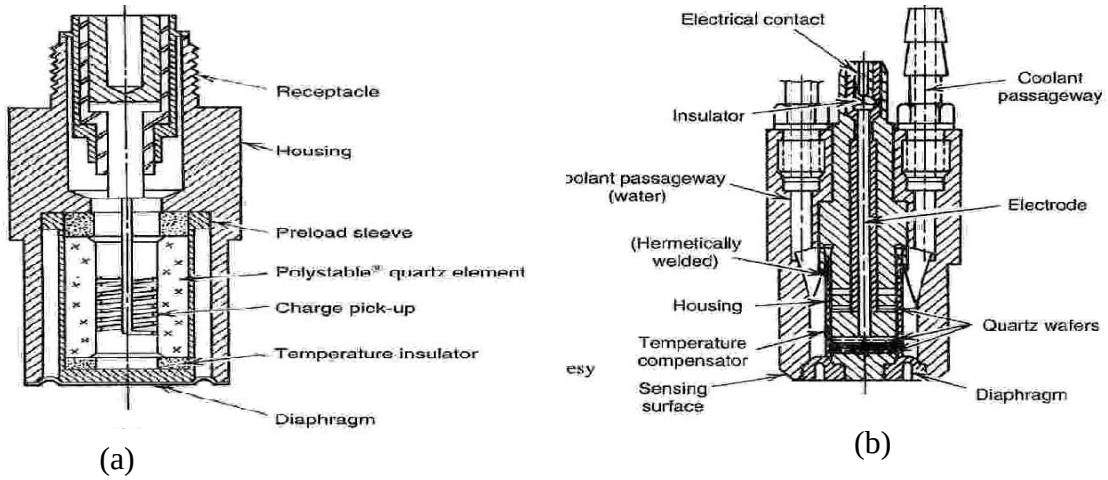

Figure 4-11 Quartz Piezoelectric Pressure Transducers. (a) Courtesy of Kistler Instrument Corp. (b) Courtesy of AVL Corp [75].

Table 4-4 Specification of pressure transducer

Make and model	Kistler ThermoCOMP®
Range	0-250bar
Linearity all ranges	<±0.5%FSO
Sensitivity shift, cooled 50±35°C	<±0.5%

4.1.9 Exhaust Gas Analyzer

Exhaust gas analyzer is shown in Figure 4-12. It is manufactured by GASMET™ which is used to measure the exhaust gases in the engine. The analyzer measures about 50 gas species in the exhaust and give their quantities in parts per million (ppm). General specifications of the gas analyzer are provided in Table 4-5.

Figure 4-12 GASMET™ Stationary FTIR Analyzer

The stationary GASMET™ FTIR analyzer consists of four systems:

1. Gasmet™ Cr-2000 gas analyzer with LN_2 detector and fast response sample cell
2. Gasmet™ sampling system
3. Heated Filter Unit
4. Gasmet™ Industrial Computer

Table 4-5 General Specifications of GASMET^{TM} FTIR Analyzer

General parameters	
Measuring Principle:	Fourier Transform Infrared, FTIR
Performance:	simultaneous analysis of up to 50 gas compounds
Response time:	typically <<25s, depending on the gas flow and measurement
Operating temperature:	15-25°C non condensing
Storage temperature:	-20 - 60°C non condensing
Power supply	100-115 or 230V / 50-60 Hz
Power consumption:	300 W
Measuring parameters	
Zero point calibration:	24 hours, calibration with nitrogen
Zero point drift:	<2% of measuring range per zero point calibration interval
Sensitivity drift:	None
Linearity deviation:	<2% of measuring range
Temperature drifts:	<2% of measuring range per 10K temperature change
Pressure Influence:	1% change of measuring value for 1% sample pressure change. Ambient pressure changes measured and compensated

4.2 Combustion Analysis

Combustion in internal combustion engine is very complex and still it is not fully understood. In order to have an insight in to combustion, Combustion analysis can be generated from the pressure reading resulted by the pressure sensors. PC-based combustion analysis hardware and software is used to acquire and analyze the pressure data. The scheme of the systems can be seen in Figure 4-13. The hardware consists of high-speed data acquisition and dedicated signal processor. The software

performs statistical and thermodynamics analysis of the pressure data at real-time. Measurements of cylinder pressure can be used to determine not only the location of peak pressure, but also the instantaneous heat release, and burn fraction. Dewetron data acquisition is used to obtain the reading of cylinder pressure, with 120 power cycles is taken as the result of the experiment and then average cycle is recorded. During the cycle of an engine useful work is only done on the power stroke. By measuring the cylinder pressure through a cycle it is possible to calculate the average pressure that is useful to analyze engine combustion. This pressure is the Indicated Mean Effective Pressure (IMEP).

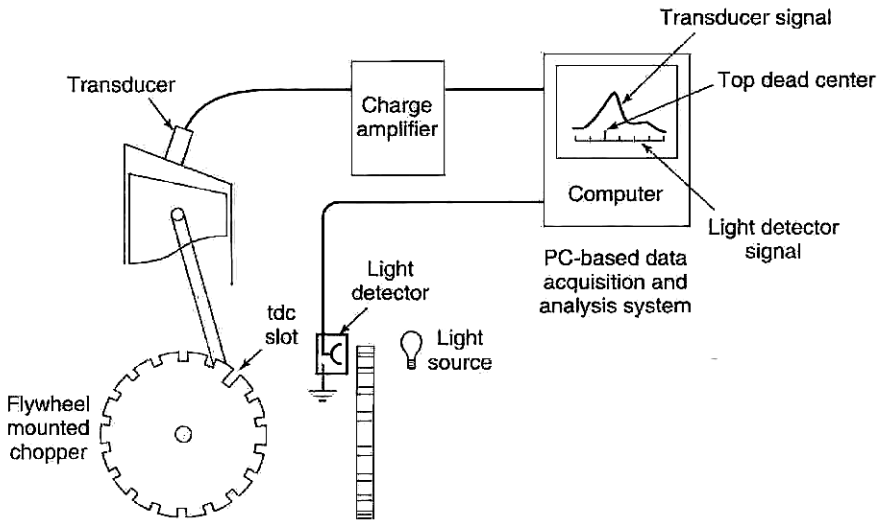

Figure 4-13 Typical Pressure Measurement System [95].

IMEP can be generally calculated by numerical integration on the PV diagram. However, this method requires a great number of sampled data per cycle in order to ensure high accuracy in calculation. There are many alternative equations to get the result of IMEP integration from cylinder pressure data, equation with the least possible error is:

$$IMEP = \frac{\Delta\theta}{V_d} \cdot \sum_{i=n_1}^{n_2} p(i) \frac{dV(i)}{d\theta} \tag{4-3}$$

Where $p(i)$ is cylinder pressure at crank angle i,

$V(i)$ is cylinder volume at crank angle i,

V_d is cylinder displacement volume, and n_1 and n_2 refers to the BDC crank angle position. Crank angle resolution, pressure transducer accuracy and engine geometry significantly affect the errors in IMEP calculations. These errors can be significantly reduced if the crank angle resolution is less than 10 crank angle degrees.

4.3 Device Calibration

Calibration process is used in order to ensure the accuracy of the experimental data. In the following experiment, calibration process was mainly done to dynamometer, pressure data acquisition system, and exhaust gas analyzer.

4.3.1 Dynamometer Calibration Process

Dynamometer was calibrated using calibrated weights as reference. The weights are put on one side of dynamometer and the reading is noted down from the control panel. After every reading the weights are increased in a sequential manner as shown in the Table 4-6.

Table 4-6 Load Sequence for Dynamometer Calibration Process

No	Weight (kg)	Torque (Nm)
1	1	4
2	2	8
3	5	20
4	10	40
5	12	48

When the dynamometer achieves its maximum reading (i.e.; 48 Nm) weights are unloaded. The reading on the control panel should be zero when all the loads are removed. Same procedure is repeated for other arm of dynamometer.

4.3.2 Pressure Data Acquisition Systems Calibration

Pressure data acquisition system is calibrated by using pressure testing device for engine.

The procedure for pressure sensor calibration was:

- Turn-on all systems
- Unplug the spark plug from its position
- Install the manual pressure testing device on the spark position
- Motoring the engine in a low rpm condition (<300 rpm)
- Measure the reading by data acquisition systems
- Compare both result from manual pressure device and pressure sensor reading

Maximum pressure was compared using this procedure. The manual pressure reading device was showing pressure gauge reading. If the pressure sensors shows the same reading with pressure gauge, then in order to get absolute pressure reading, 1 bar will be added on the whole pressure sensor reading.

4.3.3 Exhaust Gas Analyzer Calibration

Exhaust gas analyzer is calibrated before starting any experimental works. GASMET exhaust gas analyzer is already equipped with self calibration procedure. This calibration procedure is called zero calibration. Zero calibration is necessary to be done before starting the experiment. It will measure the background spectrum for subsequent sample spectrum measurement. Zero calibration can only be valid if the instrument is in steady state condition with certain cell temperature and interferometer temperature.

For zero calibration, the sample must be filled with pure substance such as N_2 to make sure that there is no unwanted sample in the test cell. FTIR system will create background data base of the pure substance analysis as the base line for the measurement process. A typical background spectrum is presented in Figure 4-14.

The background spectrum represents the actual absolute intensity of infrared radiation that is transmitted through zero gas filled sample.

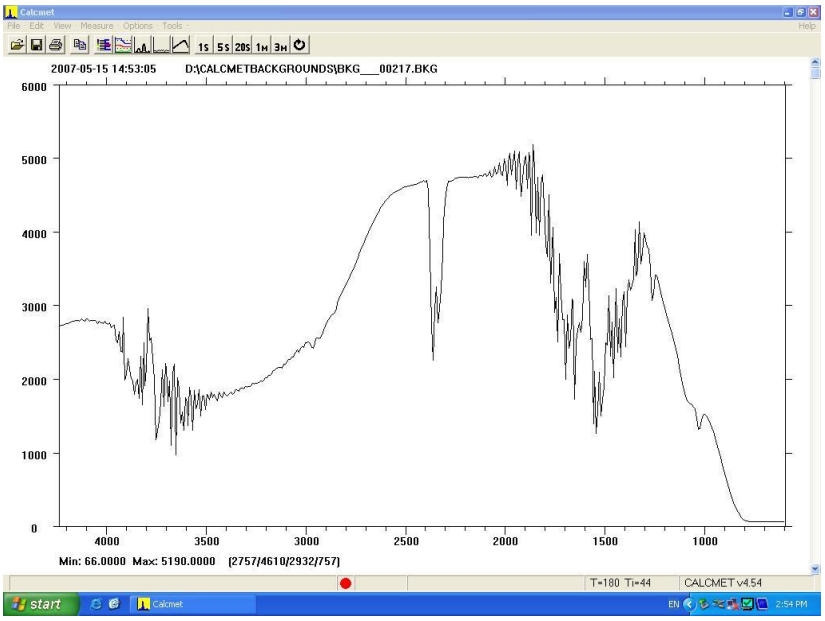

Figure 4-14 Calibration Spectrum on FTIR System for Emission Analysis

4.4 Injection Parameters and Data Collection for Boost Pressure

Injection parameters such as injection timing, injection pressure and injection spray angle have been found to have an effect on engine performance and emissions. Of all injection parameters injection timing has significant effect on engine volumetric efficiency and thus engine performance [49, 56]. For partial and port injection timings the engine will face a problem of having less volumetric efficiency because of the displacement of some of the air by natural gas as these injection timing have inlet valve open during injection. At these injection timings boost pressure will be implemented to increase the engine volumetric efficiency. Data collection for these experiments follows SAE standard for Engine performance and Testing, SAE J1995 that is Engine Power Test Code-Spark ignition and Compression ignition-Gross power rating.

4.4.1 Test Conditions

The engine test bed is a single cylinder research engine (SCRE) with a compression ratio of 14. The tests were conducted at full load condition with ignition point set at maximum brake torque (MBT). A high injection pressure, 18 bars, was used and kept constant for all experiments in a central injection system. Air fuel ratio was set at stoichiometric condition that is 17.4 for compressed natural gas in order to see the maximum output. The research has been done for speeds 2000, 2500, 3000, 3500, 4000, 4500 and 5000 rpm by varying boost pressure from 2.5 kPa (25% compressor capacity) to 10 kPa (100% compressor capacity) in the interval of 2.5 kPa at each mentioned engine speeds. Boost pressure refers to the increase in manifold pressure that is generated by the supercharging in the intake path or specifically intake manifold. This is representative of the extra air pressure that is achieved over that would be achieved without the forced induction. U-tube mercury manometer was used to measure inlet manifold pressure. Detail of boost pressure is given in Figure 4-15. Figure 4-16 shows the schematics of test set-up with supercharging and naturally aspirated condition.

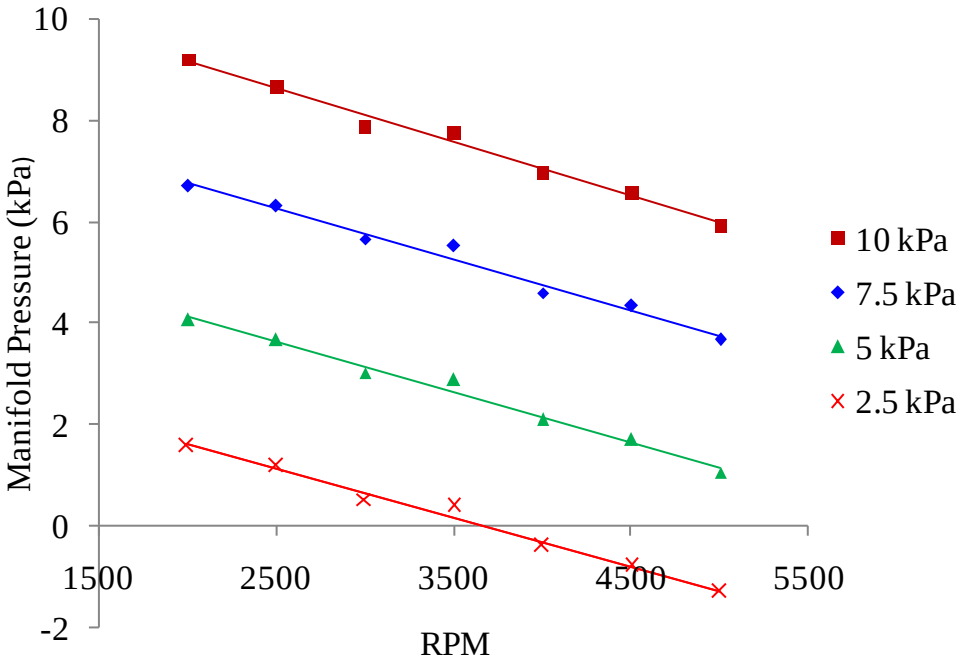

Figure 4-15 Manifold Pressure versus Engine Speed

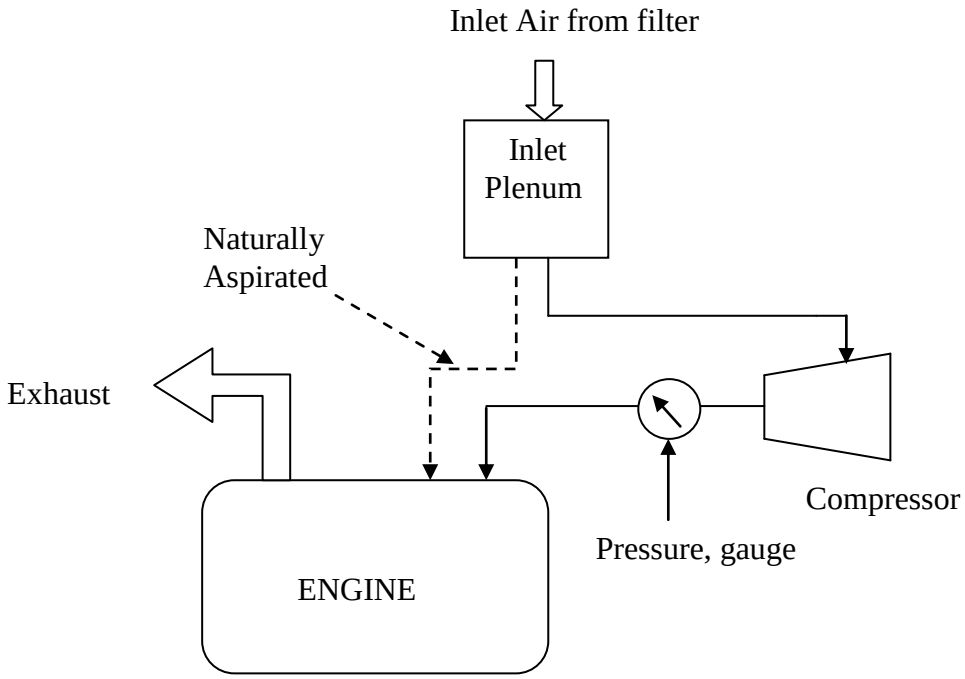

Figure 4-16 Schematic of test set-up with supercharging and naturally aspirated engine

4.4.2 Pressure Drop along the Pipe

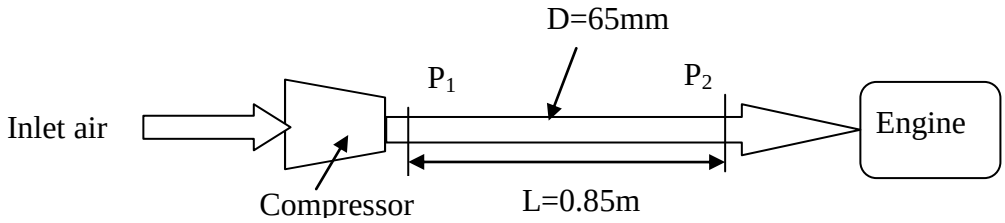

Figure 4-17 Compressor-Engine System

Figure 4-17 shows boosted engine system. After measuring boost pressure at inlet manifold there may be pressure drop in the pipe along the engine. Figure 4-18 shows the pressure drop for 10 kPa boost pressure. Pressure drop in the pipe from compressor outlet to the engine is calculated by using polyflo equation [107]. This is used for medium pressure networks.

$$Q_n = 7.57 * 10^{-4} \frac{T_n}{p_n} \sqrt{[\frac{(p_1^{\,2} - p_2^{\,2}) D^5}{fSLT}]} \qquad (4.4)$$

Where: p (bar), Q_n (m^3h^{-1})

The value of f is given by

$$\sqrt{(\frac{1}{f})} = 5.338(\mathrm{Re})^{0.076} E \tag{4.5}$$

Where: E= efficiency factor

And Reynolds number is calculated by:

$$\mathrm{Re} = \frac{Dw\rho}{\mu} \tag{4.6}$$

But

$$Q = \frac{\pi D^2}{4} w \tag{4.7}$$

Thus

$$w = \frac{4Q}{\pi D^2} \tag{4.8}$$

Substituting equation (4.8) into equation (4.6) we get

$$\mathrm{Re} = \frac{4Q\rho}{\mu D\pi} \tag{4.9}$$

Thus pressure loss in the pipe is given by:

$$p_1{}^2 - p_2{}^2 = (\frac{Q_n p_n}{7.57*10^{-4} T_n})^2 \frac{fSLT}{D^5} \tag{4.10}$$

Table 4-7 Pressure Drop along the Pipe Calculated by Using Polyflo Equation

Speed (rpm)	Q ($m^3h^{-1)}$	w (mh^{-1})	Re	f	(P_1^2-P_2^2) bar	P_1 (kPa	P_2 (kPa)	(P_1-P_2) kPa
2000	24.717	8461.87	8545.550	0.01204	4.3816E-05	10	9.979	0.0203
2500	28.661	9812.12	9909.157	0.01177	4.6881E-05	10	9.976	0.023
3000	33.976	11631.86	11746.89	0.01147	6.4201E-05	10	9.967	0.032
3500	37.449	12820.90	12947.68	0.01130	7.6852E-05	10	9.961	0.038
4000	41.979	14371.81	14513.93	0.01111	9.4908E-05	10	9.952	0.047
4500	43.187	14785.39	14931.60	0.01106	0.00010001	10	9.949	0.050
5000	45.302	15509.15	15662.52	0.01098	0.00010925	10	9.945	0.054

Table 4-8 Dynamic Viscosity of Air at Standard Atmospheric Pressure - SI Units

Temperature (t) (k)	Dynamic Viscosity (μ) (kg/m s) x 10^{-5})
150	1.0283
200	1.3289
250	1.488
300	1.983
350	2.075
400	2.286

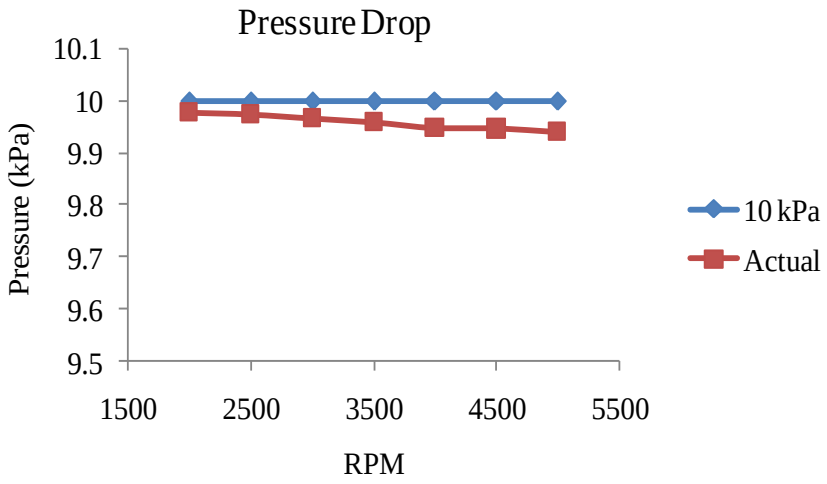

Figure 4-18 Pressure Drop along the Pipe for 10 kPa Boost Pressure

4.4.3 Injection Timing

Injection timing of 300° BTDC and 180° BTDC have inlet valve open during injection. These injection timings have penalty of volumetric efficiency due to some of the air is displaced by natural gas. At very early injection timing, 300° BTDC, the fuel was injected when intake valve starts to open. Early injection timing for direct injection systems can be considered as port injection as this injection timing has inlet valve open during injection like port injection system. Although there are differences between port injection systems and very early injection timing for direct injection systems, very early injection timing can be considered as port injection system and their mixing behavior was almost the same [57]. Partial direct injection, 180° BTDC,

is injecting fuel when inlet valve half open and half closed. Start of Injection timing was set at 300° BTDC and 180° BTDC for experimental work with homogeneous piston at stoichiometric condition. Implementation of injection timing is shown in Figure 4-19.

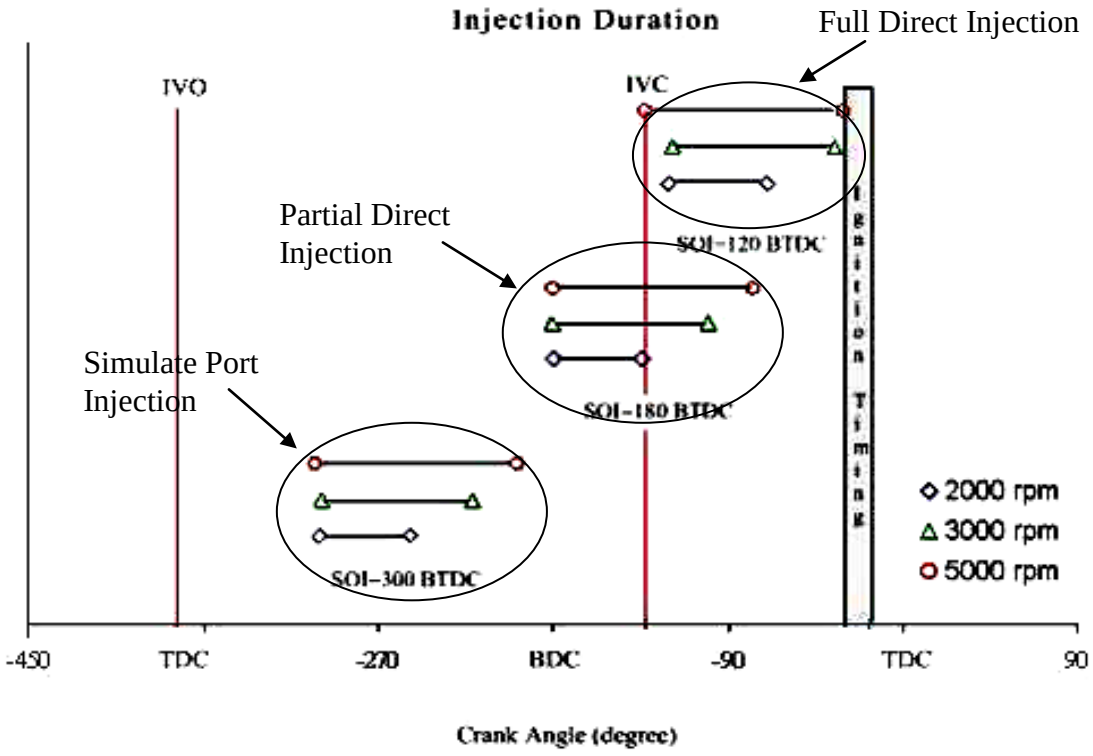

Figure 4-19 Injection Duration for Different Injection Timings

4.4.4 Injection Pressure and Injector Spray Angle

Injection pressure is kept constant at 18 bars for stoichiometric conditions. Injection pressure significantly affects the delivery rate of the injector. With increasing injection pressure, the cone angle decreases slightly that means higher injection pressure resulted in smaller injection window needed by injector to deliver the fuel required by the systems. In this research narrow angle, with 30° outward opening injector, is used and kept constant at all operating engine conditions. This is to maximize the spray penetration of natural gas.

CHAPTER 5

RESULT AND ANALYSIS

In this chapter, effects of boost pressure on engine performance, combustion and emissions are discussed. Boost pressure is tested at Partial (180° BTDC) and port (300° BTDC) injection timings to reduce the penalty of volumetric efficiency. Supercharging results are compared with naturally aspirated engine. Comparison of boost pressure results on engine performance, combustion and emissions between partial and port injection is illustrated.

5.1 Effect of Boost Pressure on Engine Performance at Partial Direct Injection, 180° BTDC.

Effects of boost pressure on engine performance parameters at partial direct injection are shown in Figure 5-1**.** Figure 5-1 (a) represents brake torque versus speed at 180° BTDC injection timing. Torque increases for all boost pressures till 3000 rpm and then starts to decrease when engine speed increased to 5000 rpm. From the graph, when inlet pressure rises the toque curve also increases for all operating engine speeds. The maximum torque achieved with boost pressure was at 3000 rpm. The benefit of torque was seen when boost pressure increased from 7.5 to 10 kPa compared to naturally aspirated engine. For boost pressure of 2.5 and 5 kPa, the torque values found lower than naturally aspirated engine for engine speeds above 2500 rpm. This is because these small boost pressures cannot capable of supplying enough amount of air at high engine speed so that the manifold pressure drops to atmospheric pressure. In this situation, the significant effect of temperature makes the air lighter and resulted in reduction of volumetric efficiency as shown in Figure 5-4.

At 2000 rpm and injection timing of 180° BTDC, boost pressures resulted 10-30% higher in torque compared to naturally aspirated engine. As the speed continues to increase the benefit in torque is decreasing due to the decrease in volumetric efficiency. For instance at 5000 rpm, boost pressures of 7.5 kPa to 10 kPa seem to have 15-20% increase in torque compared to naturally aspirated engine. The

maximum torque value is at 3000 rpm with 10 kPa boost pressure that is 32.1 Nm while 31 Nm for naturally aspirated engine.

Effect of boost pressure on brake power is illustrated in Figure 5-1 (b). For boost pressures of 7.5 kPa and 10 kPa, there is 5-25% higher brake power compared to naturally aspirated engine for all operating engine speed. For all boost pressures, power curve increases and reaches its peak point at 4000 rpm engine speed.

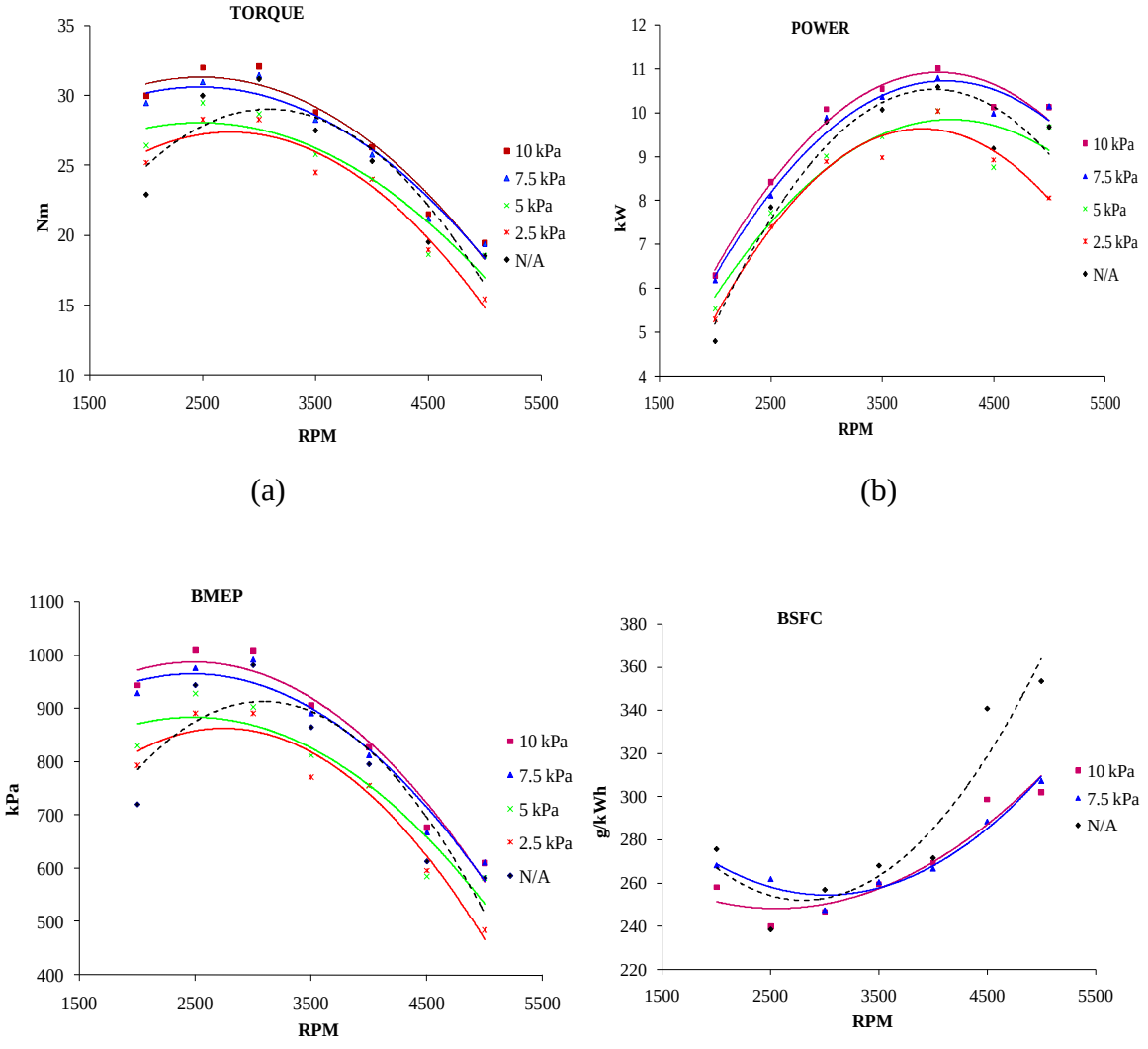

Figure 5-1 Engine Performance Results for Different Boost Pressures at 180° BTDC Injection Timing

For small boost pressures of 2.5 kPa and 5 kPa, there is better power values for speed less than 2500 rpm compared to naturally aspirated engine. At 2000 rpm, 2.5 and 5 kPa have 7 and 10% increase in power compared to naturally aspirated engine, respectively. For speed greater than 2500 rpm, power values at 2.5 kPa and 5 kPa boost pressure are lower than naturally aspirated values. This is caused by the reduction in volumetric efficiency due to the effects of temperature on the air rate for these small boost pressures compared to naturally aspirated engine. This can be verified by the actual amount of air inside the engine and effects of compressed air temperature on the density of the air entering into the engine. Actual amount of air inside the engine can be determined by using lambda from oxygen sensor, stoichiometric air fuel ratio and fuel rate injected into the engine.

Figure 5-2 illustrates actual mass of air inside the engine versus engine speed for 5 kPa, 2.5 kPa and naturally aspirated engine. From the graph, it can be seen that there is more air flow rate for boost pressure above 2.5 kPa for engine speeds lower than 2500 rpm compared to naturally aspirated engine. Beyond this engine speed, the graph illustrates that there is less amount of air inside the engine for boost pressure less than 5 kPa. This explains that the decrease in volumetric efficiency that resulted in decrease in performance is due to the decrease in actual amount of air inside the engine for these small boost pressures.

For small boost pressure, the decrease in output performance values compared to naturally aspirated engine can be proved by checking the density of air coming into the engine. At high engine speed, the significant effect of temperature (43-47^{o}c) to the air flow rate for these small boost pressures compared to naturally aspirated engine, around 30^{o}c, reduces the density of air entering into the engine cylinder. Density of air entering the cylinder is approximated by using ideal gas law (equation 3.42).

From the equation and measured values of air temperature, it can be seen that low boost pressure is mainly affected by the significant effect of temperature on the density of air. Using experimental values for temperature and pressure, density of air coming into the engine is approximated. Figure 5-3 shows density of air entering into the engine versus engine speed. At low boost pressure, temperature significantly

affects the density of air making the air lighter that resulted in decrease in performance of these small boost pressures at high engine speed compared to naturally aspirated engine. This is mainly due to at these small boost pressures and high engine speed manifold pressure drops as high engine speed requires more air and thus the significant effect of temperature resulted in decrease of air density as shown in Figure 5-3.

Engine performance parameter, Brake mean effective pressure (BMEP), is shown in Figure 5-1 (c). Brake mean effective pressure, BMEP, curve shows the same relation with the torque curve. The maximum value of BMEP is achieved at 3000 rpm for boost pressure of 10 kPa that is 1012 kPa. BMEP increases till it reaches 3000 rpm and then starts to decrease like the torque values. More benefit of BMEP is shown with boost pressure for speed less than 3000 rpm compared to BMEP of naturally aspirated engine. The benefit of BMEP starts to decrease from 30% to 15% when speed increases from 2000 to 5000 rpm for 10 kPa boost pressure. For boost pressure above 7.5 kPa there is better BMEP than naturally aspirated engine for all operating engine speeds while for boost pressure less than 5 kPa there is less performance obtained for speed greater than 2500 rpm compared to naturally aspirated engine.

Performance parameter brake specific fuel consumption, BSFC, is shown in Figure 5-1 (d). With boost pressure, brake specific fuel consumption value decreases till 3000 rpm and starts to increase when speed increased to 5000 rpm. This tells that 3000 rpm has better performance and a speed where peak performance value is achieved. 10 kPa boost pressure gives 7% and 14% lower BSFC at 2000 rpm and 5000 rpm respectively compared to naturally aspirated engine. Brake specific fuel consumption decreases with increasing boost pressure for all engine speed.

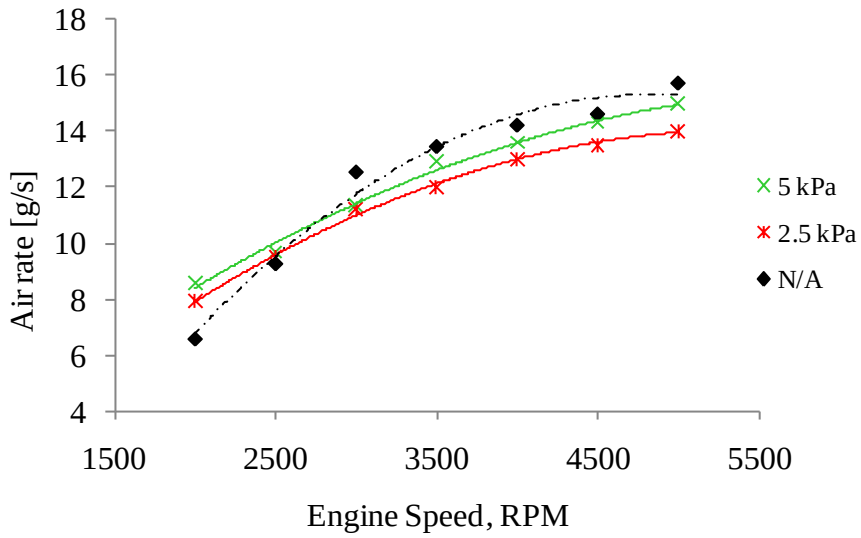

Figure 5-2 Actual Mass of Air inside Combustion Chamber versus Engine Speed

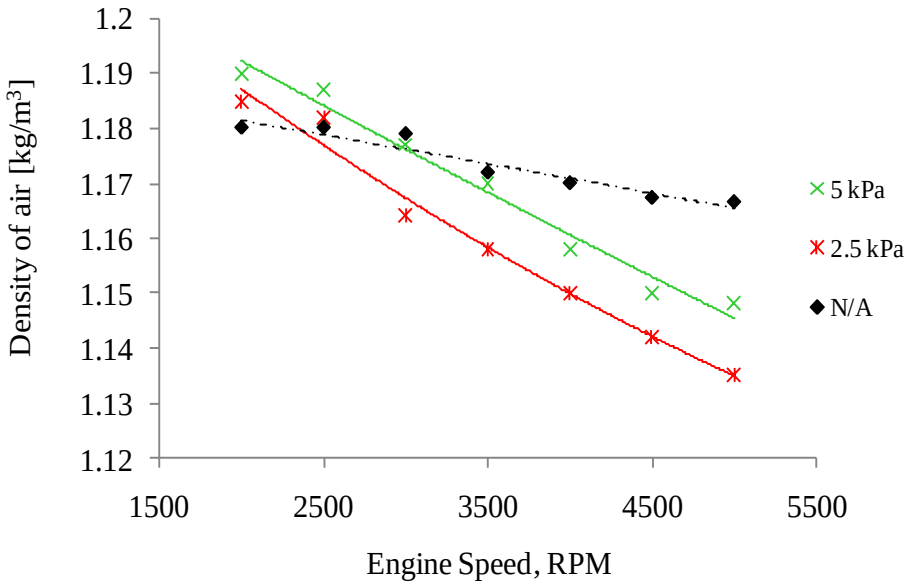

Figure 5-3 Density of Air entering into the Engine versus Engine Speed

High performance of engine has been shown with increasing boost pressure for all operating engine speed. This is mainly due to the effect of boost pressure on volumetric efficiency. Volumetric efficiency graph is shown in Figure 5-4. The graph shows that volumetric efficiency increases and reaches peak point at 3000 rpm and decreases as speed increased to 5000 rpm. The benefit of boost pressure on volumetric

efficiency decreased from 2000 to 3500 rpm and started to increase slowly as speed increased to 5000 rpm. 10 kPa has 22% and 3% higher volumetric efficiency at 2000 and 3500 rpm respectively and 5% higher at 5000 rpm compared to naturally aspirated engine. The maximum volumetric efficiency achieved with 10 kPa boost pressure is at 3000rpm and that is 1.044. The minimum volumetric efficiency achieved with 10 kPa boost pressure is 0.79 while 0.767 with naturally aspirated engine at 5000rpm. Better performance is shown with boost pressure above 7.5 kPa at all engine operating speeds because of its better volumetric efficiency as shown in Figure 5-4.

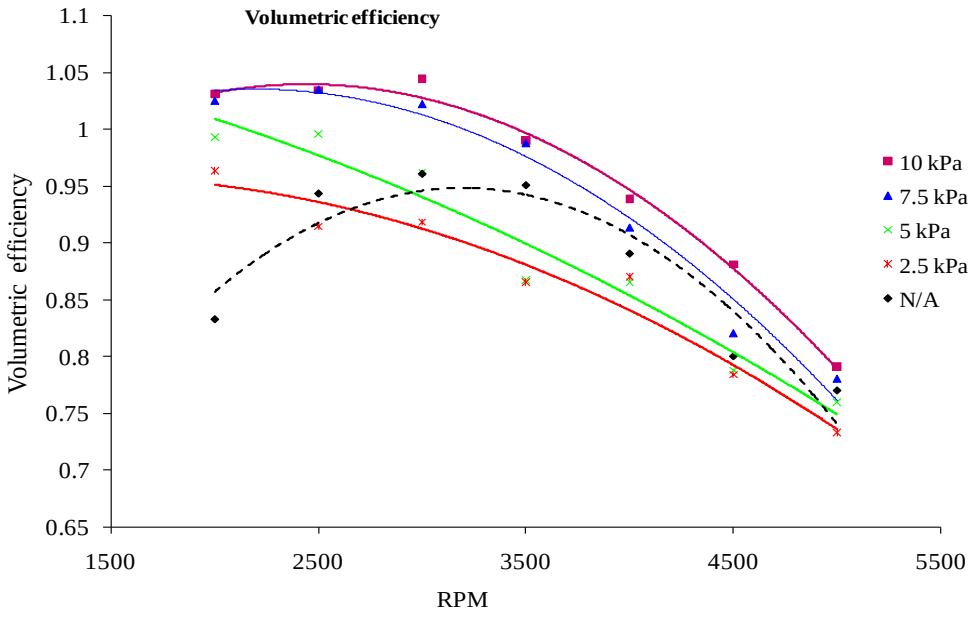

Figure 5-4 Volumetric Efficiency for Different Boost Pressures at Partial Direct Injection

5.2 Engine Performance at 300° BTDC, Port Injection Timing

Engine performance parameters are shown for 300° BTDC injection timing in Figure 5-5. Performance trends are the same like injection timing of 180° BTDC but there are variations in performance at different speeds. Figure 5-5 (a) represents brake torque versus speed at 300° BTDC injection timing. At 2000 rpm and 300° BTDC injection timing, boost pressure showed 9-22% better in torque compared to naturally

aspirated engine while it is 10-30% better in torque at 180° BTDC injection timing. For speed less than 4000 rpm, 300° BTDC injection timing performed less than 180° BTDC injection timing. This happened because of the better volumetric efficiency of partial injection for these speeds. At 5000 rpm and injection timing of 300° BTDC, 10 kPa boost pressures has an output torque of 19.5 Nm while it is 19.36 Nm at 180° BTDC injection timing. With boost pressure, injection timing of 300° BTDC gives better performance than 180° BTDC for speeds above 4000 rpm. This is due to enough time available for mixture preparation when injecting fuel early than lately for high engine speeds.

Effects of boost pressure for other performance parameters like power, brake mean effective pressure (BMEP), and brake specific fuel consumption (BSFC) at 300° BTDC injection timing are also illustrated in Figure 5-5. The graph here shows the same trends like partial direct injection. However, there are variations in performance at different engine speeds.

Effect of boost pressure on brake power is illustrated in Figure 5-5 (b). Power graph showed there are higher values for 300° BTDC injection timing for speed above 4000 rpm compared to partial direct injection. For 10 kPa boost pressure, the power achieved is 10.57 kW while it is 10.15 kW for 180° BTDC injection timing at 5000 rpm. The maximum power achieved is at 4000 rpm for both injection timings. As speed increased to 5000 rpm, the power decreased slowly for 300° BTDC than 180° BTDC injection timing.

Engine performance parameter, Brake mean effective pressure (BMEP), is shown in Figure 5-5 (c). Brake mean effective pressure (BMEP) for 300° BTDC injection timing shows the same trend like 180° BTDC. But 300° BTDC injection timing has better BMEP values than 180° BTDC injection timing for speeds above 4000 rpm for the same boost pressure. BMEP values for 10 kPa at 5000 rpm are 620kPa and 610 kPa for 300° BTDC and 180° BTDC injection timings respectively. This tells that there is a need for higher boost pressure beside optimum injection timings at high engine speeds.

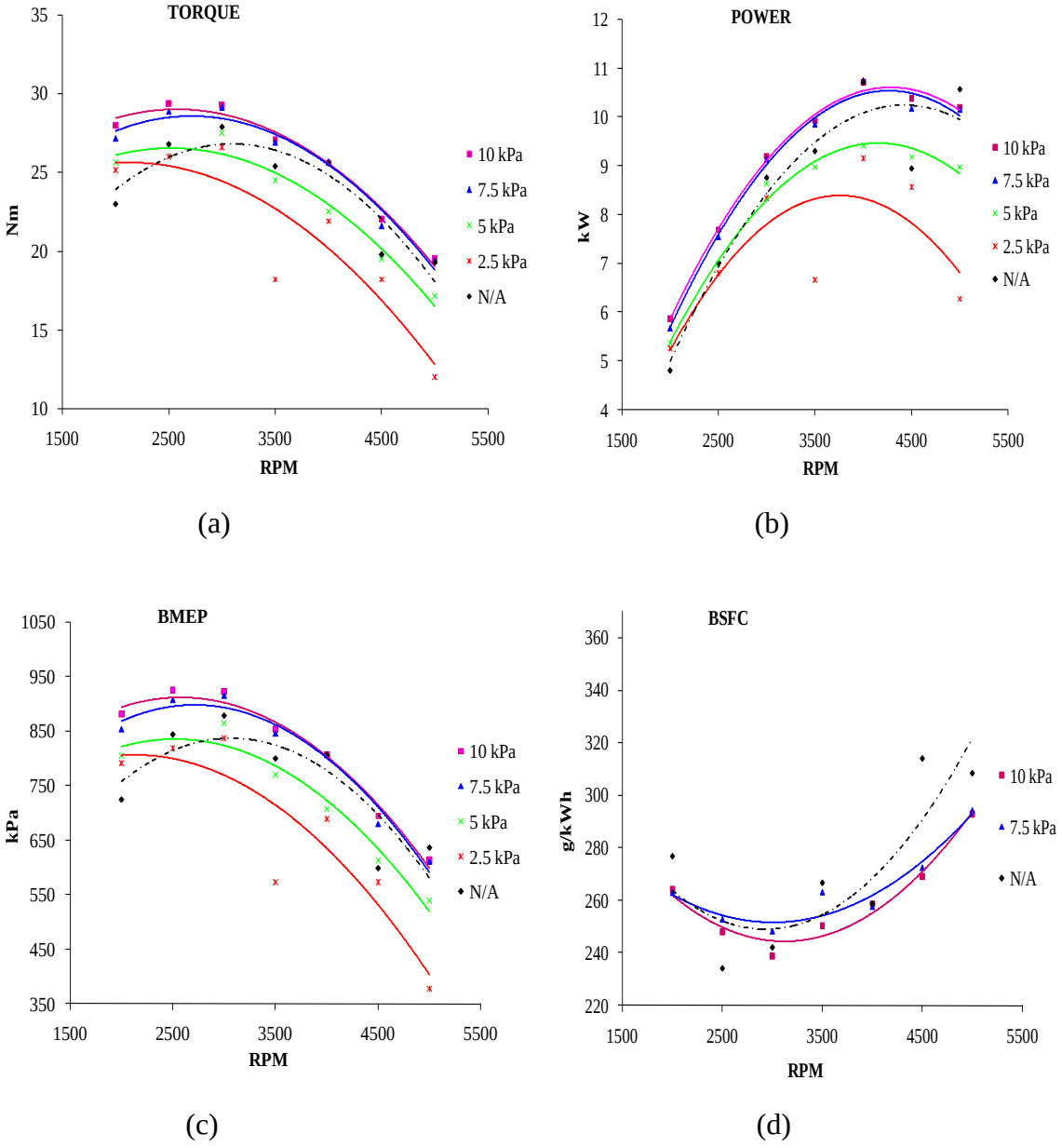

Figure 5-5 Engine Performance Results at Injection Timing of 300° BTDC for Different Boost Pressures

Performance parameter brake specific fuel consumption, BSFC, is shown in Figure 5-5 (d). Brake specific fuel consumption decreases with increasing boost pressure value. 10 kPa boost pressure has better BSFC values compared to naturally aspirated engine at all operating engine speed. With early injection timing, the benefit of boost

pressure on BSFC increases as speed increased from 2000 to 5000 rpm compared to partial direct injection.

Volumetric efficiency at early injection timing is shown in Figure 5-6. The graph shows that with boost pressure volumetric efficiency value increases and reaches peak point at 3000 rpm and starts to decrease as speed increased to 5000 rpm. The benefit of boost pressure on volumetric efficiency decreased from 2000 to 3500 rpm and started to increase slowly as speed increased to 5000 rpm. Generally, with boost pressure volumetric efficiency decreases as speed increases from 2000 rpm to 5000 rpm. The decrease in volumetric efficiency at high speed tells the need for higher boost pressure as high speeds need more air for better combustion. The maximum volumetric efficiency for boost pressure of 10 kPa is 0.97 at 2000 rpm. The minimum volumetric efficiency for 10 kPa boost pressure is 0.75 at 5000 rpm.

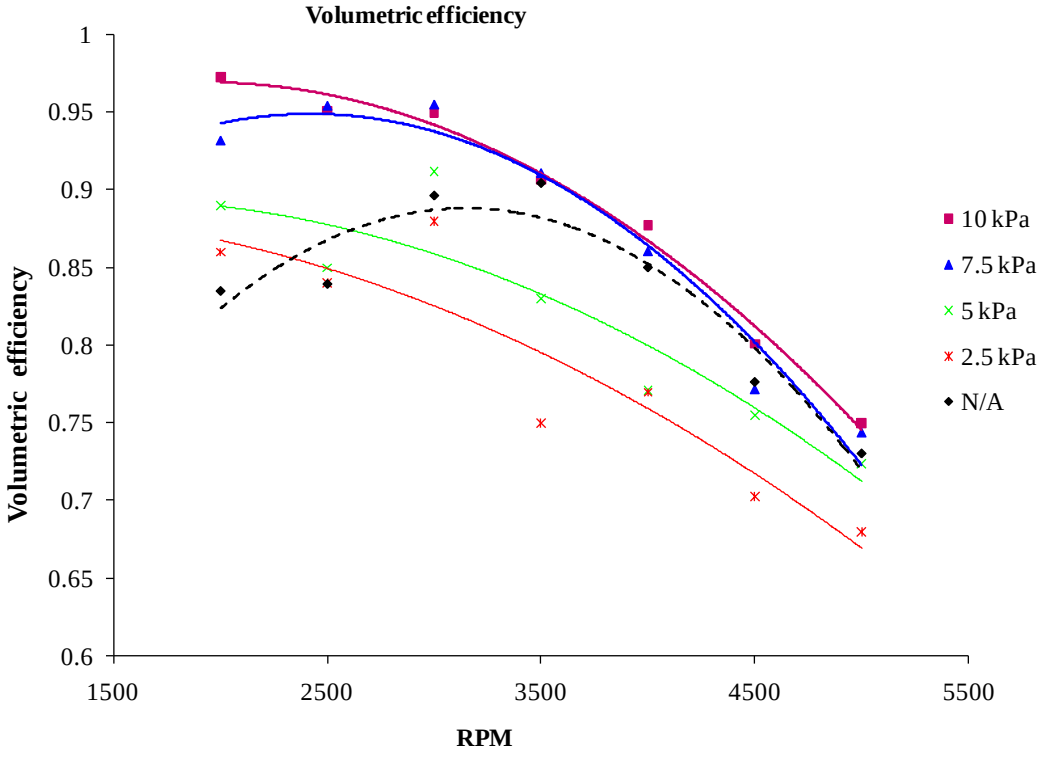

Figure 5-6 Volumetric Efficiency for Different Boost Pressures at Port Injection Timing

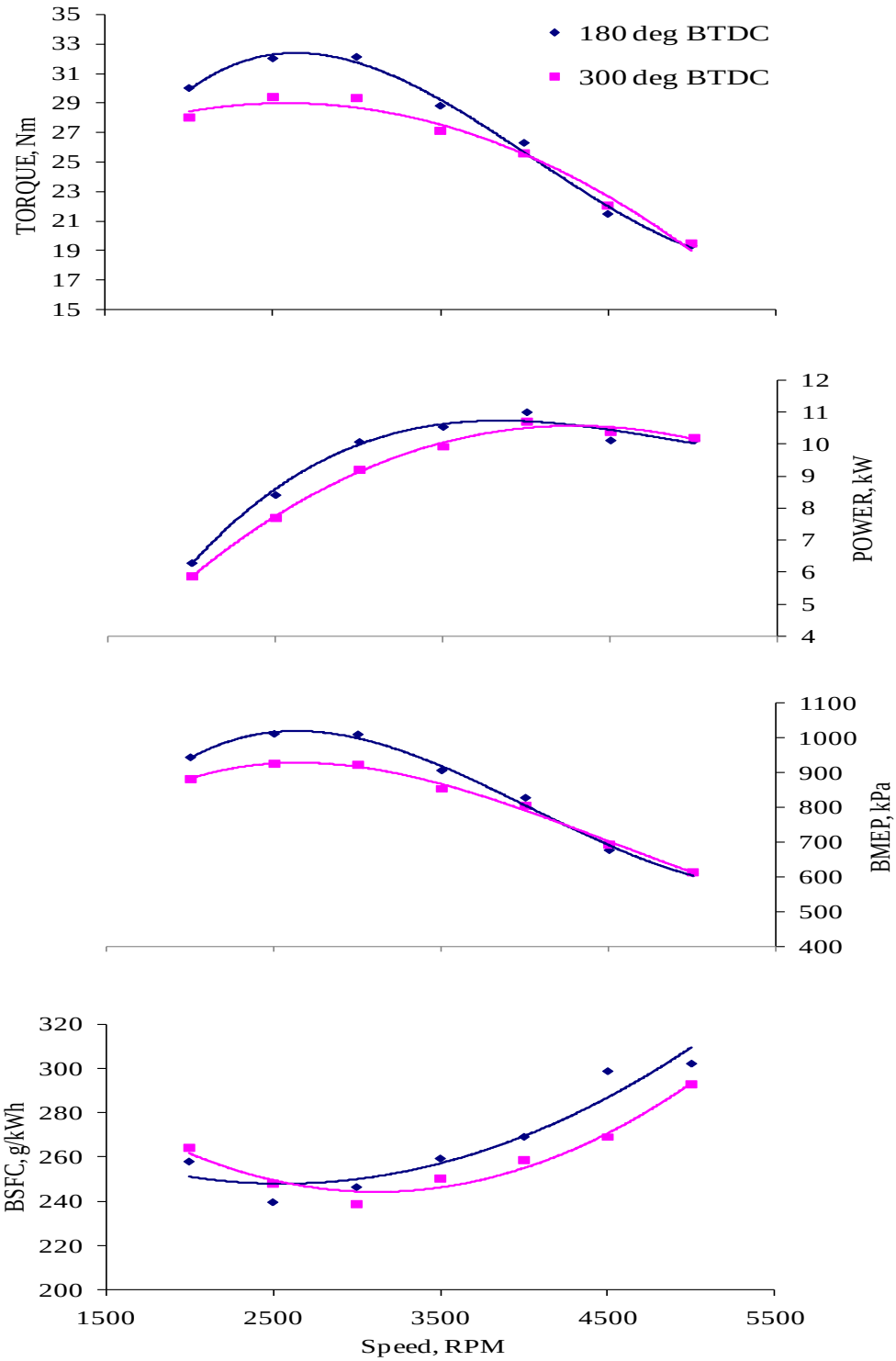

Figure 5-7 Effect of Injection Timing on Performance Values of 10 kPa Boost Pressure

Figure 5-7 compares performance values of 10 kPa boost pressure at 180° BTDC and 300° BTDC injection timings. 300° BTDC injection timing gives better performance than 180° BTDC injection timing for speeds above 4000 rpm. At 5000 rpm, 300° BTDC injection timing has an output torque of 19.5 Nm while it is 19.36 Nm at 180° BTDC injection timing. Power and BMEP curve show that 180° BTDC injection timing has better performance values than 300° BTDC injection timing for speeds less than 4000 rpm. BSFC graph shows 180° BTDC injection timing has better brake specific fuel consumption value for low engine speed while early injection timing has better result for speed above 3000 rpm. 10 kPa boost pressure has 294 g/kWh BSFC value for 300° BTDC while it is 302 g/kWh for 180° BTDC injection timing at 5000 rpm.

Generally, 300° BTDC injection timing gives better performance than 180° BTDC injection timing for speed above 4000 rpm. This is due to better mixture preparation time available for early injection timing at higher speeds compared to late injection timing. This shows additional benefit that can be achieved with boost pressure at high speeds by injecting the fuel early. While, late injection supply insufficient time for the fuel-air mixing of the late part of injected fuel bringing poor quality of mixture formation.

5.3 Effect of Boost Pressure on Engine Combustion at 180° BTDC Injection Timing

Effect of boost pressure on combustion process at 2000 rpm engine speed and partial direct injection is illustrated in Figure 5.8. In-cylinder pressure is shown in Figure 5-8 (a). Pressure profile graph shows that when boost pressure increases from 2.5 kPa to 10 kPa, pressure inside the cylinder also increases and reaches maximum value for 10 kPa boost pressure, 76 bar. For 7.5 kPa the maximum value of inside pressure is 63 bars at 13° ATDC crank angle. Better combustion with higher boost pressure may be due to better turbulence level and fast combustion with reduced ignition delay as shown in heat release graph in Figure 5-8 (b). With 10 kPa boost pressure, it is shown

that there is 0.032 kJ/CA heat release at 1.5° ATDC crank angle. For 7.5 kPa the maximum heat release is 0.031 kJ/CA at 11° ATDC crank angle.

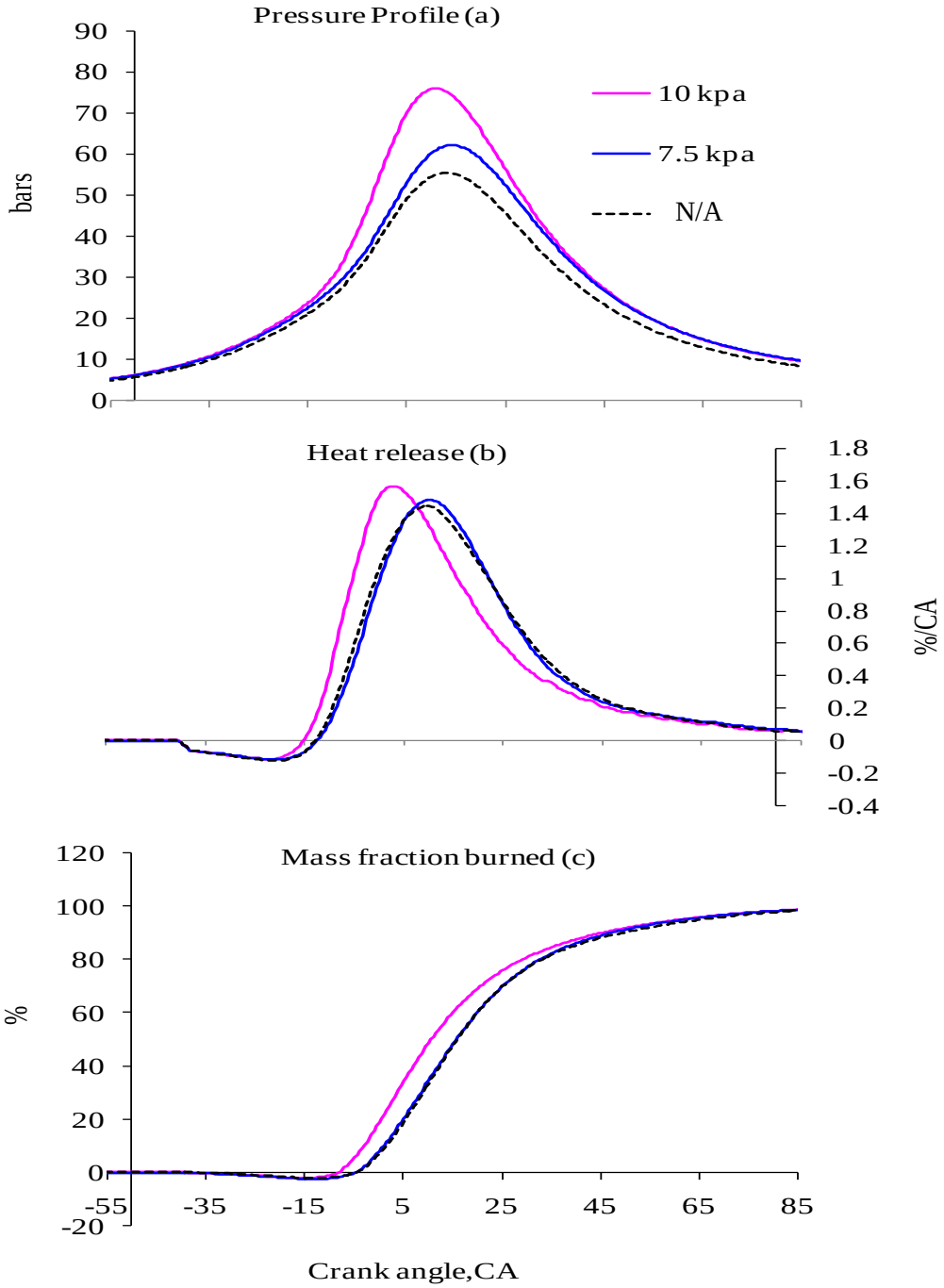

Figure 5-8 Combustion Process at 2000 rpm for Different Boost Pressures at Partial Direct Injection

Mass fraction burned at 2000 rpm is shown in Figure 5-8 (c). Fast combustion with boost pressure after ignition is shown in mass fraction burned graph. Better mass fraction burn rate is seen with boost pressure after ignition delay which results in high inside pressure and better heat release rate. With boost pressure of 10 kPa and 7.5 kPa at top dead center there are 21% and 10% mass fraction burned respectively. This shows that with increasing boost pressure there is better mass burn rate that helps the engine to produce better power.

The effect of boost pressure on combustion at engine speed of 2500 rpm is illustrated in Figure 5-9. Figure 5-9 (a) shows the in-cylinder pressure for different boost pressure at 2500 rpm. The maximum in-cylinder pressure achieved for 10 kPa boost pressure is 77.8 bars which is better than that of 2000 rpm. This is due to better volumetric efficiency as speed increased to 2500 rpm as shown in Figure 5-4. With 10 kPa and 180° BTDC injection timing, there is better heat release and the maximum value is 0.035 kJ/CA at crank angle of 3° ATDC as shown in Figure 5-9 (b). This is a reason for 10 kPa boost pressure to experience better combustion rate compared to naturally aspirated engine.

Mass fraction burn rate at 2500 rpm is illustrated in Figure 5-9 (c). At this speed, with increasing boost pressure to 10 kPa it is shown that there is better mass fraction burn rate compared to naturally aspirated condition. This is due to the better mixture preparation effect of boost pressure that results in less ignition delay as shown in the Figure 5-14. Likewise, from combustion duration graph it can be concluded that with boost pressure there is less combustion duration so that fast combustion rate after ignition delay would be resulted.

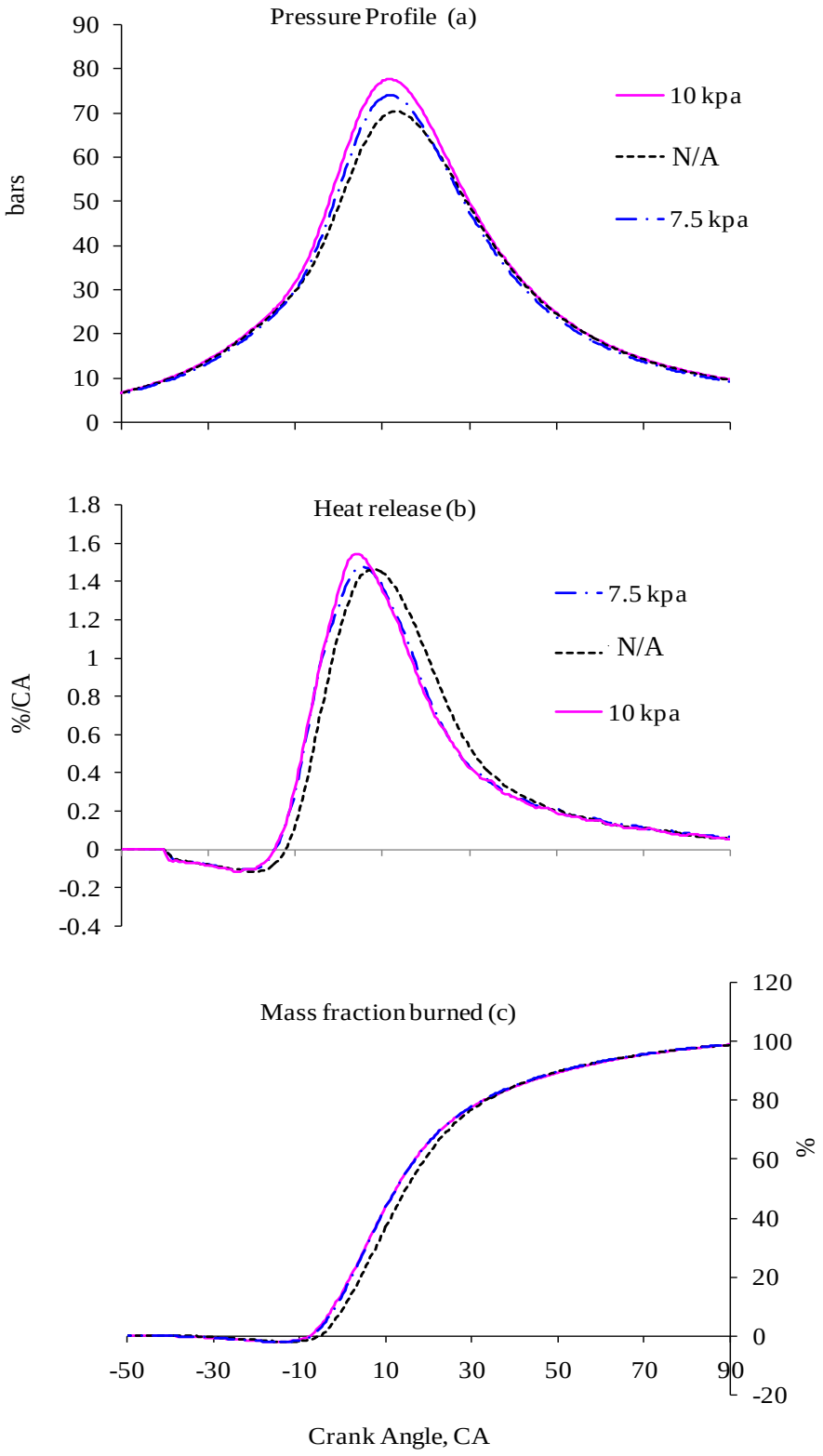

Figure 5-9 Combustion Parameters at 2500 rpm for Different Boost Pressures

The effect of boost pressure on combustion at engine speed of 3000 rpm is illustrated in Figure 5-10. Figure 5-10 (a) shows the in-cylinder pressure for different boost pressure at 3000 rpm. Partial direct injection (180° BTDC) with 10 kPa boost pressure reaches its maximum cylinder pressure at 3000 rpm which is 88 bars. The maximum pressure occurs due to better combustions inside the cylinder chamber.

Heat release rate at 3000 rpm and partial direct injection for different boost pressures is demonstrated in Figure 5-10 (b). As this speed is the engine speed where maximum performance is achieved, the graph clearly shows how heat release rate is taking place in the cylinder once the ignition starts and followed by fast flame propagation. With 10 kPa boost pressure it has been shown that there is fast heat release rate during flame propagation and reached maximum value of 0.037 kJ/CA at 0.5° BTDC while 0.036 kJ/CA at 2° ATDC crank angle for 7.5 kPa boost pressure. 5 and 2.5 kPa have 0.033 kJ/CA at crank angle of 6° ATDC and 0.03 kJ/CA at crank angle of 6.5° ATDC respectively. With naturally aspirated engine the maximum heat release is 0.0358 kJ/CA at 7° ATDC crank angle. This supports the theory of better heat release and fast combustion with increasing boost pressure. With boost pressure there is better heat release so that higher in-cylinder pressure and this resulted in better engine performance.

Mass fraction burned for boost pressures at 3000 rpm and partial direct injection is shown in Figure 5-10 (c). With increasing boost pressure from 2.5 to 10 kPa there is less ignition delay so that fast combustion before and after TDC has been observed. Mass fraction burned graph at 3000 rpm shows that there is less combustion duration with increasing boost pressure. For instance at TDC, with 10 kPa boost pressure 31.6 % of the total mixture combusted has been observed while 22.3% of the total mixture combusted observed for 7.5 kPa boost pressure. With naturally aspirated engine, it is 17.6% of the total mixture combusted has been analyzed at TDC. However, 5 and 2.5 kPa have 17.1% and 4% of mass fraction burned at TDC respectively. In addition, in combustion main stage there is fast combustion with higher boost and it is reason for higher boost pressure to have shorter heat release duration and concentrated heat release process closer to top dead center.

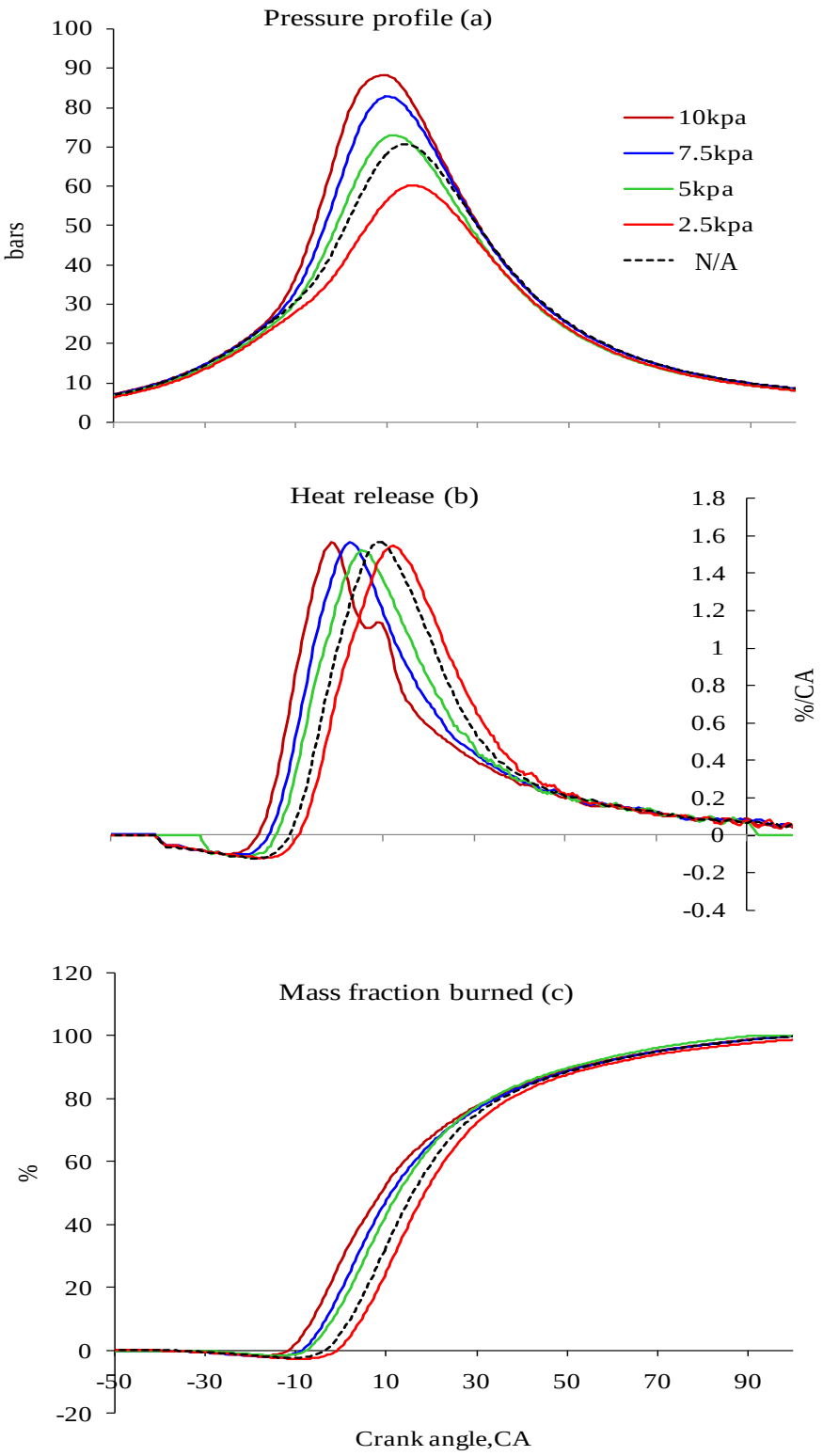

Figure 5-10 Characteristic of Combustion Parameters at 3000 rpm for Different Boost Pressures at Partial Direct Injection.

Combustion parameters at 3500 rpm are explained in Figure 5-11. Figure 5-11 (a) shows the in-cylinder pressure for different boost pressure at 3500 rpm. Maximum cylinder pressure at this speed is 68.8 bars which is much less than that of 3000 rpm for 10 kPa boost pressure. This happened due to the decrease in volumetric efficiency at 3500 rpm. And this confirms where the maximum performance achieved so that better combustion is at 3000 rpm engine speed.

Heat release and mass fraction burned at 3500 rpm and 180° BTDC injection timing are illustrated in Figure 5-11 (b) and (c) respectively. Heat release and mass fraction graph explains effect of boost pressure on combustion. The maximum heat release rate at this speed is 0.034 kJ/CA with boost pressure of 10 kPa. This maximum heat release was observed at crank angle of 6.5° after top dead centre where 27% of mixture burned and it is a phase where fast mass fraction burned takes place.

With boost pressure of 7.5 kPa, the maximum heat release rate is 0.033 kJ/CA at 7° ATDC crank angle where 25.6% mass fraction burned was observed. However, with naturally aspirated condition it has been found that the maximum heat release rate is 0.031 kJ/CA at 6.5° ATDC crank angle where 26% mass fraction burned is observed. This shows that having supercharging system of higher boost pressure would result in better heat release with more mass of fuel combusted that improves the combustion efficiency of the engine.

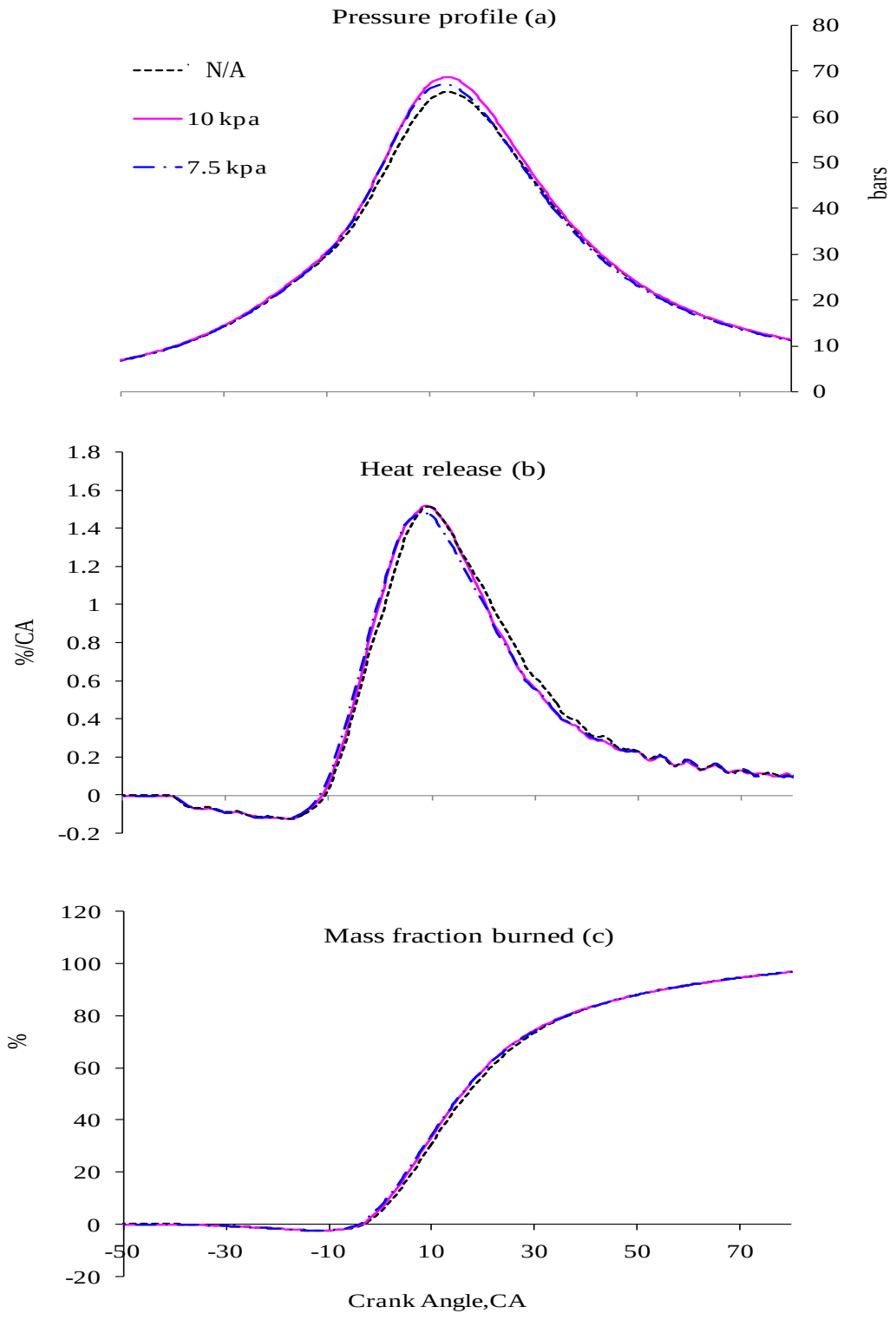

Figure 5-11 Characteristics of Combustion Parameters at 3500 rpm for Different Boost Pressures at Partial Direct Injection

Combustion process characteristics are shown for different boost pressure at 4000 rpm in Figure 5-12. Figure 5-12 (a) shows the in-cylinder pressure for different boost pressure at 4000 rpm. Here the maximum in cylinder pressure with 10 kPa boost pressure is 74 bars which is a bit higher than before. The minimum peak pressure is 58 bars with boost pressure of 2.5 kPa, while it is 71 bars with naturally aspirated engine.

Heat release and mass fraction burned at 4000 rpm and 180° BTDC injection timing are illustrated in Figure 5-12 (b) and (c) respectively. The heat release and mass fraction graph shows better combustion with increasing boost pressure. Despite higher engine speed, heat release graph shows less heat release and thus less combustion efficiency at 4000 rpm compared to 3500 rpm as shown in Figure 5-12 (b). The maximum heat release value is 0.032 kJ/CA at crank angle of 4° ATDC with boost pressure of 10 kPa.

The maximum heat release rate value of 0.028 kJ/CA, which is the minimum value compared to others boost pressure, is seen at 11° ATDC crank angle for boost pressure of 2.5 kPa while it is 0.029 kJ/CA at 7° ATDC crank angle with naturally aspirated engine. This shows that when engine speed is high the performance of 2.5 kPa boost pressure is less compared to naturally aspirated engine. This is due to at this small boost pressure the combined effect of temperature and amount of air supplied to the engine resulted in reduction of volumetric efficiency as discussed before.

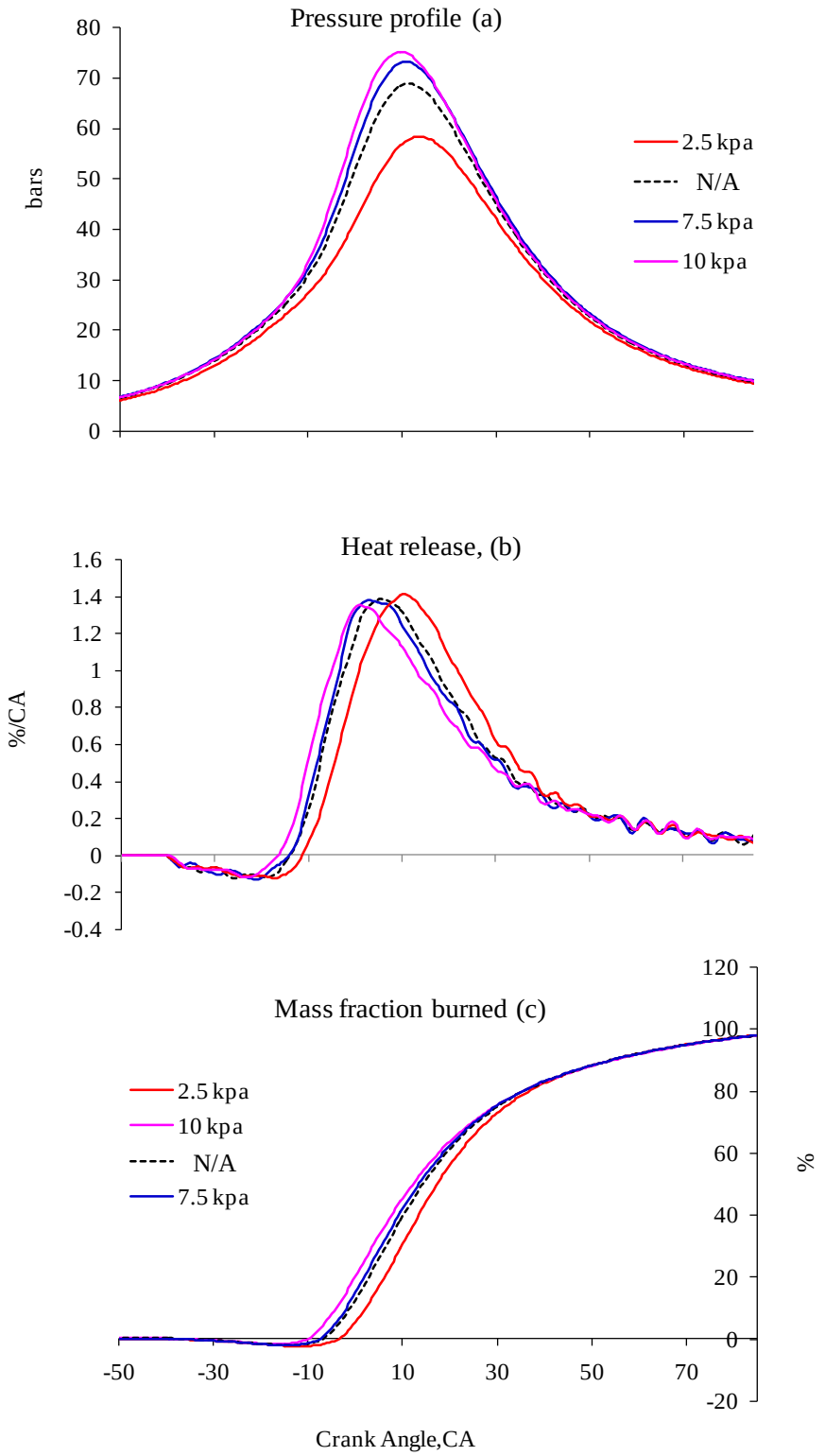

Figure 5-12 Characteristics of Combustion Processes at 4000 rpm for Different Boost Pressures at Partial Direct Injection

Combustion process characteristics at 4500 rpm with boost pressures and injection timing of 180° BTDC are illustrated in Figure 5-13. Figure 5-13 (a) shows the in-cylinder pressure for different boost pressure at 4500 rpm. The maximum peak cylinder pressure that achieved with 10 kPa boost pressure is 64.8 bars while the minimum is 58 bars with 2.5 kPa.

Heat release and mass fraction burned at 4500 rpm are illustrated in Figure 5-13 (b) and (c) respectively. Heat release rate at 4500 rpm for different boost pressure is demonstrated in Figure 5-13 (b). It has been shown that heat release rate is getting better when there is supercharging system. For instance, when boost pressure increased from 7.5 kPa to 10 kPa the trend shows there is higher slope achieved at the main stage. This explains the effect of boost pressure at the flame propagation stage making it fast and lower combustion duration of this stage. And this effect makes in-cylinder pressure to be higher as shown in Figure 5-13 (a). Heat release rate at 4500 rpm can be seen in Figure 5-13 (b). For boost pressure less than 5 kPa there are reverse conditions that have been analyzed.

Figure 5-13 (c) shows mass fraction burned rate versus crank angle for different boost pressure. As explained above, mass fraction graph at this speed shows better mass fraction burned for higher boost pressure taking the same crank angle for all supercharging pressures. This explains there is better mass fraction burned when supercharging system is implemented. Generally, heat release rate and mass fraction burned show that 180° BTDC injection timing doesn’t have enough time for mixture preparation and hence combustion efficiency is reduced at high speeds compared to early injection timing.

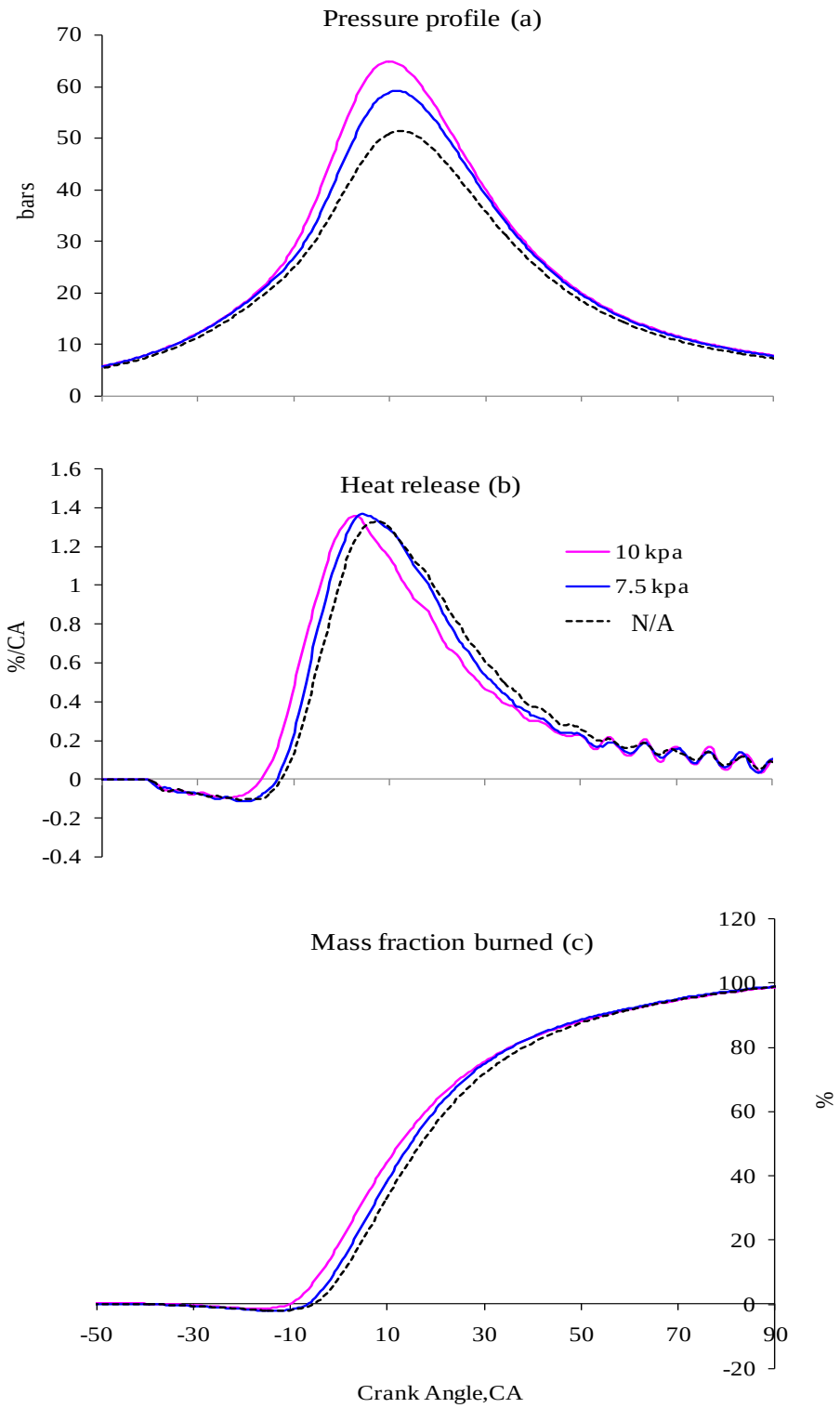

Figure 5-13 Characteristics of Combustion Parameters at 4500 rpm for Different Boost Pressures at Partial Direct Injection

At 5000 rpm engine speed and injection timing of 180° BTDC combustion is not possible when the engine is naturally aspirated as mixture preparation events should be completed before ignition timing. Partial direct injection, 180° BTDC, has been found to have less time for mixture preparation at high speeds. At high speeds mixture preparation needs enough time and thus injection timing should be advanced to early injection timing in order to get better performance of the engine. At 5000 rpm and boost pressure of 7.5 and 10 kPa, it has been found that these boost pressures have combustion event with partial direct injection. This is due to the less ignition delay and fast flame propagation of supercharging that makes mixture preparation event to take place before ignition.

5.4 Experimental Observation of Combustion Stage at Partial Direct Injection

Combustion events at injection timing of 180° BTDC are shown in Figure 5-14. Ignition advance is shown in Figure 5-14 (a). Ignition timing to get the maximum brake torque is shown to advance with boost pressure. With boost pressure above 7.5 kPa the graph shows that ignition advance to get maximum brake torque is higher compared to naturally aspirated engine. This is because of boost pressure is able to make mixture preparation faster compared to naturally aspirated engine. After ignition advance event ignition delay is shown in Figure 5-14 (b). Ignition delay illustrates the time needed for the mixture to start combustion after ignition timing. This parameter has a factor on the combustion efficiency to be better and hence to increase engine performance parameters. The graph shows ignition delay decreases with increasing boost pressure and increasing with increasing engine speed. This is due to the increase in amounts of air as engine speed increases.

Overall combustion duration for boost pressure at injection timing of 180° BTDC is shown in Figure 5-14 (c). The graph shows there is longer duration for naturally aspirated engine compared to boost pressure system. Maximum cylinder pressure for boost pressure at 180° BTDC injection timing is shown in Figure 5-14 (d). With increasing boost pressure peak pressure inside the cylinder is shown to increase. By increasing cylinder pressure the benefit of boost pressure can be seen as mentioned

above. The increase in peak cylinder pressure also figures there is better combustion inside the cylinder and this results in high performance of CNG-DI engine.

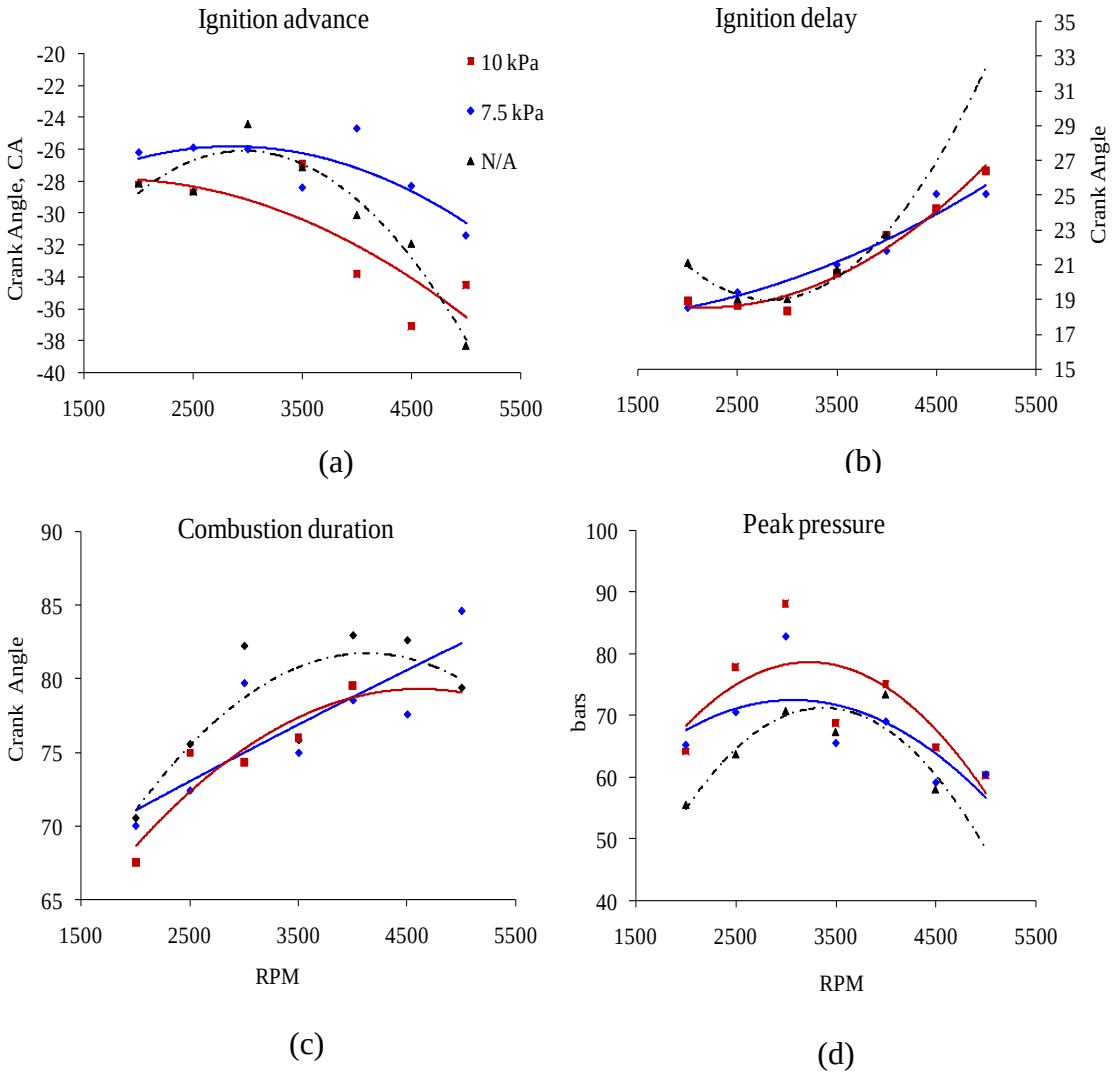

Figure 5-14 Combustion Process Characteristics for Different Boost Pressure at Partial Direct Injection

Figure 5-15 shows indicated mean effective pressure (IMEP) for different boost pressures at injection timing of 180° BTDC. IMEP shows the hypothetical constant pressure which when applied to each piston during the expansion stroke, would give the measured power. IMEP also tells the work transfer from the combustion to the

piston and indicates the combustion process. At 2000 rpm all boost pressures show higher IMEP values compared to naturally aspirated engine. The highest IMEP at this speed is ~ 12 bars with 10 kPa boost pressure while the minimum value is 9.6 bars with naturally aspirated engine. IMEP increased and reached maximum at 3000 rpm engine speed and the highest value at this speed is 12.8 bars with 10 kPa boost pressure. At 2000 rpm there is 8-20% improvement of IMEP with boost pressure of 2.5 kPa to 10 kPa whereas 2-5% improvement for boost pressure of 7.5 and 10 kPa at 3500 rpm compared to naturally aspirated engine. At 5000 rpm it has been shown that there is only 2-3% improvement in IMEP with boost pressure of 7.5 and 10 kPa. This shows that with small boost pressure there is more benefit at low speeds whereas there is not significant improvement for speed 3500 rpm and above. So there is a need to have higher boost pressure for higher speed in order to increase volumetric efficiency.

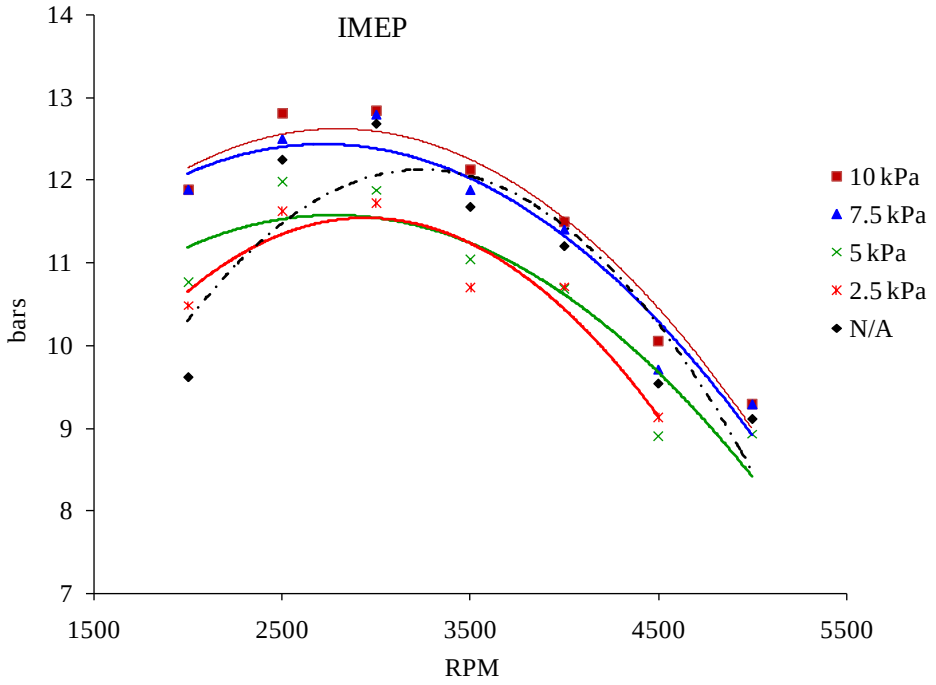

Figure 5-15 Indicated Mean Effective Pressure Characteristic for Different Boost Pressure at Partial Direct Injection.

Coefficient of variation (COV) of IMEP is shown in Figure 5-16. Coefficient of variation explains driveability of the vehicle. Heywood [51] stated that COV values above 10% would give poor driveability.COV for all operation speeds found less than 10% that shows good driveability of the vehicle for both supercharging and non supercharging pressure engine. However, having boost pressure for speed less than 3000 rpm gives lower COV value than naturally aspirated engine which tells good driveability with boost pressure at these speeds. For speed above 3000 rpm and injection timing of 180° BTDC, boost pressure is having COV value higher than naturally aspirated engine. This is due to partial direct injection that doesn't have enough time for mixture preparation at high speeds affects vehicle driveability and seems to have more effect with boost pressure. For 10 and 7.5 kPa, it is found that COV values are less than 5% at all engine speeds while it is above 5% at 2000 rpm for naturally aspirated engine. This seems to support the idea of using supercharging pressure for vehicle good driveability.

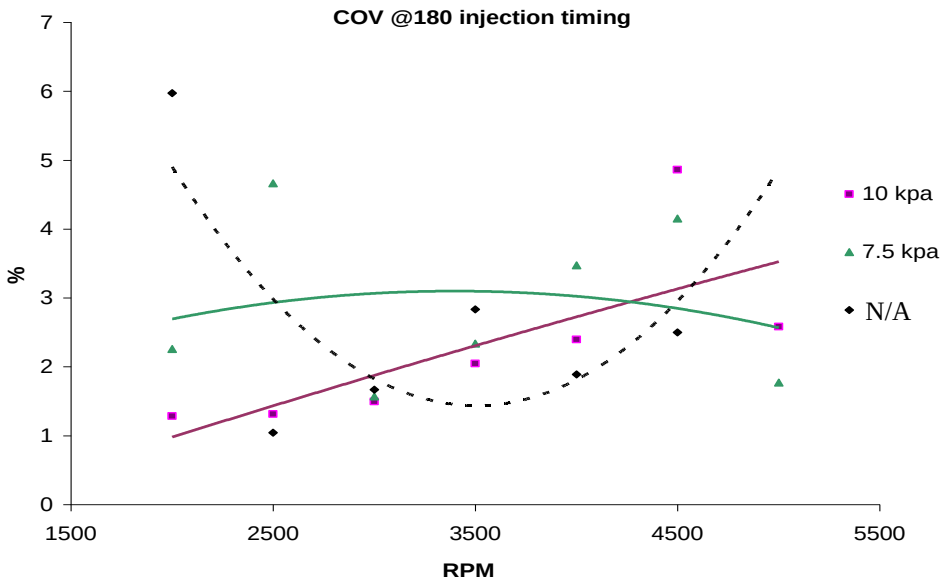

Figure 5-16 Coefficient of Variation of IMEP for Different Boost Pressure at Partial Direct Injection

Combustion efficiency at 180° BTDC for boost pressure relative to naturally aspirated engine is shown in Figure 5-17. The trends for both boost pressure and naturally aspirated engine is the same. Combustion efficiency is getting better when boost pressure starts to increase and this is a reason why boost pressure would result in better combustion inside the cylinder compared to naturally aspirated engine. The graph shows combustion efficiency increases to 3500 rpm and start to decrease when speed increased to 5000 rpm. This might be the reason for torque curve to increases till 3500 rpm and then decrease slowly as speed increased to 5000 rpm. At 2000 rpm, 10 kPa has combustion efficiency of 7% while 2% and 3% higher value than naturally aspirated engine at 3500 and 5000 rpm respectively. The better benefit at low speeds is due to better volumetric efficiency for this boost pressure. For 10 kPa boost pressure the maximum combustion efficiency is 79.6% at a speed of 3500 rpm while the minimum is 74.4% at 2000 rpm.

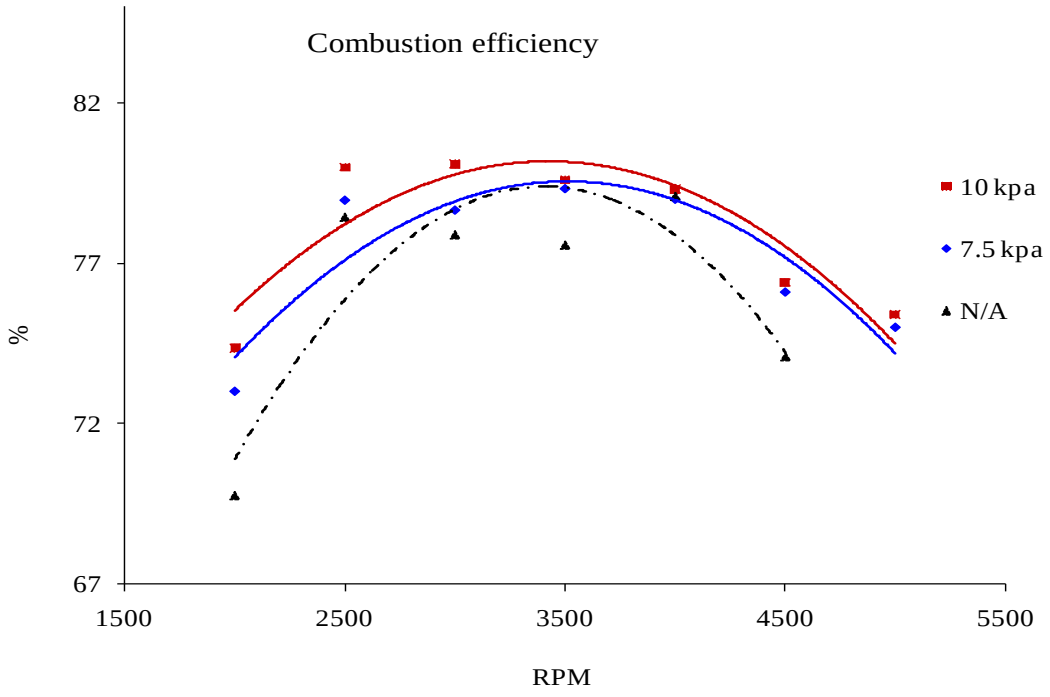

Figure 5-17 Combustion Efficiency for Different Boost Pressures at Injection Timing of 180° BTDC.

5.5 Effect of Boost Pressure on Engine Combustion at 300° BTDC Injection Timing

Effects of boost pressure with early injection timing (300° BTDC) on in-cylinder pressure at different engine operating speeds are studied in Figure 5-18. Pressure profiles are shown at operating speeds for different boost pressure. Figure 5-18 (a) shows in-cylinder pressure at 2000 rpm for different supercharging pressure at early injection timing. At this speed the maximum pressure inside the cylinder is 62.2 bars for 10 kPa boost pressure. The pressure is shown to decrease for decreasing boost pressure however it is better than naturally aspirated engine. The minimum peak pressure at this speed is 49.2 bars for naturally aspirated engine. Here 2.5 kPa has 55 bars peak inside pressure which is greater than naturally aspirated engine. This can be reason for 2.5 kPa to have better performance than naturally aspirated engine as this speed needs less air for combustion to take place. In-cylinder pressure at 2500 rpm for different boost pressure at early injection timing is shown in Figure 5-18 (b). The same condition is seen at 2500 rpm but naturally aspirated engine is having higher inside peak pressure than 5 kPa and 2.5 kPa. When engine speed increased, the amount of air needed inside the cylinder also increases and boost pressure less than 5 kPa has less air rate for the combustion and found to have less inside peak pressure.

Figure 5-18 (c) shows cylinder pressure at 3000 rpm for different boost pressures. At this speed it is shown that the maximum inside pressure for 10 kPa boost pressure is 68.6 bars and this is 12% higher compared to naturally aspirated engine. At this speed, boost pressure of 2.5 and 5 kPa have 5 and 7% lower peak pressure compared to naturally aspirated engine, respectively. Cylinder pressure at 3500 rpm is shown for different boost pressure in Figure 5-18 (d). At this speed and injection timing of 300° BTDC is where the maximum peak pressure observed compared to other operating speeds. Here the peak pressure is 72.7 bars with 10 kPa boost pressure which is 15% higher compared to naturally aspirated engine. This can be a reason for 300° BTDC injection timing to have better performance at high speed compared to 180° BTDC. The same situation is seen for speed above 3500 rpm where 300° BTDC injection timing is performing better. Cylinder pressures for different boost pressure at 4000

rpm and 4500 rpm are explained in Figure 5-18 (e) and (f). For instance, at 4000 and 4500 rpm and with boost pressure of 10 kPa there are 5% and 15% higher peak pressure compared to naturally aspirated engine, respectively. However it was 3% and 11% higher peak pressure at 180° injection timing compared to naturally aspirated engine. This shows the better performance of early injection timing at high speed compared to late injection timing.

In general, the graphs explains that for engine speeds less than 4000 rpm, 300° BTDC has less volumetric efficiency and thus less peak pressures are seen compared to partial direct injection. This is a reason for less combustion efficiency of early injection timing at low engine speeds. For speeds greater than 4000 rpm, 300° BTDC is having high cylinder peak pressure and thus results in better combustion efficiency as seen in figures below. This is because of enough mixture preparation time available for early injection timing at high engine speeds.

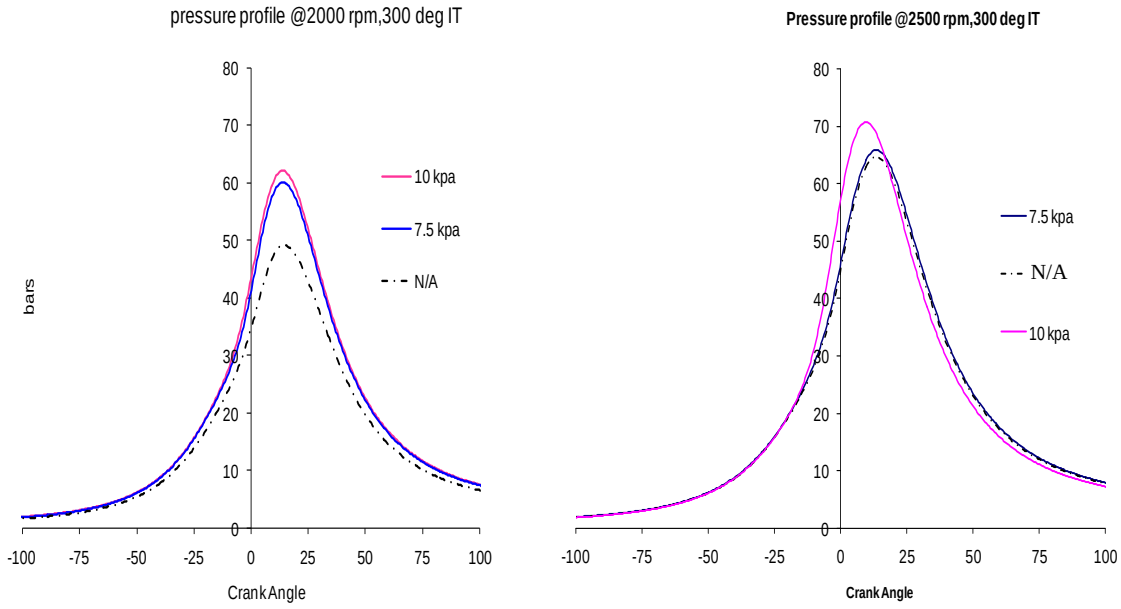

(a) (b)

Figure 5-18 In-Cylinder Pressure for Different Boost Pressures at Injection Timing of 300° BTDC.

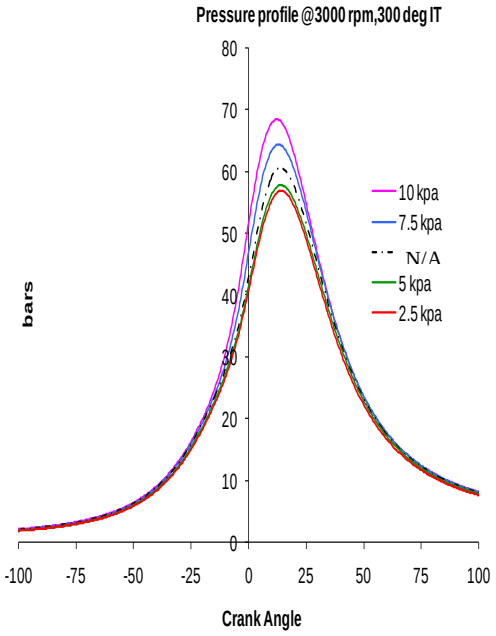

(c)

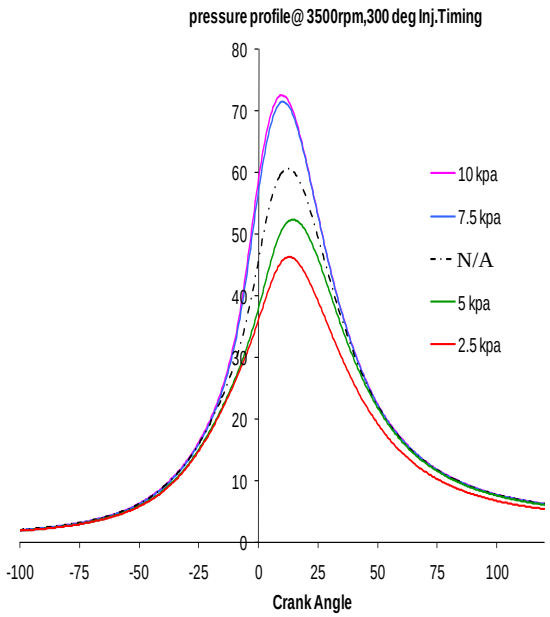

(d)

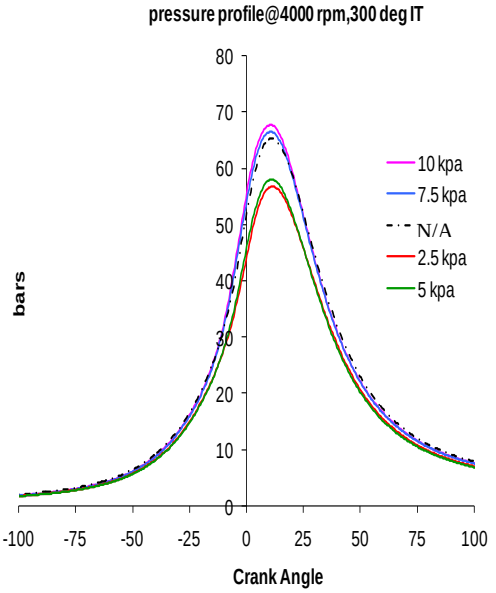

(e)

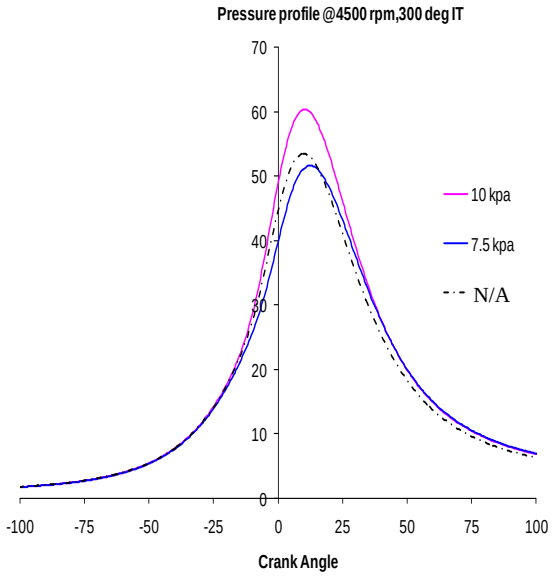

(f)

Figure 5-18 In-Cylinder Pressure for Different Boost Pressure at Injection Timing of 300° BTDC (continuation)

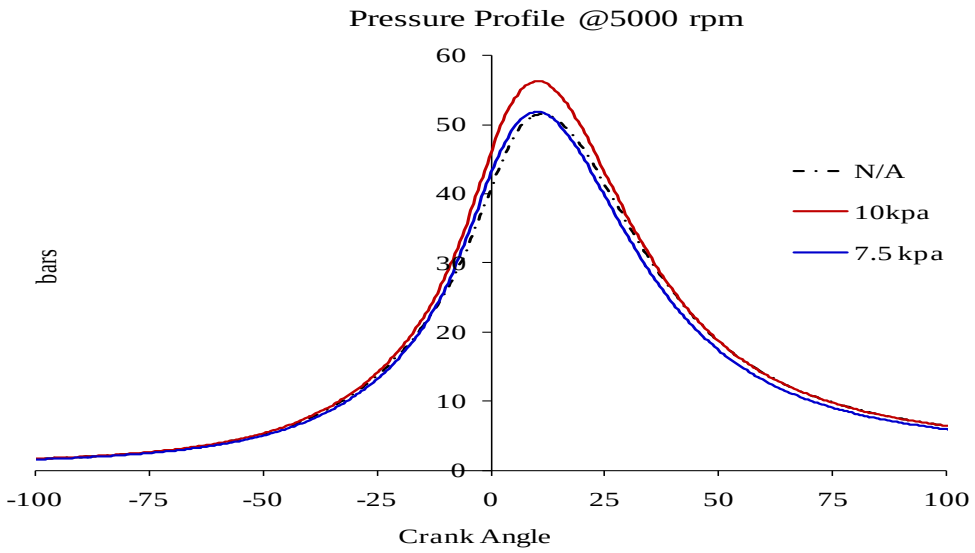

(g)

Figure 5-18 In-Cylinder Pressure for Different Boost Pressure at Injection Timing of 300° BTDC (continuation).

Heat release rate is studied for boost pressures and injection timing of 300° BTDC at operating engine speeds of 2000 to 5000 rpm in Figure 5-19. Het release rate at 2000 rpm and early injection for supercharging system is shown in Figure 5-19 (a). At 2000 rpm and boost pressure of 10 kPa, the maximum heat release rate is 0.03 kJ/CA at crank angle of 9° ATDC while it is 0.025 kJ/CA at 11° ATDC crank angle with naturally aspirated engine. This shows the better performance value of boost pressures compared to naturally aspirated engine. At this speed, with 10 kPa supercharging pressure the highest heat release value of 180° BTDC is 0.031 kJ/CA while it is 0.03 kJ/CA for 300° BTDC injection timing. This shows the better performance value of partial direct injection compared to early injection at this speed. Figure 5-19 (b) shows the heat release rate at 2500 rpm for different supercharging pressure. At 2500 rpm and injection timing of 300° BTDC, the maximum heat release for 10 kPa boost pressure is 0.03 kJ/CA at crank angle of 6.5° ATDC while it is 0.035 kJ/CA at 3° ATDC crank angle for 180° BTDC injection timing which shows the better combustion of late injection at this speed. Figure 5-19 (c) illustrates the heat release rate of supercharging system at 3000 rpm. With 10 kPa boost pressure the maximum heat release rate at 3000 rpm is 0.029 kJ/CA at 11° ATDC crank angle which is 18%

lower than that of 180° BTDC injection timing. This proves the better performance of late injection timing at 3000 rpm.

Heat release rate of supercharging system at 3500 rpm engine speed is explained in Figure 5-19 (d). At 3500 rpm and injection timing of 300° BTDC, it has been shown that the maximum heat release is with 10 kPa boost pressure that is 0.03 kJ/CA which is better than that of 3000 rpm, 0.029 kJ/CA. This shows there is no significant difference on heat release at this speed for both injection timings. At 4000 rpm and injection timing of 300° BTDC, the heat release graph in Figure 5-19 (e) shows there is 15% lower heat release than that of 180° BTDC injection timing for 10 kPa boost pressure. Heat release rate at 4500 rpm and early injection timing for different boost pressures is demonstrated in Figure 5-19 (f). At this speed the maximum heat release is 0.022 kJ/CA at 3° after top dead centre which is 12% better heat release than naturally aspirated engine. 300° BTDC injection timing has better heat release rate and combustion efficiency than 180° BTDC injection timing at speed greater than 4500 rpm. Figure 5-19 (g) shows the heat release rate at 5000 rpm for different boost pressures and early injection timing. The same event is seen at 5000 rpm where better combustion is observed for higher boost pressure and early injection timing.

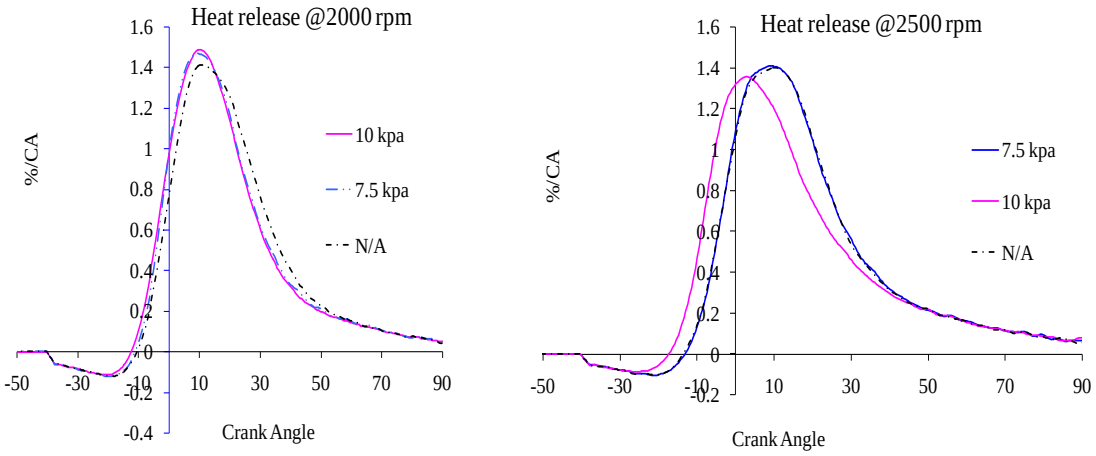

(a) (b)

Figure 5-19 Heat Release Rate for Boost Pressures at Injection Timing of 300° BTDC

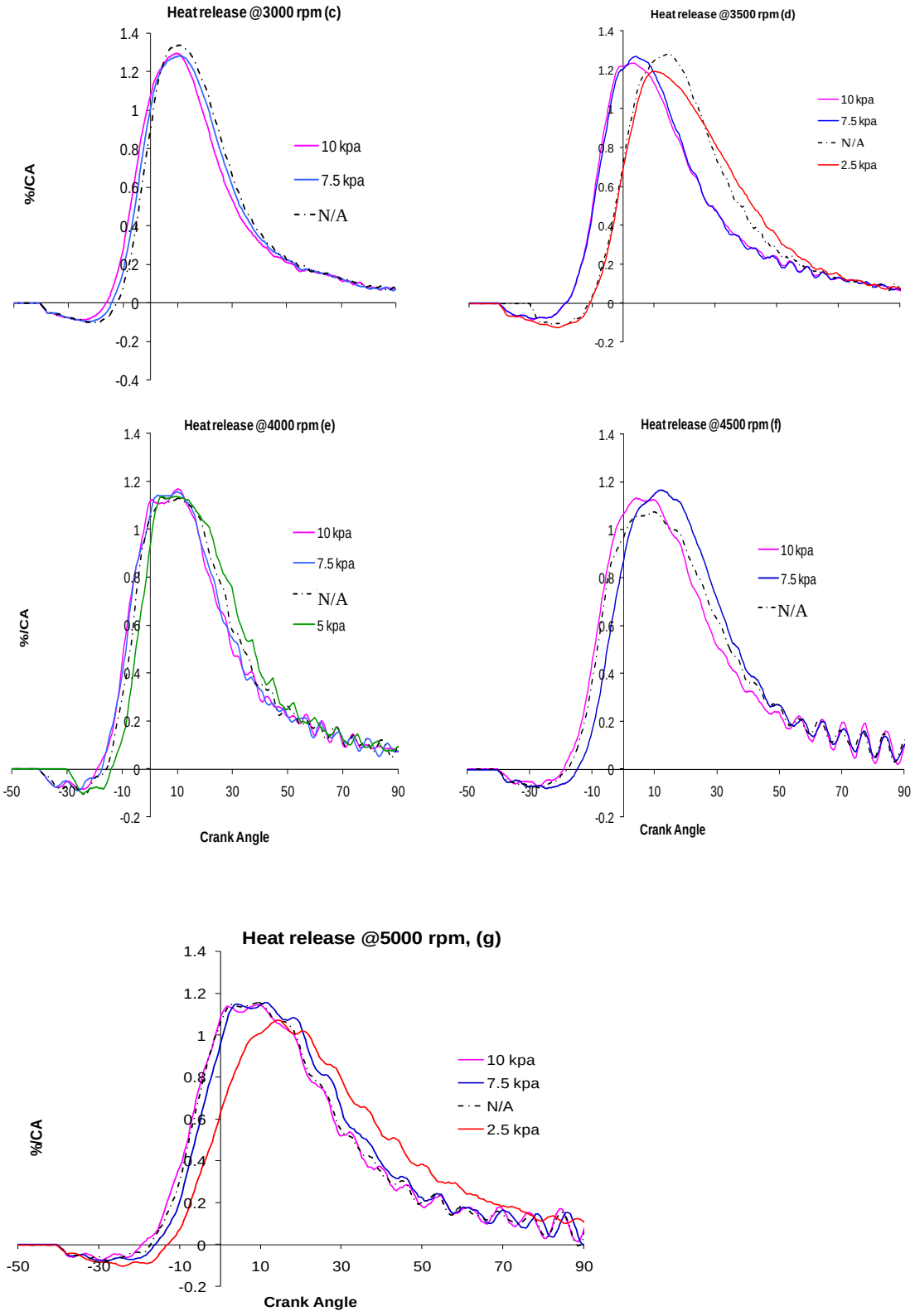

Figure 5-19 Heat Release for Boost Pressure at Injection Timing of 300° BTDC (contd.)

Mass fraction burned is explained in the following section for different boost pressures and early injection timing, 300° BTDC. Mass fraction burned is shown for engine operating speeds of 2000 to 5000 rpm and supercharging pressures in Figure 5-20. Figure 5-20 (a) shows mass fraction burned at 2000 rpm for supercharging pressures. Here it can be seen that when boost pressure becoming high ignition delay is lower and higher burn rate is followed. For instance at top dead center, 10 kPa boost pressure has 9% mass fraction burned where as 7.5 kPa boost pressure and naturally aspirated engine have 7 and 4% mass fraction burned respectively. This shows the better mass burn rate as supercharging system is implemented. Figure 5-20 (b) shows the mass fraction burned at engine speed of 2500 rpm and port injection timing. As can be seen from the graph, the flame propagation stage shows fast mass burn rate when boost pressure becomes higher. At top dead center, 10 kPa boost pressure has 15% mass fraction burned while 7.5 kPa boost pressure and naturally aspirated engine have 11 and 10% mass fraction burned, respectively. Mass fraction burned at this speed and the same crank angle like 2000 rpm shows there is better mass fraction burned as the speed increased to 2500 rpm. This is due to the better combustion efficiency of this speed compared to 2000 rpm. Mass fraction burned at 3000 rpm is shown in Figure 5-20 (c). Around this speed experimental data shows there is higher combustion heat release rate because of higher volumetric efficiency of the engine. Mass fraction burned shows the same trend like before. For instance at TDC, 10 kPa boost pressure has 16% mass fraction burned while 7.5 kPa has 12% mass fraction burned. This proves the higher the boost pressure the faster mass fraction burned in the cylinder. Figure 5-20 (d) shows the mass fraction burned at 3500 rpm engine speed. At top dead center, 10 kPa boost pressure has 24% mass fraction burned while 7.5 kPa and naturally aspirated engine have 22 and 11% mass burn rate respectively. However, 5 and 2.5 kPa boost pressure have 6 and 4% mass fraction burned at TDC respectively. Compared to other speed, the fast burn rate has been observed and this can be a reason for the maximum combustion efficiency of the engine to be at this speed.

Mass fraction burned at 4000 rpm is shown in Figure 5-20 (e). Experimental value shows mass fraction burned at this speed is less than that of 3500 rpm. For instance, at

top dead center, 10 kPa boost pressure has 20% mass fraction burned while 7.5 kPa has 19% and naturally aspirated engine has 15% mass fraction burned. However, 5 and 2.5 kPa have 14 and 13% mass fraction burned respectively. Mass fraction burned at 4500 and 5000 rpm are explained in Figure 5-20 (f) and (g). The same conclusion can be reached from the graph that when there is supercharging system it helps at all speed to have better mass fraction burned. At 45000 rpm and 10 kPa boost pressure there is 20% mass fraction burned while it is 18% mass fraction burned at 5000 rpm for the same boost pressure of 10 kPa. 7.5 kPa boost pressure has 14% mass fraction burned at 4500 rpm and it has 13% mass fraction burned at 5000 rpm at top dead centre. This shows the decrease in combustion efficiency as the speed increased from 4000 to 5000 rpm.

Mass fraction burned supports the previous idea that when there is high boost pressure there is better mass fraction burned at all operating engine speeds. Especially, with boost pressure it has been shown that there is high mass fraction rate after ignition delay and before 10° ATDC crank angle. Beside, ignition delay is shown to be less for boost pressure at all operating engine speeds. This is the reason for boost pressure to experience better combustion and hence engine performance than naturally aspirated engine.

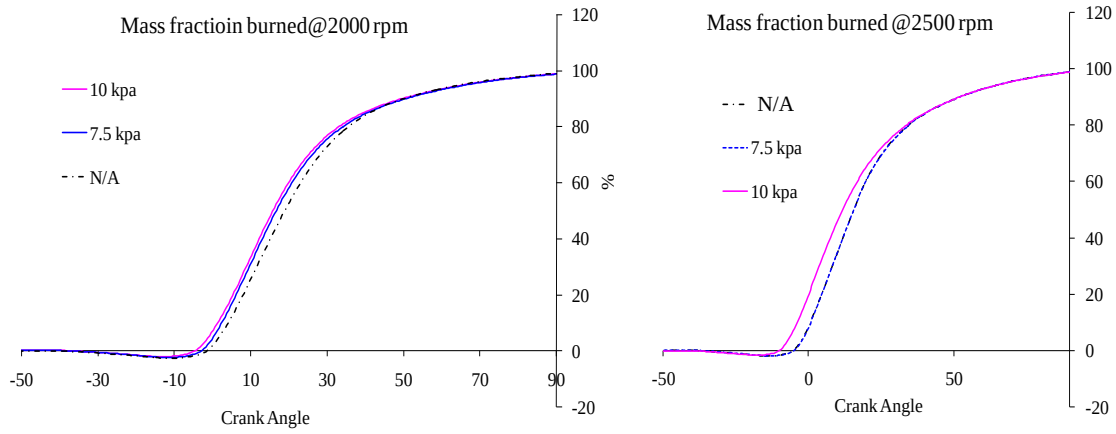

(a) (b)

Figure 5-20 Mass Fraction Burn for Boost Pressure at Injection Timing of 300° BTDC

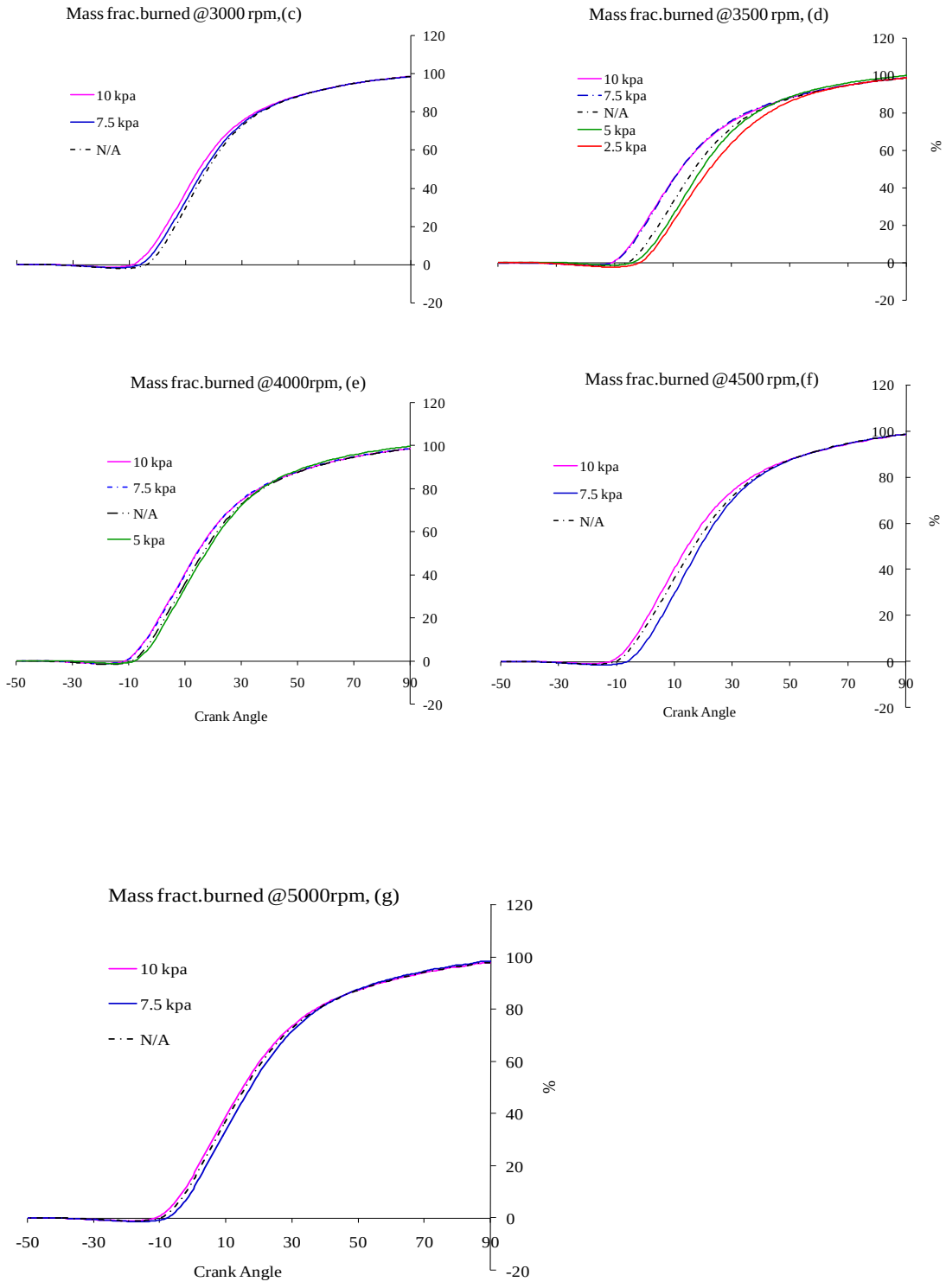

Figure 5-20 Mass Fraction Burned for Different Boost Pressures at injection Timing of 300° BTDC (continuation).

5.6 Experimental Observation of Combustion Stage for Early Injection Timing, 300° BTDC

Combustion process with boost pressure and injection timing of 300° BTDC is discussed in Figure 5-21. Here starting from ignition advance where we set to get maximum brake torque to end of combustion is discussed. Figure 5-21 (a) Shows ignition advance at 300° BTDC injection timing. At this injection timing and boost pressure of 10 kPa, ignition timing is advanced compared to naturally aspirated engine. This might be due to the better mixture preparation of supercharging that helps the combustion event to start earlier than naturally aspirated engine. Ignition delay graph is illustrated in Figure 5-21 (b). There is no significant variation in ignition delay though there is less ignition delay period is seen with supercharging system. For early injection timing and boost pressure above 7.5 kPa it is shown that there is less ignition delay period for engine speeds above 4000 rpm than speeds less than 4000 rpm compared to without supercharging. This could be a reason for 300° BTDC injection timing with supercharging to perform better for speed above 4000 rpm. This illustrates the benefit of supercharging with early injection timing on high engine speeds than on low engine speeds.

Overall combustion duration is shown in Figure 5-21 (c). This graph shows there is shorter combustion duration with boost pressure at 300° BTDC that might result in fast combustion rate of supercharging system. The graph proves as boost pressure has significant effect on combustion efficiency by making combustion duration to be completed faster compare to naturally aspirated engine. Maximum inside pressure for early injection timing is shown in Figure 5-21 (d). Here maximum inside pressure is shown to increase as boost pressure increases and this considered to have significant effect on engine combustion.

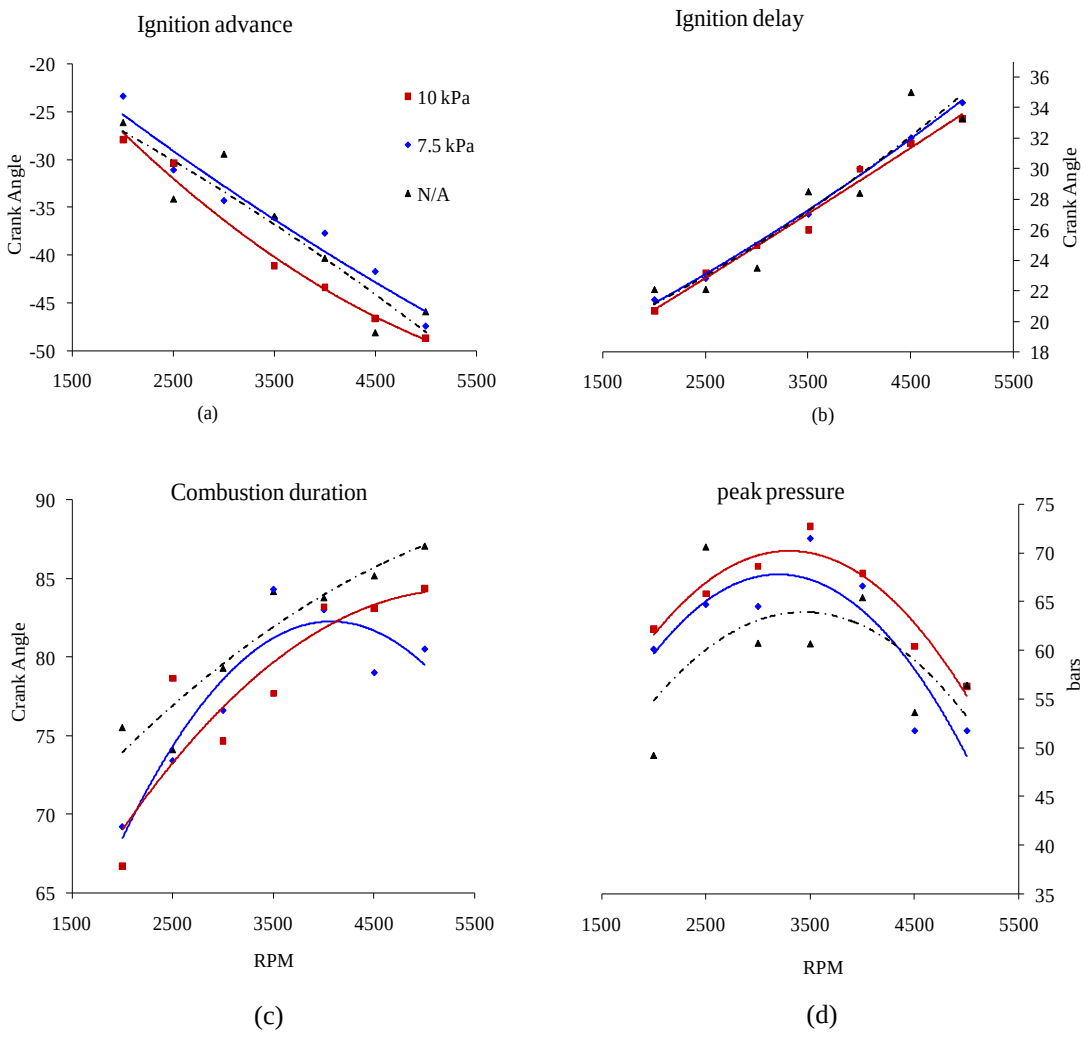

Figure 5-21 Combustion Process Characteristics for Different Boost Pressures at 300° BTDC Injection Timing

It can be concluded that early injection timing, 300° BTDC, has better combustion efficiency for speeds above 4000 rpm whereas 180° BTDC seems to have better combustion process for speeds less than 4000 rpm for the same boost pressure. With supercharging, injection timing of 180° BTDC has better combustion event with some stratification to occur that results in higher combustion efficiency at low speed. However, 180° BTDC doesn't look to have enough mixture preparation time at high speeds as these speeds need long time for mixture preparation before ignition events come.

Indicated Mean Effective Pressure (IMEP) is shown for different boost pressures at 300° BTDC injection timing in Figure 5-22. The same trend is shown here like 180° BTDC injection timing. IMEP increases till 3000 rpm and then starts to decrease as speed increased to 5000 rpm. The maximum IMEP achieved here is ~ 12 bars at 3000 rpm and 10 kPa boost pressure while it is 12.8 bars at 180° BTDC injection timing. At 2000 rpm and with boost pressure above 2.5 to 10 kPa there is 9-19% more IMEP value than naturally aspirated engine. At this speed, 300° BTDC is having 5% lower IMEP value than 180° BTDC for 10 kPa boost pressure. IMEP at 5000 rpm and 10 kPa boost pressure is ~9.5 bars for 300° BTDC injection timing while it is ~9.2 bar for 180° BTDC injection timing. In addition the graph shows better IMEP at 300° BTDC injection timing for speed above 3500 rpm compared to 180° BTDC injection timing. IMEP for speed less than 3500 rpm is having 5-9% lower IMEP value for 300° BTDC injection timing compared to 180° BTDC injection timing. As mentioned above, this is due to the better volumetric efficiency of 180° BTDC injection timing compared to 300° BTDC injection timing at low speeds.

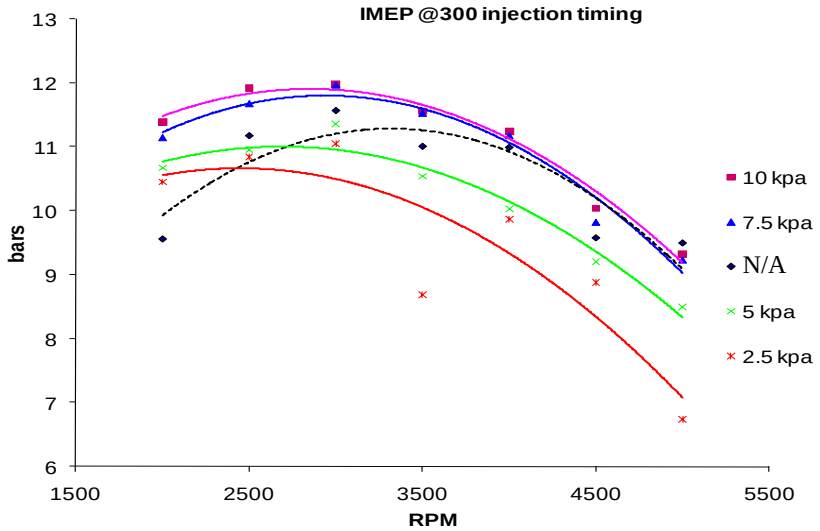

Figure 5-22 Indicated Mean Effective Pressure for Different Boost Pressure at 300° BTDC Injection Timing

Coefficient of variation (COV) of indicated mean effective pressure at injection timing of 300° BTDC is illustrated in Figure 5-23. Coefficient of variation is expected

less than 10% for good driveability of the vehicles. At 300° BTDC injection timing COV is less than 5% at all operating engine speeds for both boost pressure of 7.5 and 10 kPa. However, COV is seen above 5% for naturally aspirated engine at speeds less than 2500 rpm. Yet it is less than 10% that shows good driveability of the vehicle. COV graph shows decreasing COV values with increasing engine speed which reveals more stability of the engine with boost pressure as engine speed increases. For instance COV value at 5000 rpm for 10 kPa boost pressure is 1.6% while it is 2.6% for 180° BTDC injection timing. For speed above 3500 rpm, COV of IMEP values for 300° BTDC injection timing are found to be lower than 180° BTDC injection timing. This is a reason for 300° BTDC injection timing to experience more engine stability at high speeds compared to partial direct injection. Boost pressure above 7.5 kPa and naturally aspirated engine exhibit the lowest COV values at 5000 rpm for 300° BTDC injection timing which indicates good combustion at this speed.

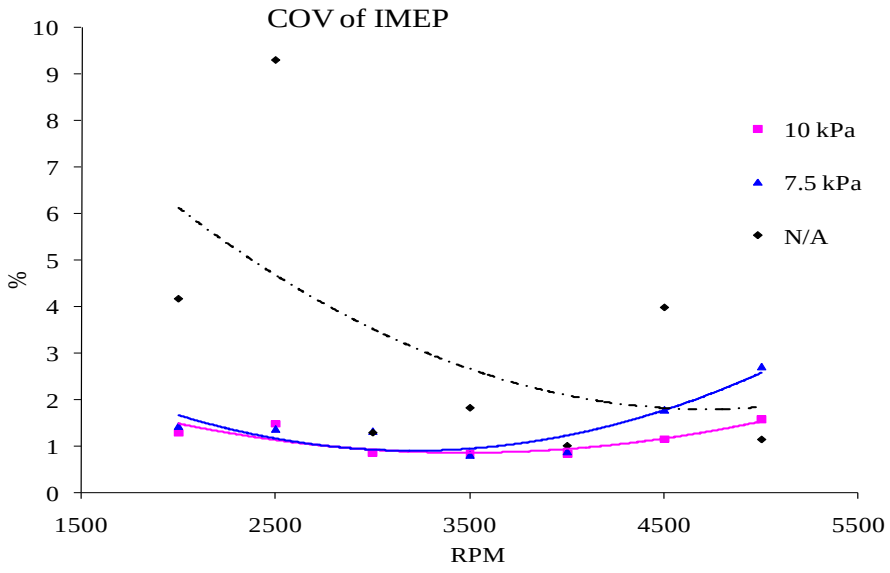

Figure 5-23 Coefficient of Variation of IMEP for Different Boost Pressures at 300° BTDC Injection Timing

Combustion efficiency for different boost pressures at 300° BTDC injection timing is illustrated in Figure 5-24. The results of combustion efficiency of boost pressure are

compared to naturally aspirated engine values that are indicated in hidden line. Combustion efficiency values increases till 4000 rpm and then decreases slowly when speed increased to 5000 rpm. Better combustion efficiency can be achieved for higher boost pressure as shown in the Figure 5-24. 300° BTDC injection timing has 4-6% higher combustion efficiency than 180° BTDC for speed greater than 3000 rpm. This illustrates the better combustion process with less COV of IMEP of 300° BTDC injection timing at high speed. With boost pressure less than 10 kPa and 300° BTDC injection timing, it has been shown that there is 1-3% lower combustion efficiency compared to 180° BTDC injection timing for engine speed less than 3500 rpm. This is because of some stratification formed at low speeds with partial direct injection that enhances combustion process.

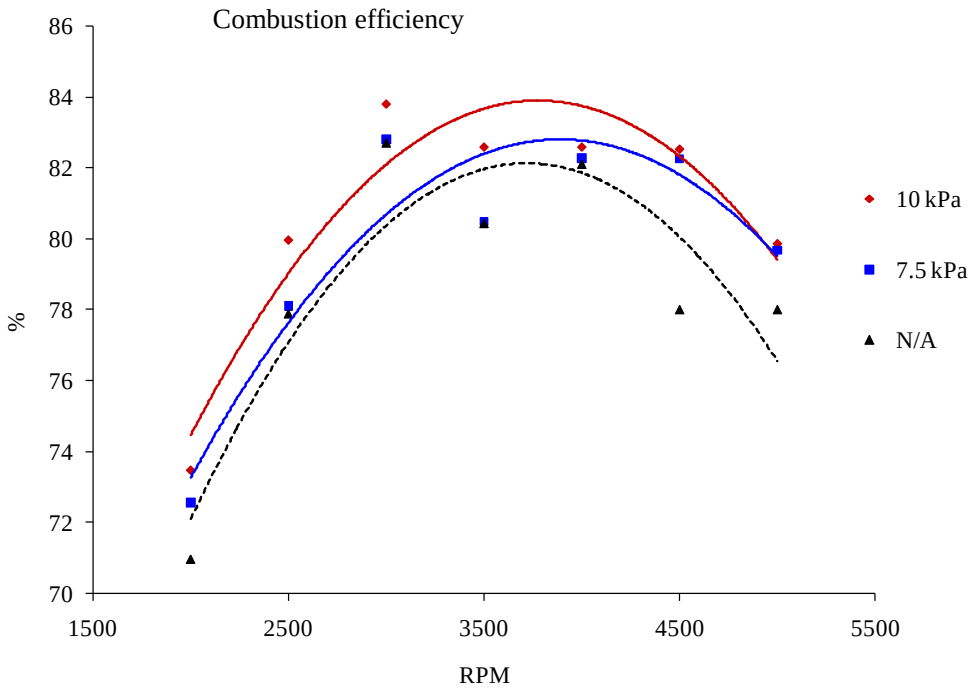

Figure 5-24 Combustion Efficiency for Different Boost Pressures at 300° BTDC Injection Timing

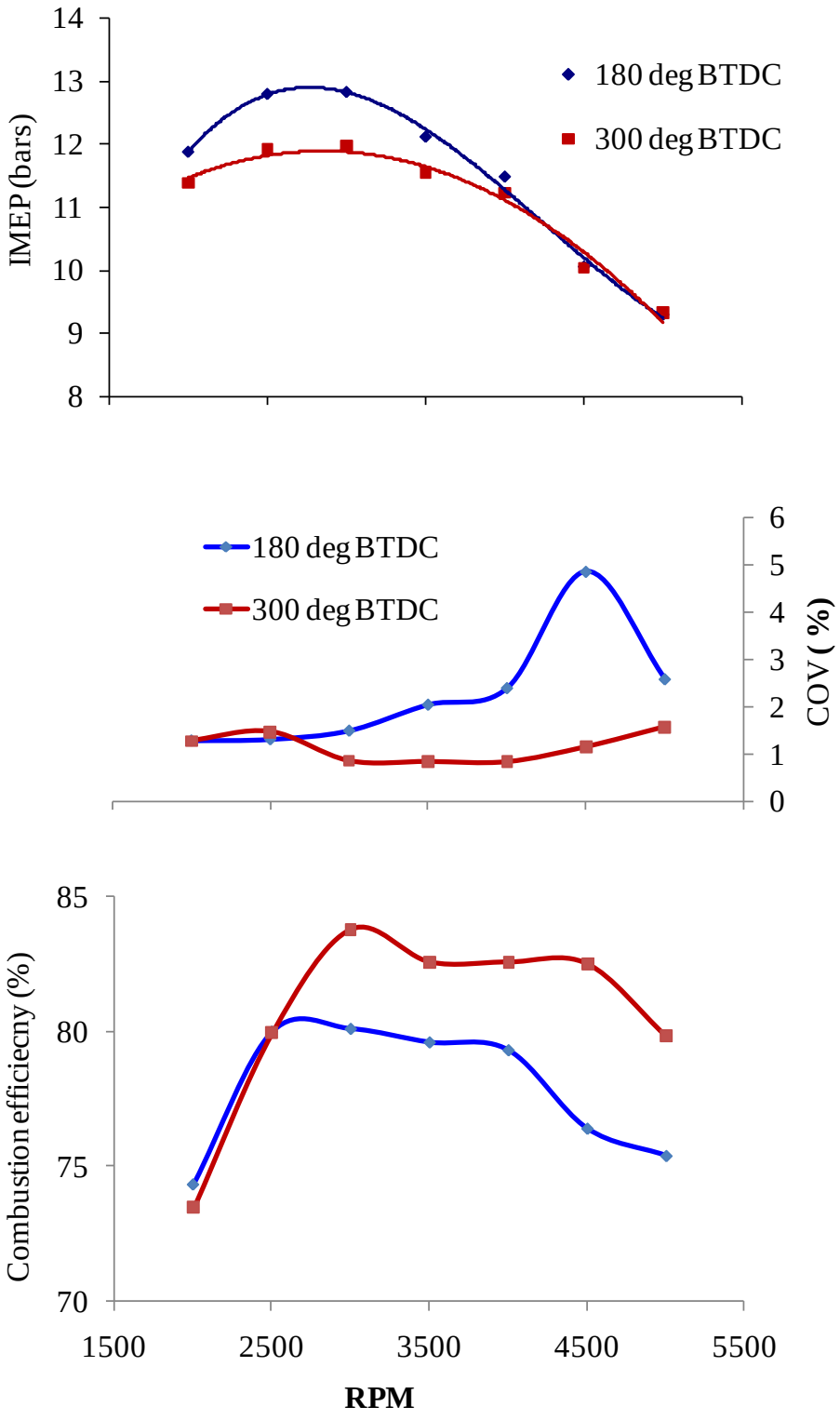

Figure 5-25 Effect of Injection Timing on IMEP, COV and Combustion Efficiency of Engine at 10 kPa Boost Pressure

IMEP, COV of IMEP and Combustion efficiency are shown for boost pressure of 10 kPa at partial direct injection and port injection timing in Figure 5-25. IMEP values for 180° BTDC injection timing is higher than 300° BTDC for speed lower than 4000 rpm. This illustrates the better performance values of early injection timing at high engine speeds. COV of IMEP and combustion efficiency graph prove that early injection timing can help supercharging system to perform better by maintaining engine stability at high speed compared to late injection timing. COV of IMEP values for both injection timing is less than 5% that shows engine stability with supercharging system at all operating engine speeds. 180° BTDC injection timing has better combustion efficiency and COV values for speed lower than 3000 rpm beside high performance values for speed less than 4000 rpm.

5.7 Effect of Boost Pressure on Engine Emissions at 180° BTDC Injection Timing

Engine emissions for different boost pressure are presented at 180° BTDC injection timing in Figure 5-26. NOx emission is shown in Figure 5-26 (a). NOx emission depends mainly on maximum temperature in combustion chamber. As stated before, boost pressure has an ability to increase in cylinder pressure and combustion temperature. In consequence, with increasing boost pressure it is shown that there is an increase in NOx emission. This is due to the fact that boost pressure can increase combustion temperature and this resulted in increase NOx emission. The variation of NOx emission increases when engine speed increased to 3000 rpm and then decrease and finally for engine speed above 4500 rpm the variation is not significant. For instance, with boost pressure of 10 kPa there is 40% and 50% higher NOx emission at 2000 and 3000 rpm respectively compared to naturally aspirated engine. The maximum NOx emission is at 3000 rpm with 10 kPa boost pressure that is 2959.8 ppm. A higher production of NOx emission when boost pressure is increased can be a reason for better combustion efficiency of supercharging system. At high engine speeds and 180° BTDC injection timing, it is shown that NOx variation is not significant. This is possibly due to improper mixture preparation as this injection timing experiences less mixture preparation period.

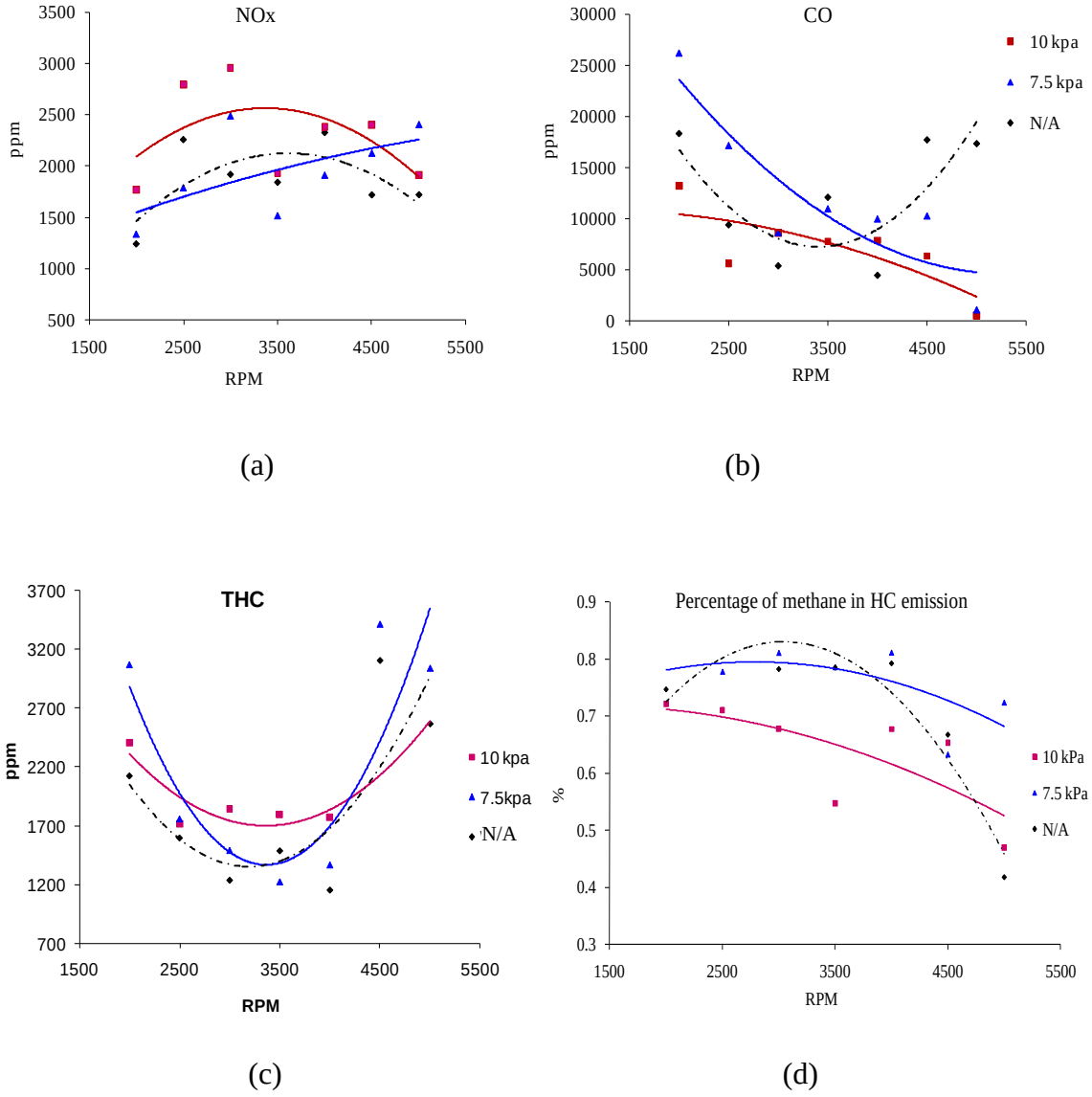

Figure 5-26 Exhaust Emissions for Different Boost Pressure at 180° BTDC Injection Timing

Carbon monoxide emission for different boost pressure at 180° BTDC injection timing is shown in Figure 5-26 (b). A decrease in carbon monoxide emission is shown as the engine speed increased from 2000 rpm to 5000 rpm. The same trend is shown for both boost pressures and naturally aspirated engine. With 7.5 kPa boost pressure CO emission doesn't have significant variation compared to naturally aspirated engine

while with 10 kPa boost pressure there is some benefit is seen as shown in Figure. For instance, at 2000 rpm and with boost pressure of 10 kPa there is 20% lower CO emission compared to naturally aspirated engine. This effect is probably due to boost pressure improves brake specific fuel consumption and thus reduce CO emission. With this boost pressure it is also shown that there is insignificant effect in CO emission variation compared to naturally aspirated engine when speed increased from 2500 to 3500 rpm. However, when speed increased from 3500 to 5000 rpm, 10 kPa boost pressure gives 5-30% lower emission than naturally aspirated engine. This shows as boost pressure increased there is reduction in CO emission because of better specific fuel consumption inside the chamber that indicates completeness of combustion.

Hydrocarbon emission is shown for different boost pressure at 180° BTDC injection timing in Figure 5-26 (c). Hydrocarbon emissions decreases when speed increased to 3500 rpm and then start to increase as speed increased to 5000 rpm for both boost pressure and naturally aspirated engine. The decrease in hydrocarbon emissions from speed 2000 rpm to 3500 rpm is due to the better combustion of 180° BTDC injection timing as this injection timing has increased volumetric efficiency when speed increased to 3000 rpm. With increased boost pressure it is seen that there is no significant variation in hydrocarbon emission. Moreover, it is shown that for small boost pressure there is no significant effect of boost pressure in hydrocarbons emissions though increased boost pressure expected to improve hydrocarbon emission.

Percentage of methane in total hydrocarbon emissions is discussed in Figure 5-26 (d). With partial direct injection and supercharging system, it has been shown that percentage of methane decreases with increasing boost pressure. With increasing engine speed percentage of methane in total hydrocarbon is also shown to decrease. For instance, with 10 kPa boost pressure the percentage of methane decreases from 70% to 40% when engine speed increased from 2000 to 5000 rpm. The same trends were shown with boost pressure of 7.5 kPa whereas percentage of methane increases till 3000 rpm and then decreases with increasing engine speed for naturally aspirated

engine. At high engine speeds, there is no significant difference in percentage of methane with small boost pressure compared to naturally aspirated engine.

5.8 Effect of Boost Pressure on Engine Emissions at 300° BTDC Injection Timing

Engine Emissions for different boost pressure at 300° BTDC injection timing are studied in Figure 5-27. NOx emission is shown for different boost pressure at port injection timing in Figure 5-27(a). NOx emission shows the same trends like 180° BTDC injection timing. Both of them show the increase in NOx emission as boost pressure is increased that reveals the better combustion with boost pressure. Higher NOx emission is mainly due to the higher temperature inside the cylinder and this happens because of higher pressure created with boost pressure that enhances the engine performance. Early injection timing shows the same event as explained in Figure below. This injection timing has higher NOx for speed greater than 3000 rpm compared to 180° BTDC injection timing. For instance, with boost pressure of 10 kPa and for speed above 3000 rpm there is 10-60% higher NOx emission compared to naturally aspirated engine while it is 5-50% higher NOx emission at 180° BTDC injection timing. This can be one reason for early injection timing seems to have better combustion efficiency at high engine speeds. For speed lower than 3000 rpm and early injection timing, there is 0-50% higher NOx emission compared to naturally aspirated engine while it is 40-50% higher NOx for partial injection,180° BTDC. This proves that 180° BTDC injection timing performs better than early injection timing for speed less than 3500 rpm for the same boost pressure.

Carbon monoxide emission with boost pressure and injection timing of 300° BTDC is demonstrated in Figure 5-27 (b). Carbon monoxide emission will tell combustion event happening in combustion chamber. Carbon monoxide emission usually happens because of incomplete combustion inside the cylinder. With boost pressure and 300° BTDC injection timing, it is shown that CO emission decreases as speed increased from 2000 to 5000 rpm. And lower emission of CO is observed with boost pressure compared to naturally aspirated engine. For instance with boost pressure of 10 kPa and for speed ranging from 2000 to 3500 rpm there is 10-50% lower CO emissions

while it is 35-50% lower emission for speed ranging from 3500 to 5000 rpm compared to naturally aspirated engine. This lower CO emission at high engine speeds compared to low speeds for early injection timing is due to better mixture preparation for high speed than low speed where weak mixing event happened with early injection timing. This is reason for early injection timing to have better performance at high engine speeds than low speeds compared to late injection timing for the same boost pressure.

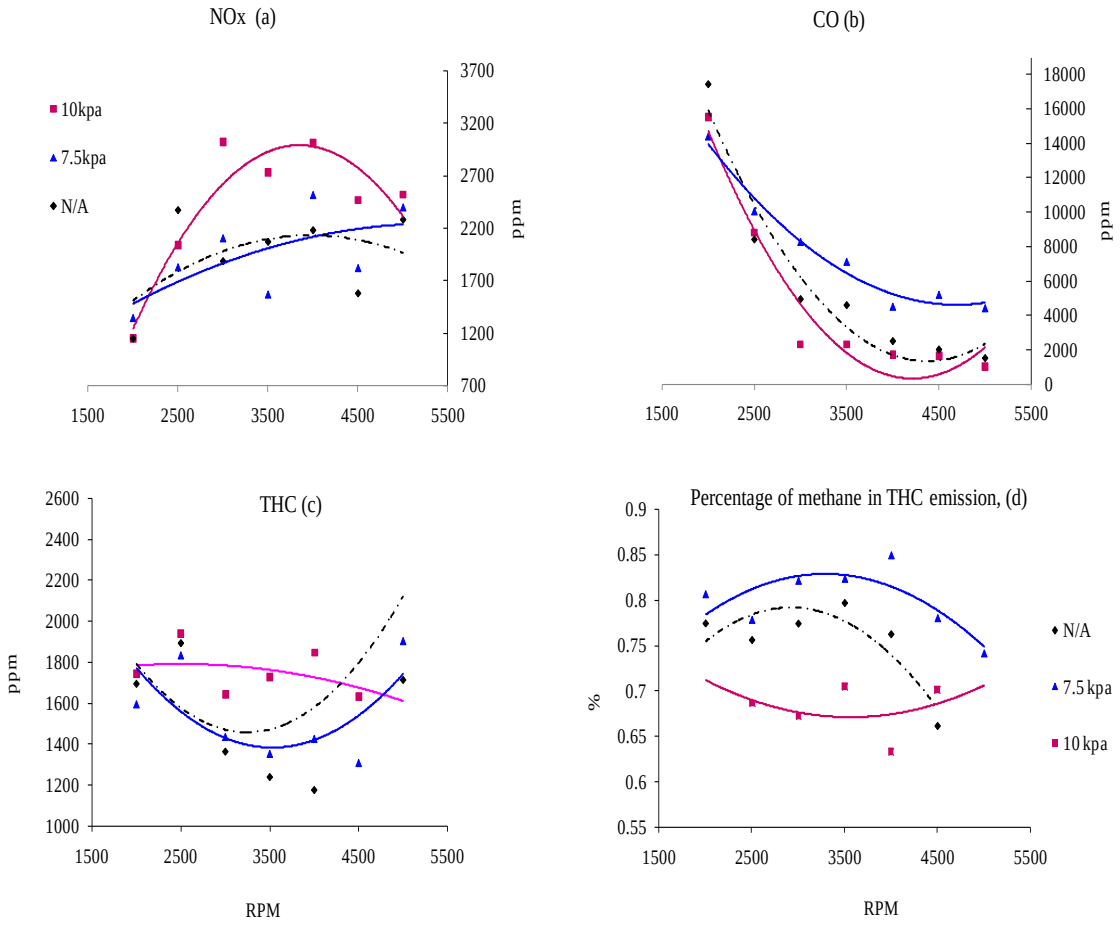

Figure 5-27 Exhaust Emissions of Boost Pressures at Injection Timing of 300° BTDC.

Total hydrocarbon emission for different boost pressure is observed and shown in Figure 5-27 (c). Hydrocarbon emission can explain the phenomena of combustion inside the combustion chamber. Less emission of hydrocarbon usually happens because of the better specific fuel consumption inside the chamber. With boost

pressure and 300° BTDC injection timing the graph shows insignificant variation in hydrocarbon emission for speed less than 4000 rpm. However, it has been shown that better hydrocarbon emission for speed above 4000 rpm compared to naturally aspirated engine. Effect of boost pressure with 300° BTDC injection timing on hydrocarbon emissions is observed for high speed while insignificant effect is revealed for speed less than 4000 rpm. This approves the better mixture preparation of early injection timing with supercharging system for speed above 4000 rpm.

Percentage of methane in total hydrocarbon emission for supercharging system at 300° BTDC injection timing is explained in Figure 5-27 (d). With early injection timing, the same event is shown like partial direct injection where percentage of methane in total hydrocarbon emission decreases with increasing boost pressure. However, with increasing engine speed percentage of methane is not decreasing like partial direct injection. For instance, with 10 kPa boost pressure percentage of methane start to decrease till 3500 rpm and slightly increase when engine speed increased to 5000 rpm. With early injection timing percentage of methane in total hydrocarbon seems to be higher for high engine speeds compared to partial direct injection. With 10 kPa boost pressure and early injection timing on average there is 6% higher percentage of methane in total hydrocarbon emissions compared to partial direct injection for speed above 3500 rpm. For both injection timing it is shown that better percentage of methane in total hydrocarbon emission is shown when boost pressure is above 7.5 kPa. This shows that having higher boost pressure at high engine speed results in fast combustion rate with improved exhaust emissions.

Figure 5-28 compares emissions of 10 kPa boost pressure between partial and early injection timings. 300° BTDC injection timing has higher NOx emission at high engine speed compared to 180° BTDC injection timing. The better performance values of 300° BTDC injection timing is supported by the higher emission of NOx and lower emission of CO at high engine speed. Early injection timing also helps THC emission to become small relative to late injection timing at high speed. This is due to late injection gives insufficient time for the fuel air-mixing of the injected fuel bringing poor quality of mixture formation and subsequently resulting in the slow

combustion rate and high HC and CO concentrations at high engine speeds compared to early injection timing. However, late injection timing results in high NOx emission while maintaining in low level of HC and CO emissions at low engine speeds compared to early injection timing.

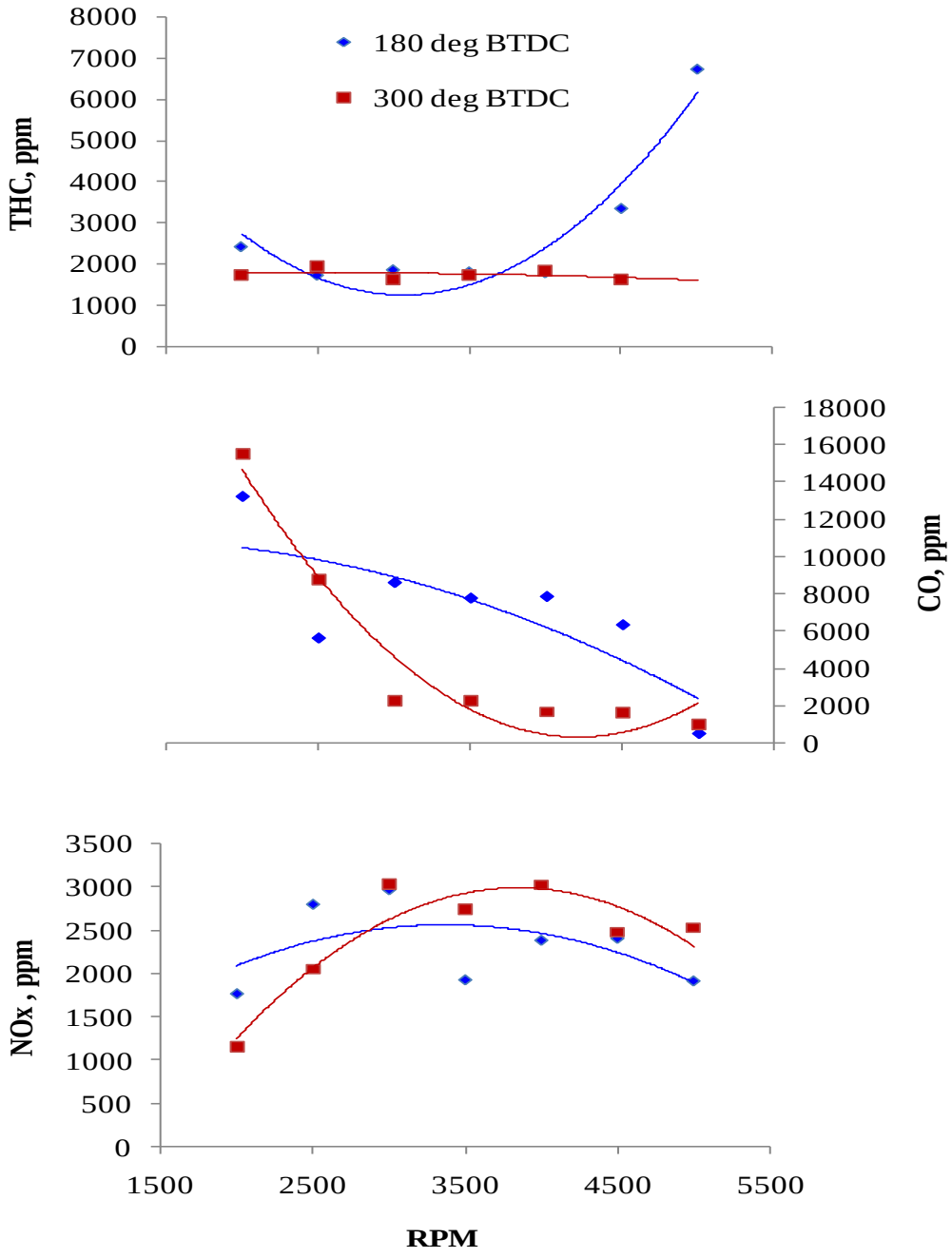

Figure 5-28 Effect of Injection Timing on Emissions of 10 kPa Boost Pressure

CHAPTER 6

CONCLUSIONS AND RECOMMENDATIONS

6.1 Conclusions

The use of direct injection to increase the performance of the engine has been verified by previous researchers. However the use of direct injection with gaseous fuels at port and partial injection was found to have penalty of volumetric efficiency. This is mainly due to the displacement of some of the air by natural gas as these two injection timings have inlet valve open during injection. For this reason the use of supercharging system has been recommended to boost the performance of the engine at these injection timings. Here small boost pressures were used to study effects of boost pressure on performance, combustion and exhaust emissions. Boost pressures were varied at injection timings of 180° and 300° BTDC for operating engine speeds of 2000 to 5000 rpm. From the result of the experiment, we can conclude that:

1. Boost pressures above 7.5 kPa resulted in a better engine performance compared to naturally aspirated engine at all engine operating speeds. Supercharging reduces the penalty due to the losses in volumetric efficiency.
2. At low speeds from 2000 to 2500 rpm, a minimum of 2.5 kPa boost pressure resulted in a better performance compared to naturally aspirated engine. However, for speeds above 2500 rpm a higher boost pressure is required to supply enough amount of air and compensate temperature effect for performance comparable to naturally aspirated engine.
3. With supercharging, early injection timing has better performance to late injection timing at engine speed above 4000 rpm. This is mainly due to the mixture preparation time available for early injection timing before ignition events happen at higher speeds.
4. With supercharging, partial direct injection has better performance at engine speeds from 2000 to 4000 rpm compared to 300° BTDC (early) injection timing. This is due to better volumetric efficiency of partial direct injection with supercharging at low engine speeds.

5. Without supercharging, there is higher cycle to cycle variation compared to supercharging system. With supercharging COV values of less than 5% are achieved at all operating engine speeds.
6. With supercharging, ignition delay period was found to be lower and results in better combustion efficiency compared to naturally aspirated engine.
7. Once combustion event happened supercharging was found to have significant effect on combustion stage making combustion duration of main stage (10-90%) smaller compared to naturally aspirated engine.
8. The lower combustion duration of supercharging system has a significant improvement in heat release and mass fraction burn rate making concentrated heat release process closer to the top dead center compared to naturally aspirated engine.
9. With boost pressure, emission of NOx is high compared to naturally aspirated engine due to high pressure and temperature in the combustion chamber.
10. With small supercharging pressure there was no significant improvement in THC emission compared to naturally aspirated engine.
11. With supercharging, CO emission was found to be lower amount than naturally aspirated engine.

6.2 Recommendations

The following is recommended as a continuation of the current research. Engine performance and combustion characteristics of lean stratified operation with supercharging need to be further studied to investigate effect of supercharging system. To further maximize engine performance of alternative fuels, Supercharging with cooling system needs to be studied. Combustion process is the most important aspect of any internal combustion engine. Analysis of combustion has been a challenge to understand and have clear picture of combustion process. Besides supercharging system, controlling combustion process will result in high performance of alternative fuels. Thus, flow and combustion flame visualization studies are recommended to fully understand the mixture formation and combustion characteristics that helps to analyze combustion process. Moreover mixture formation process in the combustion chamber is a key to control combustion process, and thus fuel injection and in-cylinder flow phenomena need to be studied further.

REFERENCES

1. d'Ambrosio, S., Spessa, E. and Vassallo, A., "Experimental Investigation of Fuel Consumption, Exhaust Emissions, and Heat release of a Small-Displacement Turbocharged CNG engine," SAE International, 2006-01-0049, 2006.
2. Tanin, K., Wickman,D., Montgomery, D., Das, v. and Reilz, R.D., "The influence of Boost pressure on Emissions and Fuel Consumption of a Heavy Duty, Single-Cylinder D.I.Diesel Engine," SAE Paper No.1999-01-0840.
3. Hiereth, H. and Prenning, P., "Charging the internal combustion engine," Springer-verlagWien, NewYork, 2003.
4. Hailin, L., "An Experimental and Analytical Examination of Gas Fuelled Spark Ignition-Engine performance and Combustion," PhD Thesis, University of Calgary, 2004.
5. Zhang, S., "The second law analysis of a spark ignition engine fueled with compressed natural gas," Msc. thesis, University of Windsor, Canada, 2002.
6. IANGV, "Pathways for Natural Gas into Advance Vehicles," G. Harris, Editor. 2002, IANGV.
7. IANGV, *IANGV* reports. 2007.
8. NGV Community library, "Compressed natural gas," http://www.ngv.com.my
9. IANGV, "Pathways for Natural Gas into Advance Vehicles," 2000: IANGV.
10. Sllveira, B.H.d., Leandro, H. and Edward, W., "Development of a Concept Vehicle for Compressed Natural Gas," SAE Brasil, 2004-01-3452, 2004.
11. Durell, E., Allen, J., Law, D. and Health, J., "Installation and development of direct injection system for a Bi-Fuel gasoline and compressed natural gas engine," Proceeding ANGVA Conference, 2000.
12. Ganesan, V., "Internal combustion engines," Tata MacGraw-Hill publisher, Third Edition, India, 2007.
13. Watson, N. and Janota, M.S., "Turbocharging the internal combustion engine," MacMillan publishers Limited, London, 1982.
14. Oullette, P., "High pressure direct injection (HPDI) of natural gas in diesel engines," Westport Innovation, Inc., Canada, 2000.

15. Remo, D., Vander, F. and Francisco, E., “Performance and Emission Analysis of the Turbocharged Spark- Ignition Engine Converted to Natural Gas,” SAE Paper No.2003-01-3726.
16. Walter, E.J. and Wenger, M., “Boosting of Turbocharger Dynamics: Simulation and Comparison of Different Solutions,” SAE Paper No.2003-01-0399.
17. Barkawi, P., Rashid, A., Ali, Y., Chuah, T.G., Hassan, M., Halim, K. and Ahmad, F., “Compressed natural gas passenger vehicle and development issues and challenges,” UPM Serdang, slangor, 2006.
18. Maji, S., Sharma, P.B. and Babu, M.K.G., “A Comparative Study of Performance and Emission Characteristics of CNG and Gasoline on a Single Cylinder S.I. Engine,” SAE, 2004-28-0038, 2004.
19. Weaver, C. S., “Natural Gas Vehicle-A Review of the State of the Art, Gaseous Fuel Technology, Performance and Emissions SP-798,” SAE, Inc., Warrendale, PA, pp. 35-55, 1989.
20. IANGV, Natural Gas Vehicle Industry Position Paper, 1997.
21. Mistry, C.S., "Comparative Assassment on Performance of Multi cylinder Engine Using CNG, LPG and Petrol as a Fuel," SAE International, 2005-01-1056, 2005.
22. Kato, K., Yasadu, A. and Masuda, M., "Development of Engine for Natural Gas Vehicle," SAE, 1999-01-0574, 1999.
23. Atkinson, C.M., Traver, M.L. and Tennant, C.J., "Exhaust Emissions and Combustion Stability in a Bi-Fuel Spark Ignition Engine," SAE International, 950458, 1995.
24. Dunn, M., "State of the Art and Future Developments in Natural Gas Engine Technologies," Proceedings of DEER 2003:Diesel Engine Emissions Reduction Newport, Rhode Island, August 2003.
25. Pischinger, S., Umierski, M. and Huchtebrock, B., "New CNG Concepts for Passanger Cars: High Torque Engines with Superior Fuel Consumption," SAE, 2003-01-2264, 2003.
26. Achleitner, E., Backer, H. and Funaioli, A., "Direct Injection Systems for Otto Engines," SAE, 2007-01-1416, 2007.

27. Einewall, P. and Jőnsson, O., "Ultra-clean natural gas engine with closed-loop lambda control, high turbulence combustion chamber, EGR and a three-way catalyst," Lund University, 2000.
28. Catania, A.E., d'Ambrosio, S., Misul, D. and Spessa, E., "High-Boost C.R. Diesel Engine: A Feasibility Study of Performance Enhancement and Exhaust-Gas Power Cogeneration," SAE Paper No.2002-01-2814.
29. Nafis, A., and Razique, M.A., "Simulation and Experimental studies on combustion and performance characteristics for a turbocharged and natural aspirated multi-cylinder compression ignition Engine," SAE Paper No. 2006-01-3487.
30. George, S., Morris, G., Dixon, J., Pearce, D. and Heslop, G., "Optimal boost control for an electrical supercharging application," SAE Paper No.2004-01-0523.
31. Sugihara, H., Aoyagi, Y., Shin, S. and Joko, I., "Effect of high boost turbocharging on combustion characteristics and improving its low engine speed torque," SAE Paper No. 920046.
32. Buckland, J., Jeff Cook, J., llya, K. and Jing, S., "Technology Assessment of Boosted Direct Injection Stratified Charge Gasoline Engines," SAE Paper No.2000-01-0249.
33. Alasdair, C. and Hugh, B., "Lean Boost and External Exhaust gas Recirculation for High Load Controlled Auto-ignition," SAE Paper No. 2005-01-3744.
34. Stone, R., "Introduction to Internal Combustion Engines," 3rd ed., SAE International, 1999.
35. Mello, P., Pelliza, G. and Cataluna, R., "Evaluation of the maximum horsepower of vehicles converted for use with natural gas fuel," Fuel, 85(14-15), pp. 2180-2186, 2006.
36. Loukanine, V.N., Khatchiya, A.S. and Shishlov, I.V., "Analysis of Different Ways to Develop Low-Emission Natural Gas Engines," In NGV Yokohama, Japan: ANGVA, 2000.
37. Czerwinski, J., Comte, P. and Zimmerli, Y., "Investigations of the Gas Injection System on a HD-CNG Engine," SAE 2003-01-0625, 2003.

38. IANGV, *IANGV* reports, 2000.
39. Kim, J. and Carley, D., "Development of direct injection CNG engine," NGV report, 2000.
40. Ishiyama, T., Shioji, M., Tanaka, H. and Nakai, S., "Implementation of direct fuel-injection for higher efficiency in natural gas engines," Proceedings of the eighth international conference & exhibition on natural gas vehicles pp.1, 2002.
41. Arcoumanis, C., Hu, Z., Vafidis, C. and Whitelaw, J.H., "Tumbling motion: A mechanism for turbulence enhancement in spark ignition engines," SAE 900060.
42. Endres, H., Neuber, H.J. and Wurms, R., "Influence of swirl and tumble on economy and emissions of multivalve SI engine," SAE 920516.
43. Zhao, K., "Study on combustion system of a spark ignition natural gas engine," Journal of Tongji University, 26(1), pp. 1-8, 1998.
44. Arcoumanis, C., "Injection natural gas engine for light duty applications," IMEchE, C588 (013), 2001.
45. Hayashida, M., Yamato, T. and Sekino, H., "Investigation of Performance and Fuel Distribution of a Direct Injection Gas Engine Using LIF Measurement," SAE 1999-01-3291 JSAE 9938046, 1999.
46. Hassaneen, A.E., Vaede, K.S. and Bawady, A., "A Study of the Flame Development and Rapid Burn Durations in a Lean-Burn Fuel Injected Natural Gas S.I. Engine," SAE, 981384, 1998.
47. Zuo, C. and Zhao, K., "Study on the combustion system of a spark ignition natural gas engine," Dearborn, MI, USA: SAE, Warrendale, PA, USA, 1998.
48. Zhao, F., Harrington, D.L. and Lai, M.C., "Automotive Gasoline Direct-Injection Engines," SAE International, 2002.
49. Huang, Z., Shiga, S. and Ueda, T., "Feasibility of CNG DI Stratified Combustion Using a Spark-Ignited Rapid Compression Machine," In the fifth International Symposium on Diagnostic and Modeling of Combustion in Internal Combustion Engines, Nagoya: Comodia, 2001.
50. Achleitner, E., Backer, H. and Funaioli, A., "Direct Injection Systems for Otto Engines," SAE, 2007-01-1416, 2007.

51. Heywood, J.B., “Internal Combustion Engine Fundamentals,” McGraw-Hill, 1998.
52. Shiga, S., Ozone, S. and Machacon, H.T., “A study of the combustion and emission characteristics of compressed natural gas direct-injection stratified combustion using a rapid compression machine,” Combustion and Flame, pp. 1-10, 2002.
53. Shiga, S., Ueda, T. and Ishii, H., “Basic Aspect of Combustion of CNG In-cylinder Direct-Injection with Spark-Ignition,” SAE International, 2005-26-352, 2005.
54. Kuwahara, K., Ueda, K., and Ando, H., “Mixing control Strategy for Engine Performance Improvement in a Gasoline Direct Injection Engine”, SAE Paper 980158, 1998.
55. Huang, Z., Shiga, S. and Ueda, T., “Basic Characteristics of direct injection combustion fuelled with compressed natural gas and gasoline using a rapid compression machine,” Proc. Instn Mech. Engrs. Part D: j. Automobile Engineering, 2003.
56. Huang, Z., Shiga, S. and Ueda, T., “Combustion characteristics of natural gas direct injection combustion under various fuel injection timings,” Proc. Instn Mech. Engrs. Part D: j. Automobile Engineering, pp. 935-941, 2003.
57. Huang, Z., Shiga, S. and Ueda, T., “Effect of Fuel Injection Timing Relative to Ignition Timing on the Natural-Gas Direct-Injection Combustion,” Journal of Engineering for Gas Turbines and Power ASME, pp. 53-61, 2003.
58. Huang, Z., Shiga, S. and Ueda, T., “Correlation of ignitability with injection timing for direct injection combustion fuelled with compressed natural gas and gasoline,” Proceedings of the Institution of Mechanical Engineers, Part D: Journal of Automobile Engineering, pp. 499-506, 2003.
59. Goto, Y., “Mixture formation and ignition in a direct injection natural gas engine,” JSME International Journal, Series B, 1999. 42(2), pp. 268-274.
60. Wang, J., Zuohua, H. and Bing, L., “Effect of fuel injection timings and hydrogen fraction on combustion characteristics of direct-injection engine,” Hsi-An Chiao Tung Ta Hsueh/Journal of Xi'an Jiaotong University, pp. 767-770, 2006.

61. Kim, C.U. and Bae, C.S., “Speculated hydrocarbon emissions from a gas-fuelled spark-ignition engine with various operating parameters,” Proceedings of the Institution of Mechanical Engineers, Part D: Journal of Automobile Engineering, pp. 795-808, 2000.
62. Kakuho, A., Yamaguchi, K. and Fukuda, T., “A Study of Air-Fuel Mixture Formation in Direct-Injection SI Engine,” SAE, 2004-01-1946, 2004.
63. Ortmann, R., Raimann, J. and Wuerfel, G., “Methods and Analysis of Fuel Injection, Mixture Preparation and Charge Stratification in Different Direct Injected SI Engine,” SAE, 2001-01-0970, 20001.
64. Aleiferis, P.G., Hardalupas, Y., Taylor, A.M.K.P., Ishii, K. and Urata, Y., “Flame chemiluminescence studies of cyclic combustion variations and air-to-fuel ratio of the reacting mixture in a lean-burn stratified-charge spark-ignition engine,” Combustion and Flame 136, pp. 72–90, 2004.
65. Aleiferis, P.G., Taylor, A.M.K.P., Ishii, K. and Urata, Y., “The nature of early flame development in a lean-burn stratified-charge spark-ignition engine,” Combustion and Flame 136, pp 283–302, 2004.
66. Cho, H.M. and He, B.Q., “Spark Ignition natural gas engines - A review,” Energy Conversion and Management, 2006.
67. Aslam, M.U., Masjuki, H.H., Kalam, M.A., Abdesselam, H., Mahlia, T.M.I. and Amalina, M.A., “An experimental investigation of CNG as an alternative fuel for a retrofitted gasoline vehicle,” Fuel 85, pp. 717-724, 2006.
68. Nylund, N., Laurikko, J. and Ikonen, M., “Pathways for natural gas into advanced vehicles,” IANGV, 2002.
69. Maji, S., Sharma, P.B. and Babu, M.K.G., “Experimental Investigations on Performance and Emission Characteristics of CNG in a Spark Ignition Engine,” SAE International, 2005-26-344, 2005.
70. Nylund, N.O., Laurikko, J. and Ikonen, M., “Pathways for natural gas into advanced vehicles,” IANGV Edited Draft Report 2002; Version 30.8.2002.
71. Martin, D. and Beldan, P., “Boosted Engine Systems Optimization Approach,” SAE Paper 981976, 1998.

72. Stokes, J., Lakes, T.H. and Osborne, R.J., "A Gasoline Engine Concept for Improved Fuel Economy–The Lean Boost System," SAE Paper No.2000-01-2902.
73. New, J., Criddle, M. and Brown, J., "Application of an Electrical Boosting System to a small, Four-Cylinder S.I. Engine," SAE Paper No.2003-32-0039
74. Shao, J., Ogura, M., Liu, Y. and Yoshino, M., "Performance of a New Axially Movable Vane Turbocharger," SAE Paper 961747, 1996.
75. Hu, X., "An advanced turbocharger model for the internal combustion engine," Phd thesis, Purdue Universtiy, 2000.
76. Podevin, P. and Descombes, G., "Effect of supercharging pressure on internal combustion engine performance and pollutant emissions," paper, France.
77. Joseph, A., "A turbocharger unsteady performance model for the GT-Power internal combustion engine simulation" Phd thesis, Purdue University, 2002.
78. Agarwal, A., "Multi-Dimensional modeling of natural gas ignition, combustion and pollutant formation in direct injection engines" Phd thesis, University of Michigan, 1998.
79. Catania, A.E., Misuld, D. and Spessa, E., "Conversion of a Multivalve Gasoline Engine to Run on CNG," SAE International, 2000-01-0673, 2000.
80. Catania, A.E., Misuld, D. and Spessa, E., "A refined two-zone heat release model for combustion analysis in SI engines," JSME International Journal, Series B: Fluids and Thermal Engineering, pp. 75-85, 2003.
81. Kim, J.M., Han, S.B. and Raine, R.R., "Combustion Stability of Natural Gas Engine Operating at Idle," SAE, 2005-01-3446, 2005.
82. Freund, E., "The future of technologies to reduce CO_2 emission of road transport," In Technology future presentation, Paris, 2006.
83. Kalam, M.A., Masjuki, H.H. and Maleque, M.A., "Gasoline engine operated on compressed natural gas," Proc. Advances in Malaysian Energy Research (AMER), Malaysia, pp. 307–316, 2001.
84. Nylund, N.O. and Lawson, A., "Exhaust emissions from natural gas vehicles," Report prepared for the IANGV Technical Committee, 2000.
85. Varde, K. S., Cherng, J. C., Bailey, C. J. and Majewski, W. A., "Emissions and their Control in Natural Gas Fueled Engines," Automotive Emissions and

Catalyst Technology SP-938, Society of Automotive Engineers, Inc., Warrendale, PA, pp. 63-76, 1992.

86. Baird, B. and Gollahalli, S. R., "Emissions and Efficiency of a SI Engine Fueled with a Natural Gas and Propane mixture," Proceedings of 2000 International Joint Power Generation Conference Miami Beach, Florida, July 23-26, 2000.
87. Suga, T., Muraishi, T. and Bienenfeld, R., "Potential of a low emission Natural gas Vehicle for the 21th Century," Yokohama, Japan: IANGV, 2000.
88. Majid, Z.A., Yaacob, Z. and Piau, M.P.K.I., "Natural gas motorcycle-emission," IANGV, 2000.
89. Beroun, S. and Martins, J., "The Development of Gas (CNG, LPG and H_2) Engines for Buses and Trucks and their Emission and Cycle Variability," SAE, 2001-01-0144, 2001.
90. Cattelan, A. and Wallace, J., "Exhaust Emission and Energy Consumption Effects from Hydrogen Supplementation of Natural Gas, Alternate Fuels Emissions and Technology," SP-1115, SAE, Inc., Warrendale, PA, pp. 155-165, 1995.
91. Uger, K., "Study on prediction of the effects of design and operating parameters on NOx emissions from a lean burn natural gas engine," Energy Conversion and Management 44, pp. 907–921, 2003.
92. Loffer, G., Sieber, R., Harasek, M., Hofbauer, H., Hauss, R. and Landauf, J., "NOx Formation in natural gas combustion-a new simplified reaction scheme for CFD calculations," Fuel 85, pp. 513-523, 2006.
93. Alkidas, A.C., "Combustion-chamber crevices: the major source of engine-out hydrocarbon emissions under fully warmed conditions," Progress in Energy and Combustion Science, pp. 253–273, 1999.
94. Ferguson, C. R., KirkPatrick, A. T., "Internal Combustion Engine Applied Thermo sciences," John Wiley & Sons, Inc., 2001.
95. Krieger, R. B., and Borman, G. L., "The Computation of Apparent Heat Release for Internal Combustion Engines," ASME paper 66-WA/DGP-4, ASME, 1966.

96. Esfahanian, V., Salavati, A., Nasr, A. and Mirosohil, M., "Simulation and Comparison of the Performance of CNG and Gasoline Engines Using Flame Propagation Model Considering the Effects of Some of the Parameters of Combustion Chamber," ANGVA International Conference, Malaysia, 2005.
97. Rassweiler, G.M. and Withrow, L., "Motion Pictures of Engine Flames Correlated with Pressure Cards," SAE Trans., Vol. 47, pp. 185-204, 1938.
98. Nagano, M., Watanabe, S., Sukegawa, Y. and Amou, K., "Port-injection Engine-control System for Environmental Protection," SAE International, 2002.
99. Richard, B. and Fred, S., "Internal combustion engine handbook," SAE international, Canada, 2002.
100. Bielaczyc, P., Pajdowski, P. and Szczotka, A., "Particulate matter Emissions for Different type of Fuel Supplying System of Spark Ignition and Compression Ignition Engines," Journal of Kones Combustion Engines, VoIB, No 1-2, 2001.
101. Mintz, M.M., Wang, M.Q. and Vyas, A.D., "Fuel-Cycle Energy and Emissions Impacts of Propulsion System/Fuel Alternatives for Tripled Fuel-Economy Vehicles," SAE, 1999-01-1118, 1999.
102. Cheung, H. and Heywood, J., "Evaluation of a One-zone Burn Rate Analysis Procedure Using Production SI Engine Pressure Data," SAE paper 932749, 1993.
103. Grimm, B.M. and Johnson, T., "Review of Simple Heat Release Computation," SAE International, 900445, 1990.
104. SAE J1349, "Engine Power Test Code – Spark Ignition and Compression Ignition – Net Power Rating," SAE Standard Handbook, 1995.
105. Klein, M., "A Specific Heat Ratio Model and Compression Ratio Estimation," Thesis No: 1104, Division of Vehicular Systems, Linköping University, SE–581 83 Linköping, Sweden, 2004.
106. Moran, M.J. and Shapiro, H.N., "Fundamental of Engineering Thermodynamics," third ed., Wiley, New York, pp. 590-610, 1995.
107. Andrzej, J., Osiadacz., "Simulation and Analysis of Gas Networks," PhD DSc, the Control Systems Center UMIST, Manchester, UK, 1987.

APPENDIX A

Properties of Natural Gas Used in the Study

Component	Leanest	Richest	Unit
Methane	96.42	89.04	%
Ethane	2.29	5.85	%
Propane	0.23	1.28	%
Iso-Butane	0.03	0.14	%
N-Butane	0.02	0.10	%
Iso-Pentane	N/A	N/A	%
N-Pentane	N/A	N/A	%
N-Hexane	N/A	N/A	%
Condensate	0.00	0.02	%
Nitrogen	0.44	0.47	%
CO_2	0.57	3.09	%
Gross Heating Value	38130	38960	kJ/kg